MECHANISMS OF INFLAMMATION RESOLUTION IN A MURINE MODEL OF LYME ARTHRITIS

A Dissertation

Presented to

The Faculty of the Graduate School

at the

University of Missouri

In Partial Fulfillment

of the Requirements for the Degree

Doctor of Philosophy

In Microbiology

By

CHRISTA DANIELLE JACKSON

Dr. Charles Robert Brown, Dissertation Advisor

May 2023

The undersigned, appointed by the dean of the Graduate School, have examined the dissertation entitled:

MECHANISMS OF INFLAMMATION RESOLUTION

IN A MURINE MODEL OF LYME ARTHRITIS

Presented by Christa D. Jackson,

a candidate for the degree of Doctor of Philosophy,

and hereby certify that, in their opinion, it is worthy of acceptance.

Certified

by_____

Charles R. Brown

Professor of Veterinary Pathobiology

Accepted

by_____

Jerod A. Skyberg

Associate Professor of Veterinary Pathobiology

Accepted

by_____

Deborah M. Anderson

Professor of Veterinary Pathobiology

Accepted

by_____

Bumsuk Hahm

Professor of Molecular Microbiology and Immunology

Accepted

by_____

Adam G. Schrum

Associate Professor of Molecular Microbiology and Immunology

DEDICATION

To family and friends, both old and new, without whom I would not be here today. Much love to you all.

ACKNOWLEDGEMENTS

I would first like to thank my dissertation committee, who challenged and supported me from the very beginning. I appreciate the thoughtful questions, constructive criticism, and encouragement that I received from Drs. Deb Anderson, Bumsuk Hahm, and Adam Schrum. I would especially like to thank Dr. Jerod Skyberg for the countless hours he spent discussing my data, helping me troubleshoot flow cytometry, and mentoring me.

Thank you to our collaborators who graciously shared their time, equipment, and expertise. Thanks to Drs. David Gozal, Abdelnaby Khalyfa, and Mohammad Badran at the University of Missouri-Columbia School of Medicine (SOM) for their collaboration on the sleep study design and in overseeing the sleep fragmentation portion of those studies. Thanks also to Dr. Steven Segal, also at the University of Missouri-Columbia SOM, for providing us the opportunity to perform intravital microscopy.

I'd like to thank those in the Molecular Pathogenesis and Therapeutics graduate program, the Department of Veterinary Pathobiology, and the Department of Molecular Microbiology and Immunology. Thanks to the incredible instructors and tireless administrative staff for your help along the way, and thanks to the OAR staff for taking care of our mice. I'd also like to thank my peers, whose constant support has sustained me. I treasure the dear friends I've made in classes and through the MPTGSO. I'd also like to thank the Connaway

gang, with whom I've learned and grown as a scientist and as a person. Special thanks to Dr. Alexis Dadelahi, who was always willing to help troubleshoot my experiments and discuss my data, who encouraged me and kept me grounded, and who, most importantly, introduced me to disc golf.

Many thanks to my undergraduate research mentor, Dr. C. Joel Funk at John Brown University, whose instruction and endless encouragement gave me the confidence to pursue graduate school and a career in research. I am forever grateful for the education I received at JBU and the community I found in Bell Science Hall.

Most importantly, I'd like to thank my dissertation advisor and mentor, Dr. Charles Brown, without whom none of this work would have been possible. Through the highs and lows, you have remained a patient and steadfast guide. You taught me how to think like a scientist, and it is because of you that I have the confidence to forge ahead.

TABLE OF CONTENTS

LIST OF FIGURES AND TABLES

Figures

Tables

MECHANISMS OF INFLAMMATION RESOLUTION IN A MURINE MODEL OF LYME ARTHRITIS

Christa D. Jackson

Dr. Charles R. Brown, Dissertation supervisor

ABSTRACT

In some patients, Lyme arthritis persists despite antibiotic clearance of *Borrelia burgdorferi*, indicating an underlying defect in inflammation resolution mechanisms. In the murine model of Lyme arthritis (mLA), *B. burgdorferi* infection of C3H/HeJ mice induces a self-limiting arthritis, allowing the study of both the development and resolution of inflammation. Our primary interest is the role of bioactive lipid mediators in mLA inflammation. Here we showed that 12/15-LO activity is required for efficient mLA resolution and that LXA_4 may therapeutically ameliorate mLA by reducing edema and remodeling joint macrophage populations. We demonstrated that PGE_2 is not required for mLA resolution, but mLA may instead resolve more efficiently in PGE_2-deficient mPGES-$1^{-/-}$ mice due to enhanced bacterial control in the joint. Further, disruption of early inflammation in mPGES-$1^{-/-}$ mice by PGE_2 addback worsened arthritis outcomes. We also designed an *in vivo* staining method to characterize neutrophil reverse transendothelial migration from the inflamed site. Lastly, we demonstrated that sleep fragmentation impairs *B. burgdorferi* clearance from the joint and prevents efficient mLA resolution. These findings strengthen our understanding of inflammation resolution and may help identify therapeutic targets to ameliorate human LA and other inflammatory diseases.

CHAPTER 1

INTRODUCTION

Lyme Disease

Lyme disease (LD) remains a global health concern as the most common vector-borne disease in the Northern Hemisphere, with the CDC estimating 476,000 new cases in the US each year [1]. The majority of reported US cases are distributed throughout the Northeast and upper Midwest states [2], roughly matching the distribution of its vector in temperate climates. However, recent studies suggest that the geographic distribution of *Ixodes* ticks is expanding, which could lead to increased incidence of LD globally [3]. While most LD patients recover uneventfully following antibiotic treatment, undiagnosed or misdiagnosed patients, as well as some treated patients, can experience debilitating long-term sequelae including neuroborreliosis, carditis, and arthritis (as rev. in [4]). The mechanisms precipitating many of these systemic sequelae are poorly understood, and there is no vaccine available for humans.

History of Lyme Disease

The characterization of Lyme disease began when a rash of apparent juvenile rheumatoid arthritis cases were noticed in the communities near Lyme, Connecticut in the 1970s. These cases seemingly appeared around the same time of year, and many patients pre- or co-manifested with a bullseye rash (also called an erythema migrans) [5]. Local mothers reached out to investigators at

Yale University who recognized the similarity of the disease pathogenesis to cases following documented *Ixodes ricinus* tick bites in Europe. In line with European scientists' hypothesis that a spirochete could be causing the condition, researchers at Rocky Mountain Laboratories were able to isolate spirochetes from blood, skin, and cerebrospinal fluid samples from patients with erythema migrans [6]. Using DNA-DNA hybridization, the isolated spirochete was identified as a member of the *Borrelia* genus and eventually named *Borrelia burgdorferi* (*Bb*) in honor of its discoverer, Willy Burgdorfer [7].

Enzootic cycle and transmission of **Borrelia burgdorferi**

The causative agents of Lyme disease are *Borrelia* species spirochetes transmitted by ixodid ticks [2]. Individual *Borrelia* species are preferentially vectored by specific tick species; thus, different regions have distinct tick/*Borrelia* combinations causing LD [8]. For example, LD in the US is caused by *Borrelia burgdorferi* in *Ixodes scapularis* ticks, while *B. garinii* and *B. afzelii* in *I. ricinus* ticks are responsible for most borrelioses in Europe and Asia [9]. Though clinical manifestations differ between tick/spirochete combinations, the overall mechanism of transmission and pathogenesis is similar, leading to this family of spirochetes to be referred to as *Borrelia burgdorferi sensu lato* (rev. by [10]).

Ticks usually acquire the spirochete during larval feeding from small rodent reservoirs [11], where spirochetes respond to chemotactic signaling induced by larval feeding [12]. Ticks maintain infection trans-stadially (through subsequent

life stages and molting), but do not pass on the infection trans-ovarially [8]. Ticks are most likely to transmit *Bb* to humans during their nymphal feeding, where humans are considered an incidental host [8]. Because of the changes that must occur for *Bb* to prepare for life in a mammalian host (discussed below), transmission is more likely to occur after 48hr+ attachment [13]. It is unknown whether infected humans can transmit *Bb* to ticks.

In addition to altered metabolism, *Bb* modify their protein/lipoprotein surface expression when transitioning between tick and mammalian hosts. The most well-characterized example of this transition is in the expression of outer surface proteins (Osp). During tick acquisition, the *Bb* Rrp2/RpoN/RpoS transcriptional pathway is downregulated to allow de-repression of tick-phase genes, including OspA [11], a lipoprotein required for *Bb* colonization of tick midgut epithelium and sustained residence in ticks [14]. Conversely, nymphal bloodmeal intake triggers upregulation of the Rrp2/RpoN/RpoS transcriptional pathway, resulting in repression of OspA and induction of OspC in its place. OspC is required to establish early infection, although *Bb* downregulates the immunogenic OspC soon after mammalian colonization as an immune evasion mechanism [15].

As *Bb* does not produce any known toxins (including endotoxin [16]), tissue damage associated with *Bb* infection is a result of the host immune response against it. To survive in the mammalian host, *Bb* has developed a number of strategies to evade immune detection. Downregulation of OspC after the

infection is established allows *Bb* to evade OspC-specific antibodies [15]. Similarly, *Bb* utilizes a system of antigenic variation at its *vls* locus to thwart VlsE-specific antibody-mediated recognition and clearance [17]. Further, surface expression of *Bb*CRASP (complement regulator-acquiring surface protein) lipoproteins prevents activation of the alternative complement pathway [18]. These strategies permit *Bb* to establish infection and promote subsequent systemic dissemination and colonization of the mammalian host.

Clinical manifestations and pathogenesis

After transmission to a mammalian host, *Bb* establishes a localized cutaneous infection with the help of tick salivary components which help *Bb* evade early detection by suppressing the local immune response at the bite site [19]. Recruitment of T cells to the site of infection results in formation of one or more erythema migrans [20] in 70-80% of patients [21]. Erythema are characteristically bullseye-shaped but may be more homogeneous during early infection [22]. Aside from this rash, early signs of LD include non-specific flu-like symptoms such as fever, fatigue, and general malaise [23]. Early-stage, localized LD is usually resolved with a course of oral antibiotics [24].

If LD patients are left untreated, *Bb* will disseminate throughout the body via blood and/or lymph to colonize various tissues. At this stage, disseminated skin colonization may lead to the formation of secondary erythema and/or development of acrodermatitis chronica atrophicans (ACA) [25]. Late-stage

borreliosis can also result in systemic sequelae including Lyme carditis, Lyme neuroborreliosis, and Lyme arthritis (LA) [4]. The development of these systemic conditions largely depends on which *Borrelia* strain is acquired, where *B. afzelii* most frequently causes ACA, *B. garinii* is the most neurotropic, and *B. burgdorferi* is the most arthritogenic [9, 22].

Following transmission of *Bb* into the mammalian host, TLR2-mediated recognition of *Bb* lipoproteins by dermal macrophages and dendritic cells initiates an inflammatory response, with TLR2/TLR1 heterodimers activating the MAPK signaling pathway, leading to activation of NF-κB and subsequent production of proinflammatory mediators [26]. These mediators recruit leukocytes to the site of infection to clear the bacteria [27]. Infiltrating neutrophils kill bacteria via phagocytosis, oxidative burst, lytic enzymes, and neutrophil extracellular traps (NETs) [28]. Antibody opsonization of *Bb* boosts their phagocytosis by macrophages and neutrophils [29]. T cell-independent production of IgM boosts initial spirochete clearance [15], while later T-cell dependent development of *Bb*-specific IgG, predominantly IgG1 and IgG3, contributes to spirochete clearance by inducing opsonization and activating complement [29]. Indeed, passive immunization using sera from *Bb*-infected mice can provide protection against *Bb* infection in naïve C3H mice [30].

Both innate and acquired immunity are required for efficient clearance of *Bb* from most tissues, although mice never fully clear the spirochete [31]. TLR2$^{-/-}$ and MyD88$^{-/-}$ mice with defective innate immune responses have significantly

elevated levels of *Bb* in ears, hearts, and ankles up to 8 weeks post-infection (pi) [26, 32]. Antibody responses are still intact in these mice, as passive immunization of WT animals with sera from *Bb*-infected TLR2$^{-/-}$ or MyD88$^{-/-}$ mice is still protective. Therefore, the intact humoral responses were not sufficient to control *Bb* burdens in these tissues in the absence of innate immunity. Conversely, severe combined immunodeficiency (*scid*) mice did not clear spirochetes from joint synovium or blood for over six months, and *Bb* was still identifiable by histological staining in the myocardium at 161 dpi [33]. In another study, *scid* mice passively immunized with *Bb*-specific sera prior to infection with *Bb* cleared the spirochete from the joint by 15 dpi [34]. Lastly, one study used single and double TLR2$^{-/-}$/*scid* mice to determine the relative contribution of innate and adaptive immunity, and while TLR2$^{-/-}$ mice had higher levels of *Bb* in several tissues up to eight weeks pi compared to *scid* mice, this difference was not significant [35]. Therefore, the contribution of both arms of immunity should be considered when investigating mechanisms of bacterial control as antibody opsonization likely plays a major role in *Bb* clearance by innate immune cells.

Lyme Arthritis

Lyme arthritis is most commonly found in *B. burgdorferi sensu stricto*-endemic areas in the US, where LA occurs in about 80% of untreated Lyme patients [21]. LA incidence is much lower in Europe where other *Borrelia* species are more common, with only 3% of LD patients presenting with arthritis [4]. LA often manifests as a recurring asymmetrical inflammation of one or more large, weight-

bearing joints, especially the knee [36]. Clinical diagnosis in patients with arthritic manifestations relies on positive serology [37] and is supported by elevated white blood cell counts in synovial fluid, with neutrophil predominance [38], and PCR detection of *Bb* in synovial fluid [22]. In one US study, LA onset was reported between 4 days to 2 years after infection, with a mean of 6 months [36]. Acute LA is treated with a course of oral antibiotics with NSAIDs for pain relief, but up to 10% of patients have a recurrent or persistent arthritis even after antibiotic treatment [22]. Synovial tissue in patients who present with this antibiotic-refractory LA are culture and PCR-negative for *Bb*, and reemergent *Bb* infections have not been described at any point, even during active arthritis flareup [39]. As these patients present with a recurring LA despite no evident infection, this condition is referred to as postinfectious Lyme arthritis (pLA; as rev. by [24]).

The pathogenesis of LA is typical of an acute inflammatory response to active infection, with synovitis, robust monocyte and neutrophil infiltrate, and production of inflammatory mediators, although bone damage and/or joint erosion is not common [37]. In pLA, however, the synovial lesion more closely resembles that found in rheumatoid arthritis (RA), with elevated fibroblast proliferation and monocyte infiltration, microvasculature damage, and occasional cartilage damage and/or bone erosion [24, 40]. Unlike RA, pLA will eventually resolve, usually between 1-2 years, and this can be aided by the use of disease-modifying antirheumatic drugs (DMARDs) [39]. While the etiology of pLA is unknown, patients with excessive inflammatory responses to *Bb* infection may

develop autoantibodies, and IgG4 autoantibody titers increase with severity of fibrosis and microvascular damage in pLA [29]. Alternatively, while spirochetes are cleared from the synovium, *Bb* peptidoglycan is difficult to clear and may remain in the joint for several years post-treatment [41]. Thus, persistent *Bb* peptidoglycan antigen may drive inflammatory responses during pLA.

Regardless of the specific etiology, development of pLA is correlated with excessive inflammation during *Bb* infection and a subsequent inability to properly downregulate inflammatory mechanisms and/or upregulate pro-resolving mechanisms after spirochete clearance. Therefore, future studies should seek to identify therapeutic targets that modulate inflammatory responses, especially those related to pro-resolving mechanisms, to treat or prevent pLA.

The inflammatory response

Acute inflammation in response to infection or injury is a critical immune defense mechanism that mediates pathogen removal and tissue repair. Following infection or tissue damage, tissue-resident immune cells recognize pathogen-associated molecular patterns (PAMPs) and/or danger-associated molecular patterns (DAMPs) and secrete proinflammatory cytokines and chemokines to activate the endothelium, potentiating the recruitment of leukocytes to the site. Circulating leukocytes respond to the chemokine gradient coming from the site, travelling towards and extravasating into the site of inflammation. During infection, infiltrating immune cells phagocytose and kill pathogens and mediate

clearance of cellular debris from the site. Acute inflammation is typically self-limiting, with resolution and a return to tissue homeostasis occurring after removal of the offending agent and subsequent tissue repair [42]. However, dysregulation of resolution mechanisms can lead to a chronic inflammatory state, with continued production of proinflammatory mediators by a persistent immune infiltrate. Indeed, low-level chronic inflammation is a common underlying factor in a number of prevalent health conditions, including cardiovascular and neurodegenerative diseases, cancer, obesity, and rheumatoid arthritis, among others [43]. There is, therefore, a critical need to develop therapeutic strategies which can prevent or ameliorate chronic inflammation.

Mediators of inflammation resolution

Inflammation resolution is the process by which homeostasis is restored following injury or infectious insult. One of the central events of inflammation resolution is clearance of neutrophils from the site of inflammation. Though neutrophils are critical responders to inflammatory stimuli, excessive neutrophil recruitment and activation can be detrimental to tissue integrity [44]. Therefore, two key components of inflammation resolution include the cessation of neutrophil recruitment to the site and the apoptosis and subsequent efferocytosis of neutrophils at the site by phagocytes.

Inflammation resolution was once considered a passive process whereby the inflammatory response stopped after the pathogen was removed or the wound

was healed, after which tissue homeostasis was restored. However, we now understand that inflammation resolution is an active process that is purposefully initiated and tightly controlled [45]. Indeed, there is mounting evidence that the resolution program is set in motion during early inflammation, and that disruption of early inflammatory processes may negatively impact resolution outcomes [46].

As with development of inflammation, resolution is coordinated by myriad signaling molecules produced by immune and other local cells, including proteins (e.g. chemokines and cytokines) and bioactive lipid mediators such as eicosanoids and specialized pro-resolving mediators (SPM). Eicosanoids are arachidonic acid (AA)-derived lipids that play a role in both the induction and resolution of inflammation [47], whereas SPM are a functional class of lipids derived from omega-3 fatty acids, such as docosahexaeneoic acid (DHA) or eicosapentaenoic acid (EPA), that are characterized by pro-resolving activity in a number of disease models [48]. Enzyme activity, substrate availability, and receptor expression all affect the ability of eicosanoids and SPM to modulate inflammation, and temporal regulation of bioactive lipid class-switching from proinflammatory to pro-resolving is critical to the timely resolution of inflammation and restoration of homeostasis [49].

Bioactive lipid mediators: Cyclooxygenase products

Upon cellular activation, AA is released from the cell membrane by cytosolic phospholipase 2 ($cPLA_2$) and metabolized by cyclooxygenases (COX) or

lipoxygenases (LO) to produce pro- and anti-inflammatory/pro-resolving eicosanoids (Fig 1.1A) [47]. COX enzymes are found in two isoforms, COX-1 and COX-2. COX-1 is expressed constitutively throughout the body while COX-2 is specifically induced during inflammatory responses, especially in monocytes and macrophages [50]. Both enzymes metabolize AA to make prostaglandin H_2 (PGH_2), which can then be further metabolized by other enzymes to produce prostanoids including thromboxanes, prostacyclin, and prostaglandins [51]. Many prostanoids are considered canonically proinflammatory, making COX a therapeutic anti-inflammatory target. Indeed, several nonsteroidal anti-inflammatory drugs (NSAIDs), including ibuprofen and aspirin, prevent prostaglandin production by inhibiting the activity of COX enzymes (rev. by [47]).

Prostaglandin E_2 (PGE_2) is considered to be the most important prostanoid during inflammation as it is highly produced in inflammatory sites and is one of the more potent COX products, with well-described roles in vasodilation, vascular permeability, cell proliferation, angiogenesis, and apoptosis [50]. However, PGE_2 has also been shown to have anti-inflammatory and pro-resolving actions. PGE_2 signaling through E prostanoid receptors EP2 and EP4 suppresses chemokine production and reprograms macrophages towards a pro-resolution phenotype, including production of TGF-β [52, 53]. Levy et al. demonstrated that PGE_2 could facilitate eicosanoid class-switching from the proinflammatory 5-LO pathway to the anti-inflammatory and pro-resolving 12/15-LO pathway, permitting SPM synthesis [49]. PGE_2 can also have opposite effects on NF-κB, as it has been

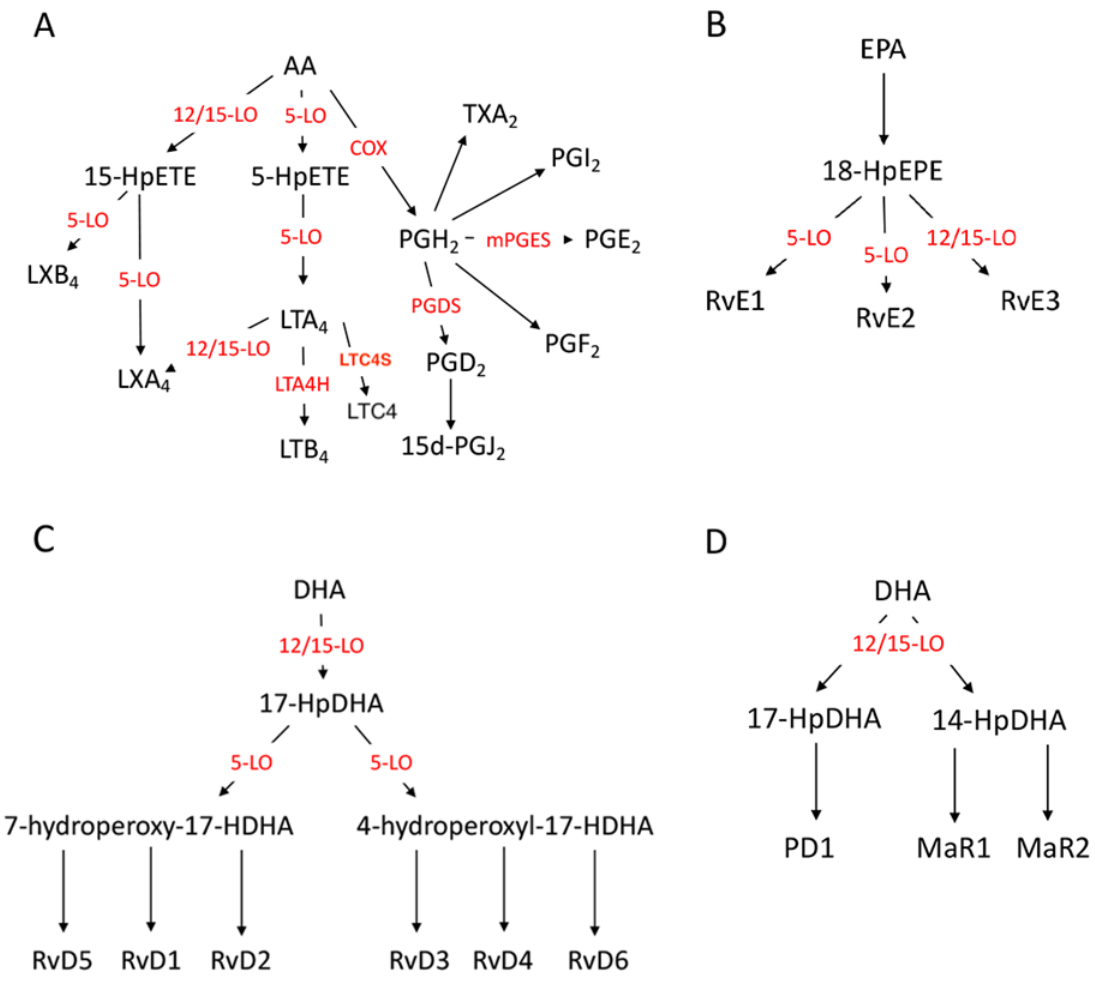

Figure 1.1. Biosynthesis of eicosanoids and SPM.

A brief overview of enzymatic pathways involved in eicosanoid and SPM biosynthesis. (A) Metabolism of arachidonic acid by COX-2, 5-LO, and 12/15-LO leads to synthesis of prostanoids, leukotrienes, and lipoxins. (B) Metabolism of EPA by 5-LO or 12/15-LO results in production of E-series resolvins. (C) Serial metabolism of DHA by 12/15-LO and 5-LO produces D-series resolvins. (D) Metabolism of DHA by 12/15-LO leads to production of protectin D1 and maresins. Red text denotes enzymes and black text denotes lipid metabolites.

shown to activate NF-κB during inflammation initiation [54] but PGE_2 production downstream of COX-2 activity can act as negative feedback by inhibiting the translocation of the NF-κB p65 subunit to prevent further COX-2 transcription [55]. Therefore, the differential roles of PGE_2 in inflammation are context-dependent, with concentration, source, localization, receptor expression, and timing all determining its overall effect.

Bioactive lipid mediators: Lipoxygenase products

AA can also be metabolized by two lipoxygenases, 5-LO and 12/15-LO (in mice; 12- and 15-LO are separate enzymes in humans) (Fig 1.1A). 5-LO is responsible for the synthesis of leukotrienes, including leukotriene B_4 (LTB_4), a potent proinflammatory lipid that activates circulating neutrophils, facilitating their diapedesis out of the vasculature and into the site of inflammation [56]. Serial lipoxygenation of AA by 5-LO and 12/15-LO produces lipoxins (lipoxygenase interaction products) [57]. Lipoxin A_4 (LXA_4) in particular has been well-characterized as a pro-resolving mediator. LXA_4 signaling through its high-affinity receptor mFpr2 (in mice; ALX/FPR2 in humans) can inhibit LTB_4- and fMLP-induced neutrophil chemotaxis [58]. LXA_4 can also promote phagocytosis of apoptotic neutrophils by macrophages [59, 60], which stimulates remodeling of efferocytosing macrophages towards a pro-resolving phenotype [61, 62]. 12/15-LO and 5-LO can also metabolize EPA and DHA to make SPM, including protectins, maresins, and E- and D-series resolvins (Fig 1.1B-D). Some of the pro-resolving actions of SPM include limiting neutrophil infiltration, enhancing

macrophage phagocytosis, suppressing neutrophil extracellular trap (NET) release, inhibiting platelet activation, and controlling bacterial and viral infections (as elegantly reviewed by [63]). Due to this wide array of pro-resolving effects, lipoxins and SPM have been investigated as potential therapeutics since their discovery, both alone and in combination with other treatments [63-65]. However, expanding our understanding of the roles of these endogenous mediators remains critical to both understanding the pathogenesis of inflammation and designing therapeutic strategies to ameliorate or prevent chronic inflammation.

A murine model of Lyme arthritis

In the murine model of Lyme arthritis (mLA), arthritis-susceptible C3H/HeJ mice [66] infected with *Bb* develop a self-limiting inflammatory arthritis characterized by a robust immune infiltrate and synovial hyperplasia in the tibiotarsal joint, which peaks around two to three weeks pi and then spontaneously resolves [67]. Development of mLA is mediated by innate immunity and is independent of acquired immunity, as demonstrated by the ability of *Rag1*$^{-/-}$, *scid*, and MHC-II-deficient mice to all develop arthritis [68-70]. As mLA is initiated by the presence of live spirochetes in the joint, so is mLA resolution correlated to the removal of *Bb* from the joint [34, 66, 69]. The key events in mLA development and resolution are briefly depicted in Figure 1.2.

However, spirochete clearance alone is not sufficient for mLA resolution, as demonstrated by the inability of mice deficient in COX-2, 5-LO, or BLT1 to

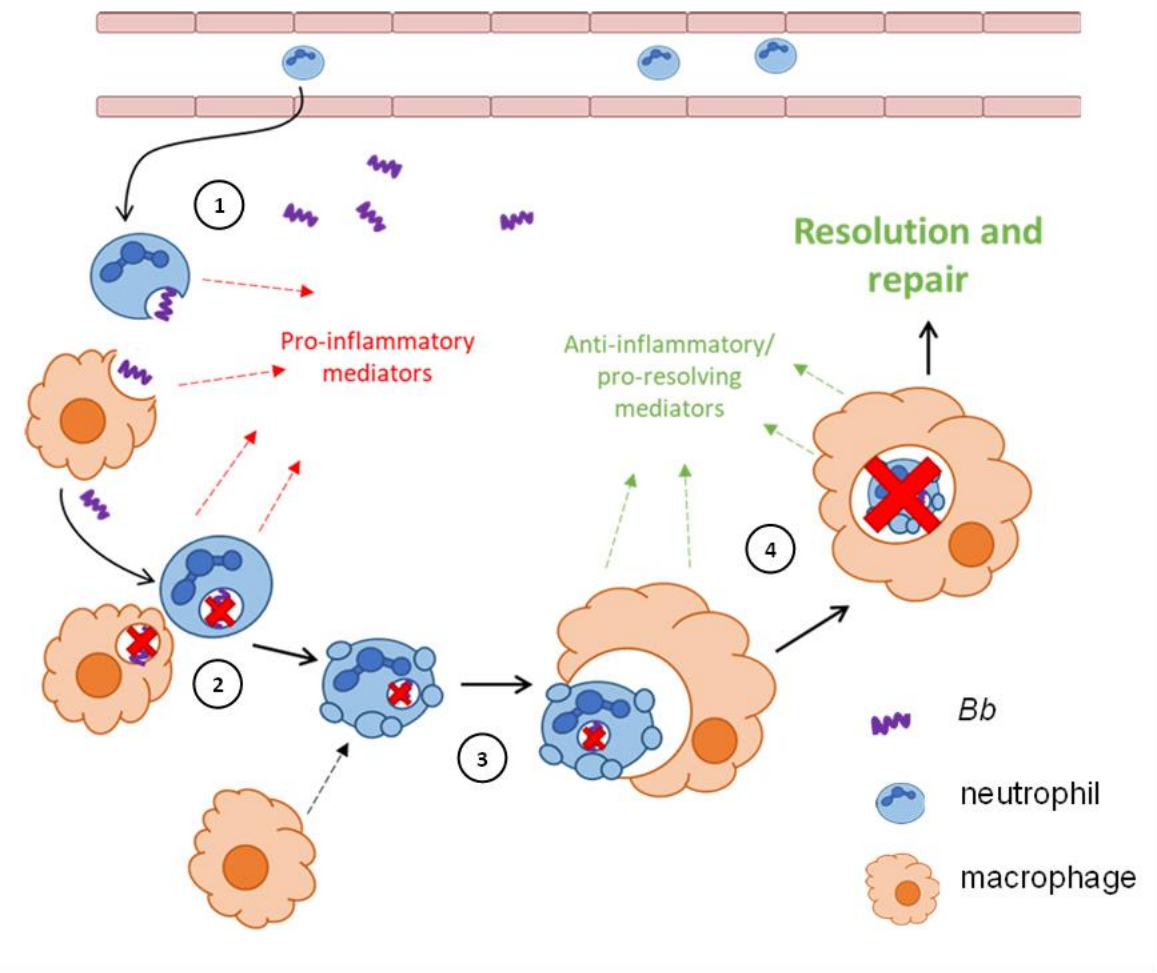

Figure 1.2. Key inflammatory events during mLA.

(1) During mLA, leukocytes responding to inflammatory signals are recruited to the site of infection to phagocytose and kill *Bb*. (2) After phagocytosing *Bb*, neutrophils begin to undergo apoptosis. (3) Neutrophils secrete “find me” signals to attract macrophages and express “eat me” molecules to help facilitate efferocytosis. (4) Following efferocytosis, macrophages are reprogrammed to produce anti-inflammatory and pro-resolving mediators, promoting inflammation resolution and tissue repair.

resolve mLA despite joint pathogen control similar to WT mice at 35 dpi [71-73]. 5-LO$^{-/-}$ (*Alox5*$^{-/-}$) mice are unable to synthesize lipoxins and most resolvins, which may contribute to inefficient resolution. However, studies using mLA in BLT1$^{-/-}$ mice demonstrated that the specific lack of LTB_4 signaling also led to a resolution defect, as LTB_4:BLT1 signaling can promote assembly of the death-inducing signaling complex, a component of the extrinsic apoptosis pathway [73]. Without LTB_4:BLT1 signaling, it was proposed that more cells would undergo necrosis secondary to apoptosis, thereby amplifying inflammation [73]. Thus, a breakdown in either pathogen removal and/or in the clearance of inflammatory infiltrate may delay or prevent mLA resolution.

While these mechanisms are plausible explanations for the mLA resolution defect in 5-LO$^{-/-}$ and BLT1$^{-/-}$ (*Ltb4r*$^{-/-}$) mice, less work has been done to investigate the mechanism behind the non-resolving mLA phenotype seen in COX-2$^{-/-}$ (*Ptgs2*$^{-/-}$) mice. As PGE_2 may be involved in facilitating lipid mediator class-switching in mLA, the absence of PGE_2 in these COX-2$^{-/-}$ mice may result in suboptimal induction of pro-resolution mechanisms. In one study, pharmacological inhibition of COX-2 during early mLA only (up to 14 dpi) was sufficient to prevent efficient mLA resolution, with robust inflammatory infiltrate persisting in the joint up to 35 dpi [71]. PGE_2 is the predominant AA-derived COX-2 metabolite in *Bb*-infected joints from around 7-14 dpi [74], so we may hypothesize that the lack of PGE_2 in COX-2$^{-/-}$ mice dysregulates the pro-resolution lipid mediator class switch, ultimately leading to prolonged

inflammation in the joint. These findings also support the hypothesis that resolution programs are initiated during early inflammation, such that disruption of early inflammatory mechanisms may be deleterious to overall outcomes.

Purpose and experimental approach

While we can appreciate that eicosanoids play a critical role in inflammation resolution in mLA, we seek to further understand the mechanisms required for resolution by identifying key bioactive lipids and characterizing their role in arthritis resolution. As one aspect contributing to pLA pathogenesis appears to be an inability to downregulate inflammation after pathogen removal, we can use mLA to study the factors that contribute to the development and resolution of arthritis in response to *Bb* infection in order to identify potential therapeutic targets for human LA and pLA patients.

The first data chapter demonstrates the contribution of bioactive lipid mediators downstream of 12/15-LO to successful inflammation resolution in mLA, with additional studies investigating the therapeutic use of 12/15-LO metabolite LXA_4 to ameliorate arthritis outcomes. The second data chapter builds off of the COX-$2^{-/-}$ mouse study by determining the specific contribution of PGE_2 to mLA resolution using PGE_2-deficient mice. Subsequent chapters explore other factors which may contribute to mLA development and resolution, including an alternative mechanism for neutrophil removal from the site of inflammation and the contribution of sleep to mLA outcomes.

CHAPTER 2

MATERIALS AND METHODS

Animals

All mice are on a C3H/HeJ background. 12/15-LO knockout mice (B6.129S2-*Alox15*^{tm1Fun}/J stock #002778) were purchased from The Jackson Laboratory (Bar Harbor, ME) and backcrossed to a C3H/HeJ background for at least ten generations in our colony. BLT1/2$^{-/-}$ (*Ltb4r/Ltb4r2*$^{-/-}$ and mPGES-1$^{-/-}$ (*Ptges*$^{-/-}$) mice on a C57BL/6 background were also backcrossed to a C3H/HeJ background for at least ten generations in our colony. Approximately equal numbers of male and female mice were used for *in vivo* experiments and as the source of bone marrow-derived cells. Animals were housed in a specific pathogen-free facility and given sterile food and water *ad libitum*. All studies were conducted in accordance with the Animal Care and Use Committee of the University of Missouri.

Bacteria and infections

A low-passage virulent N40 strain *B. burgdorferi* [75] was grown to log phase in complete Barbour-Stoenner-Kelly (BSK)-H media (Sigma, St. Louis, MO) at 32°C [76]. For *in vivo* infections, 5x10^4 spirochetes in 50µL incomplete BSK-H media (without rabbit serum) were injected into each hind footpad [77]. For *in vitro* studies, *Bb* was used at a multiplicity of infection (MOI) of 10 [77].

Ankle swelling and arthritis assessment

Ankle swelling was monitored by measuring the thickest cranio-caudal portion of the tibiotarsal joint using a metric caliper. In most cases, the baseline (0 dpi) values were subtracted from weekly measurements to determine the increase in ankle diameter [78]. In two experiments (Fig 6.1&2), ankle diameter was only taken at sacrifice. After sacrifice, one ankle from each mouse was harvested for histological staining. Histology samples were preserved in formalin and submitted to the University of Missouri Veterinary Medicine Diagnostic Lab (VMDL) for hematoxylin and eosin (H&E) staining. Sections were scored for arthritis severity on a scale of 0 to 4 as described [79]. Briefly, a score of 0 represents no evident inflammatory cells, 1 represents 1-10% inflammatory cells, 2 represents 11-25%, 3 represents 26-50% and 4 represents inflammation involving more than 50% of the section. Sections were scored in a double-blind manner by two trained individuals and the average score of each sample was plotted.

Tissue harvest and processing for flow cytometry

Ankles: Following sacrifice, ankle joints were completely degloved, excess muscle was trimmed, and samples were cut at the knee to avoid bone marrow exposure and/or contamination. Harvested joints were digested in collagenase/dispase with DNase I, rocking for 1 hr at room temperature (RT). After incubation, ankles were shredded with rat-tooth forceps, taking special care to disarticulate the ankle joint without breaking the bone. Cells were then strained through a 70 μm filter before being washed and stained for flow cytometry.

Knees: To avoid contaminating samples with bone marrow cells, bones were not cut around the knee, but instead the femur was disarticulated from the hip and the tibia from the foot, leaving the knee joint intact. Muscle was cut off halfway down each bone so that the only tissue left surrounded the knee. As with ankles, knees were incubated in collagenase/dispase with DNase I for 1 hr and then shredded with forceps, disarticulating the knee joint. Cells were strained from the shredded tissue, washed, and stained for flow cytometry.

Blood: Blood was collected via cardiac puncture and temporarily stored in EDTA to prevent coagulation (purple-top blood collection tube). Red blood cells (RBCs) were removed using two rounds of ACK lysis buffer and remaining cells were washed and stained for flow cytometry.

Lungs: To avoid contaminating lung tissue samples with circulating leukocytes, sacrificed animals were first perfused of blood with 10ml of sterile PBS. Then the lobes of the lung, except for the left lobe, were taken from the mouse, cut into small pieces, and incubated in collagenase IV (500 units) with DNase for 1 hr. Lung pieces were then ground on a cell strainer using a syringe plunger, washed, and stained for flow cytometry.

Bone marrow: Bone marrow was harvested from the tibias and femurs of each mouse, washed, and stained for flow cytometry.

For all tissues coming from *in vivo*-stained mice, samples were processed in a dark biosafety cabinet to protect against photobleaching.

Cell staining for flow cytometry

Single cell suspensions from either *in vivo* or *in vitro* samples were stained for flow cytometry as described [80]. About $5x10^5$ cells were incubated in a 96-well U-bottom plate with Fc block (anti-CD16/CD32; eBioscience) then surface-stained as indicated with the following antibodies: CD45.2 PE, F4/80 APC, Ly-6G PE-Cy7, and Ly-6C FITC from eBioscience or CD11b Pacific Blue™ from BioLegend. Cells were washed and fixed in 4% paraformaldehyde. For each sample, 50,000 events were analyzed using a BD LSRFortessa X-20 flow cytometer and data analysis was performed using FlowJo 10.8.1 software.

Measuring B. burgdorferi *loads*

Harvested ankles were flash frozen in liquid nitrogen and homogenized with a hammer. DNA was then isolated using TRIzol reagent (Invitrogen) according to manufacturer's specifications, followed by an ethanol precipitation step for DNA cleanup as needed. qPCR was performed using Power SYBR Green PCR Master Mix (Applied Biosystems) and results for *B. burgdorferi* flagellin (*flaB*) expression were normalized to mouse nidogen (*Nid1*) and reported as copies of *flaB* per 1000 copies of *Nid1* [79].

Determination of serum antibody levels

Blood was collected from experimental mice using cardiac puncture and serum was separated by gravity. *Bb*-specific IgM and IgG levels in the sera of infected

mice were then determined by enzyme-linked immunosorbent assay, as described [26].

RNA isolation, cDNA generation, and qPCR

RNA from ankle tissue was isolated using TRIzol reagent according to manufacturer's specifications (Invitrogen). RNA from *in vitro* cultures was isolated using a Qiagen RNeasy kit. cDNA was synthesized using a High-Capacity cDNA Reverse Transcription Kit (Applied Biosystems). qPCR was performed using Power SYBR Green PCR Master Mix and target gene expression was calculated by -ΔΔCt compared to housekeeping genes *Nid1* for tissue samples or *Gapdh* for *in vitro* experiments. Relative expression was calculated as $\log_2$ fold change from D0 (uninfected) tissue samples or unstimulated BMDM. Primers used are listed in Table 2.1. Alternatively, samples were run on a Mouse Inflammatory Cytokines & Receptors PCR Array from Qiagen (PAM-011Z). *Gapdh* was also used as the housekeeping gene for this PCR array.

Bone marrow-derived macrophage (BMDM) generation

Bone marrow was isolated from mouse tibias and femurs and allowed to differentiate for 6 days in DMEM supplemented with 30% L929 cell-conditioned medium, 10% FBS and 1% penicillin/streptomycin (P/S) at 37°C in 5% CO_2, with media replacement on day 3. Adherent cells were scraped, washed, and plated to adhere overnight at 37°C in 5% CO_2 before use. $1x10^6$ BMDM/well were used

Table 2.1. List of primer sequences used for qPCR.

Gene	Primer sequence	
B. burgdorferi flaB	F	5'- TCT TTT CTC TGG TGA GGG AGC T- 3'
	R	5'- TCC TTC CTG TTG AAC ACC CTC T- 3'
Mouse *Nid1*	F	5'- AGG GCA GAA TGC CTG AAC C- 3'
	R	5'- AGG ATA CTG GAG CCC TTC GAG- 3'
Mouse *Alox15*	F	5'- GCG ACG CTG CCC AAT CCT AAT C- 3'
	R	5'- CAT ATG GCC ACG CTG TTT TCT ACC- 3'
Mouse *Gapdh*	F	5'- GTG GAC CTC ATG GCC TAC AT- 3'
	R	5'- GGG TGC AGC GAA CTT TAT TG- 3'
Mouse *mFpr2*	F	5'- CTG AAT GGA TCA GAA GTG GTG G- 3'
	R	5'- CCC AAA TCA CTA GTC CAT TGC C- 3'
Mouse *Ptges*	F	5'- GAG CCC ACC GCA ACG ACA TG- 3'
	R	5'- CAG ATG GTG GGC CAC CTC CC- 3'

in experiments measuring transcript or eicosanoid production and $2.5x10^5$ BMDM/well were used in efferocytosis experiments.

Bone marrow neutrophil (BMN) isolation and apoptosis

Bone marrow was isolated from mouse tibias and femurs and enriched for neutrophils by separation on a 2-step Histopaque gradient (1.119 g/ml and 1.083 g/ml; MilliporeSigma) at 700x*g* for 30 minutes at RT as described [81]. RBC contamination was eliminated using ACK lysis buffer. Cells were then resuspended in RPMI 1640 with 10% FBS and 1% P/S, plated, and incubated for 24 hr at 37°C in 5% CO_2 to allow spontaneous apoptosis. Apoptosis was determined using the PE Annexin V Apoptosis Detection Kit I (BD Biosciences).

Efferocytosis assay

BMN were harvested as described above, labeled with CellTrace Far Red Cell Proliferation Kit (APC-Cy7) (ThermoFisher Scientific), and rested for 24 hours at 37°C in 5% CO_2 to allow spontaneous apoptosis. Labeled apoptotic BMN (AN) were added to BMDM (2:1) and incubated for 4 hr at 37°C in 5% CO_2. Cells were then washed and stained with CD45.2 PE and F4/80 APC for flow cytometry with 50,000 events collected per sample. Efferocytosis was determined to have occurred in cells which were $CD45.2^+F4/80^+APC\text{-}Cy7^+$.

Lipid quantification

WT, 12/15-LO$^{-/-}$, or mPGES-1$^{-/-}$ BMDM were cultured with or without *B. burgdorferi* (MOI 10) for 2 hours, after which supernatant was harvested and run on a LXA_4 EIA kit (Cayman Chemical).

Exogenous LXA_4 administration

WT C3H mice were treated intraperitoneally (i.p.) with 100µl of either vehicle control (10% EtOH in PBS) or 1µg LXA_4 (Cayman Chemical) [82, 83] in PBS on 18, 19, and 20 dpi.

Exogenous PGE_2 administration

mPGES-1$^{-/-}$ C3H mice were treated i.p. with 100µl vehicle control (10% EtOH in PBS) or 100µg PGE_2 (Cayman Chemical) in sterile PBS on either 7, 8, and 9 dpi or 18, 19, and 20 dpi.

In vivo *staining*

As adapted from previous methodology [84], mice were injected with 2µg biotinylated anti-Ly-6G or anti-CD4 monoclonal antibody (mAb) in 100µL sterile PBS via tail vein (intravenous, i.v.). Immediately afterwards, 0.1µg of Alexa Fluor 647-tagged streptavidin (AF647-SA) was delivered in 10µL sterile PBS into the knee joint through the patellar tendon. Visualization of the patellar tendon was made easier by removal of hair over the joint.

Experimental sleep fragmentation

Animals undergoing experimental sleep fragmentation (SF) were kept in custom SF housing units in which a mechanical bar sweeps just above the cage floor from one side to another. In these experiments, the bar swept across the cage once every two minutes (30 sweeps/hour) for 12 hours during the light period (6am to 6pm). This mechanism is nearly silent and helps to reduce handling stress in mice by automating SF conditions [85]. These experiments were performed with sleep experts Drs. David Gozal and Abdelnaby Khalyfa in the University of Missouri School of Medicine, so they oversaw the experimental sleep fragmentation aspect of these experiments.

Statistics

Data is presented as mean +/- standard deviation unless otherwise indicated. When representative data from two experiments is shown, it is noted in the figure legend. Data consisting of two parametric groups were compared using an unpaired, two-tailed Student's t test. Significance among three or more parametric groups was assessed by one-way ANOVA with Tukey's post-test unless the groups were all compared to a single control, in which case Dunnett's test was used. Statistical significance of histology scores was determined by a nonparametric Mann-Whitney U test if between two groups and by a Kruskal-Wallis one-way ANOVA if between three or more groups. Significance was set at $p<0.05$ for all tests.

CHAPTER 3

12/15-LO IS REQUIRED FOR EFFICIENT INFLAMMATION RESOLUTION IN A MURINE MODEL OF LYME ARTHRITIS

Introduction

Following acute inflammation, timely resolution is required to recover homeostasis and prevent further tissue damage. To promote the switch to a pro-resolution program, several endogenous mediators are released at the site of inflammation, including metabolites downstream of 12/15-LO such as lipoxins and specialized pro-resolving mediators (SPM). These lipids support inflammation resolution through a variety of mechanisms, including inhibition of inflammatory leukocyte recruitment, induction of neutrophil apoptosis and efferocytosis, and reprogramming of macrophages towards a pro-resolving phenotype [63]. Previous studies demonstrate a clear role for lipoxins and SPM in regulating inflammation in degenerative or autoimmune arthritis in humans and in mouse models of arthritis [86]. Studies in RA patients demonstrated that lower levels of circulating SPM could clearly distinguish active RA patients from healthy controls, indicating a correlation between SPM expression and disease status [87, 88]. Further, elevated synovial 15-LO expression in active RA patients [89] was positively correlated with upstream PGE_2 signaling and downstream LXA_4 production in synovial fluid [90], implicating LXA_4 as a negative feedback mechanism for proinflammatory mediator production in RA. In mice, 12/15-LO deficiency resulted in exacerbated arthritis in the K/BxN serum transfer arthritis

model, with increased proinflammatory gene expression and reduced LXA_4 levels in affected joints [91]. Using this same model, prophylactic treatment with 17*R*-resolvin D1 or resolvin D3 improved arthritis clinical scores, reduced edema, and inhibited leukocyte migration [87, 92]. Similarly, treatment with exogenous LXA_4 promoted resolution in a zymosan-induced arthritis model by reducing edema formation and joint leukocyte infiltration [93]. These studies reveal a critical role for 12/15-LO products in the resolution of joint inflammation and demonstrate that treatment with lipoxins or SPM may improve arthritis outcomes.

In the murine model of Lyme arthritis (mLA), arthritis-susceptible C3H/HeJ mice [66] infected with *B. burgdorferi* develop an inflammatory arthritis characterized by robust inflammatory cell infiltrate and synovial hyperplasia in the tibiotarsal joint, followed by spontaneous resolution starting around three to four weeks post-infection [67]. While mLA resolution correlates with antibody-mediated spirochete clearance from the joint [94], disruption of eicosanoid production or signaling has adverse effects on mLA resolution despite sufficient bacterial control, mimicking postinfectious LA in humans [71-73]. Indeed, we previously demonstrated that pharmacological inhibition or genetic deletion of eicosanoid metabolic enzymes COX-2 or 5-LO resulted in defective mLA resolution with persistent immune infiltrate [71, 72]. A potential shared mechanism behind the resolution defects in these knockout mice strains lies in the ability of these enzymes and their metabolites to either cooperate with or regulate the enzyme 12/15-LO to promote the synthesis of LXA_4 and other SPM [49, 57, 95, 96].

Therefore, a breakdown in 12/15-LO induction or activity prevents production of these pro-resolution lipid metabolites and may contribute to the mLA resolution defects seen in COX-2$^{-/-}$ and 5-LO$^{-/-}$ mice.

The impact of 12/15-LO products on LA pathogenesis has not yet been investigated in human patients or in mouse models of Lyme arthritis. This represents a substantial gap given (1) the presentation of inflammatory arthritis despite no evidence of infection in patients with pLA [24], (2) our previous findings that eicosanoids play a critical role in inflammation resolution in mLA [71-73], and (3) the known ability of pro-resolving lipids downstream of 12/15-LO to ameliorate inflammation in other models of disease, including arthritis [86]. Therefore, we designed this study to examine the contribution of 12/15-LO to the development and resolution of mLA and investigate the therapeutic capacity of 12/15-LO metabolite LXA_4 to improve arthritis outcomes.

Results

mLA resolution is defective in C3H 12/15-LO$^{-/-}$ mice

LXA_4 and SPM are metabolites of 12/15-LO activity that are well-characterized for their ability to mediate resolution in various models of inflammation, including arthritis [86]. We first characterized the expression of *Alox15*, the gene which encodes 12/15-LO in mice, during the time course of mLA. We found that *Alox15* transcript was significantly upregulated in ankle joints of *Bb*-infected mice at 28 dpi compared to baseline (0 dpi; Fig 3.1). The timing of this increase suggested a

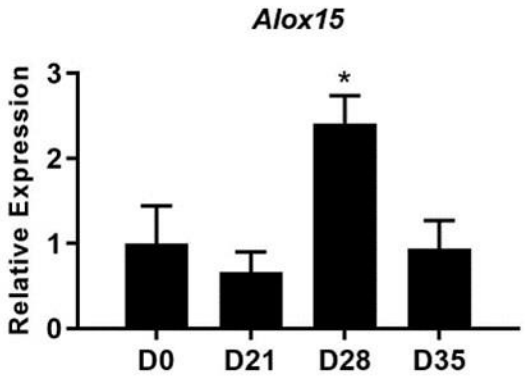

Figure 3.1. Expression of *Alox15* mRNA over the time course of mLA.

WT C3H mice were infected with *Bb* and groups of mice were sacrificed on the indicated days. *Alox15* transcript in ankle joints was quantified by RT-qPCR, normalized to *Nid1*, and reported relative to D0 (uninfected) levels. n=10/group. *p<0.05 by one way-ANOVA with Dunnett's test, compared to D0.

role for 12/15-LO metabolites in the resolution of mLA and we hypothesized that 12/15-LO activity would be required for efficient arthritis resolution. To test this hypothesis, we infected arthritis-susceptible C3H WT and 12/15-LO$^{-/-}$ mice with *Bb* and followed arthritis progression. We found that 12/15-LO-deficiency did not affect arthritis development but did impact arthritis resolution. Ankle swelling was similar between the two strains up to 14 dpi, which was near the peak of ankle swelling in WT mice. In the 12/15-LO$^{-/-}$ mice, ankle edema remained significantly higher throughout the remaining time course (35 dpi) while joint swelling in the WT mice receded (Fig 3.2A). Comparing arthritis severity scores at specific time points, WT and 12/15-LO$^{-/-}$ scores were similar at 21 dpi, again suggesting that the development of arthritis was similar between the two mouse strains (Fig 3.2B). On 28 and 35 dpi, however, severity scores in the 12/15-LO$^{-/-}$ joints were significantly higher than WT. This is readily apparent in the representative histology images from 35 dpi (Fig 3.2C). On 60 dpi there were no significant differences in severity scores between the mouse strains although the 12/15-LO$^{-/-}$ scores remained higher even at this late time point. When looking at the severity scores over time it is clear inflammation in the WT mice began to resolve after 21 dpi while resolution was significantly delayed in the 12/15-LO$^{-/-}$ joints.

Humoral immune response and control of joint spirochete loads

In C3H mice, Lyme arthritis resolution is correlated with spirochete clearance from the ankle joints [94].Therefore, we sought to determine if the defect in efficient arthritis resolution in 12/15-LO$^{-/-}$ mice could be the result of a compromised humoral immune response and poor spirochete clearance from

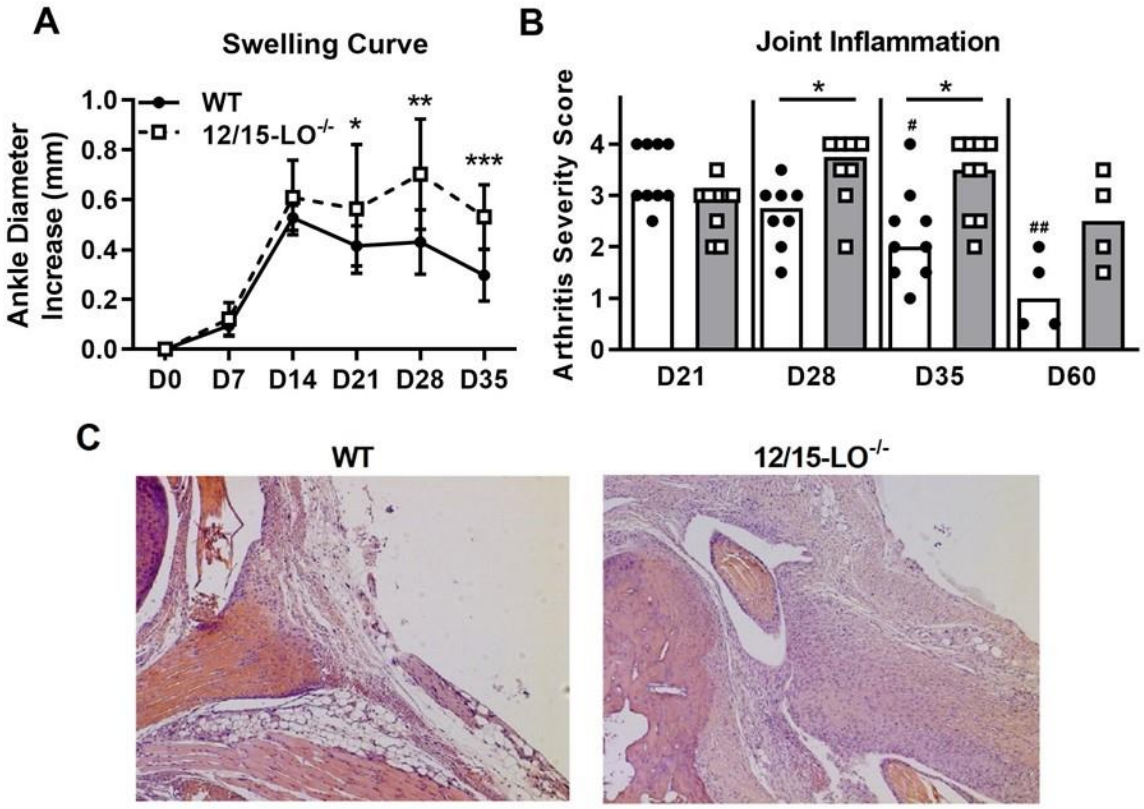

Figure 3.2. 12/15-LO$^{-/-}$ C3H mice display defective mLA resolution.

C3H WT and 12/15-LO$^{-/-}$ mice were infected with *Bb* and mLA was followed over time. (A) Ankle swelling curve throughout mLA displayed as diameter change from D0 (uninfected). n=10/group. *p<0.05, **p<0.01, ***p<0.001 by t-test between strains per timepoint. (B) Arthritis severity scores as determined by histological analysis of H&E-stained ankle joints (scale 0-4) from mice sacrificed on the indicated days. Bars represent median values. n=4-9/group. Data from two experiments were combined to increase the n value for D21, D28, and D35 groups. *p<0.05 by Mann-Whitney U test. $^{\#}$p<0.05, $^{\#\#}$p<0.01, by Kruskal-Wallis test with Dunnett's test compared to D21 of the respective strain. (C) Representative histology from WT and 12/15-LO$^{-/-}$ ankles at D35. Pictures are of the same general location and orientation of the joint. Data in A is representative of two experiments.

joint tissues. Since antibodies are an important component of spirochete clearance [94], we collected serum from WT and 12/15-LO$^{-/-}$ mice throughout the time course of mLA and measured *Bb*-specific antibody levels. As shown in Fig 3.3A, 12/15-LO$^{-/-}$ mice successfully mounted a humoral response to *Bb* infection and produced levels of *Borrelia*-specific IgM no different than WT mice. 12/15-LO$^{-/-}$ mice also produced significantly higher levels of *Borrelia*-specific IgG at 21 dpi compared to WT, but IgG levels were not different at later time points (Fig 3.3B). Lastly, we confirmed that the anti-*Bb* response mounted by 12/15-LO$^{-/-}$ mice was sufficient to control *Bb* growth in infected ankles to a similar extent as in WT mice (Fig 3.3C). These data suggest 12/15-LO activity has little effect on the development of an anti-*Borrelia* humoral response and that a defect in *Bb* clearance from the infected joints is not driving the non-resolution of arthritis in the 12/15-LO$^{-/-}$ mice.

12/15-LO$^{-/-}$ mice have persistent immune cell infiltrate during late mLA

As shown in representative histology (Fig 3.2C), we observed that 12/15-LO$^{-/-}$ mice had elevated cellular infiltrate in arthritic ankles at 35 dpi, even as cellular infiltrate decreased over time in WT mice. We used flow cytometry to quantify innate immune cell infiltrates present in ankles during arthritis progression in 12/15-LO$^{-/-}$ and WT mice (Fig 3.4A&B). Macrophage (CD45.2^{+}F4/80^{+}) and neutrophil (CD45.2^{+}Ly-6G^{hi}) populations in ankle tissue peaked around 21 dpi and then significantly declined throughout the remaining time course in WT mice. However, in 12/15-LO$^{-/-}$ mice, both macrophage and neutrophil populations in the

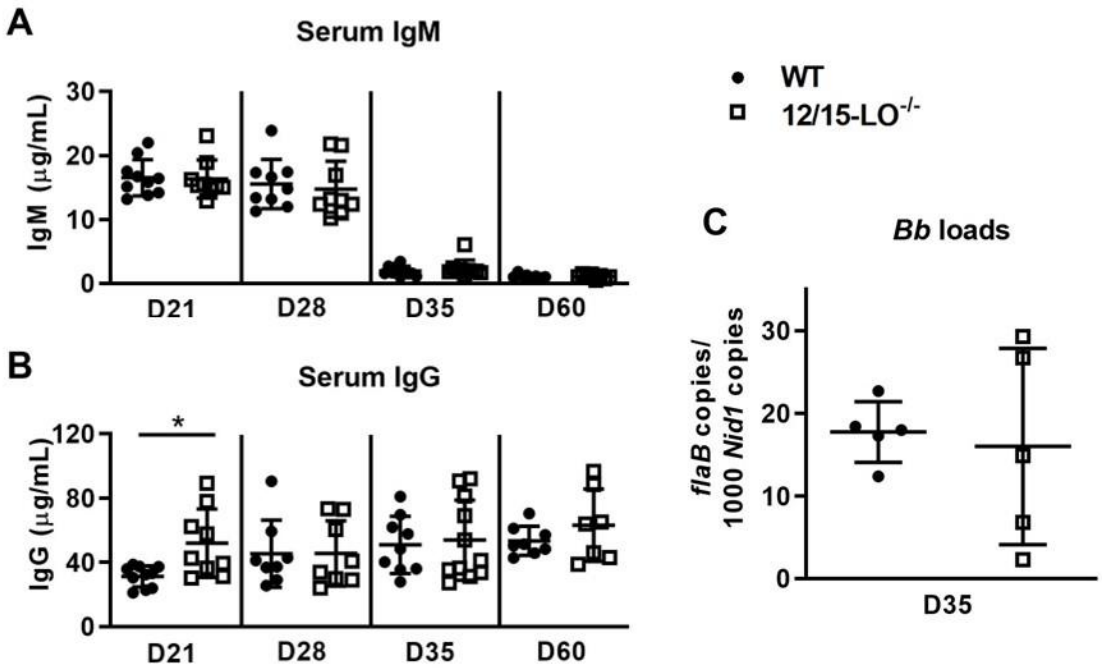

Figure 3.3. 12/15-LO deficiency does not affect the anti-*Borrelia* antibody response.

C3H WT and 12/15-LO$^{-/-}$ mice were infected with *Bb* and sacrificed on the indicated dpi. Blood was collected and *Bb*-specific serum IgM (A) and IgG (B) levels were determined by ELISA. n=7-10/group. *p<0.05 by t-test between strains per timepoint. (C) *Bb* loads in ankles at D35 by qPCR. n=5/group.

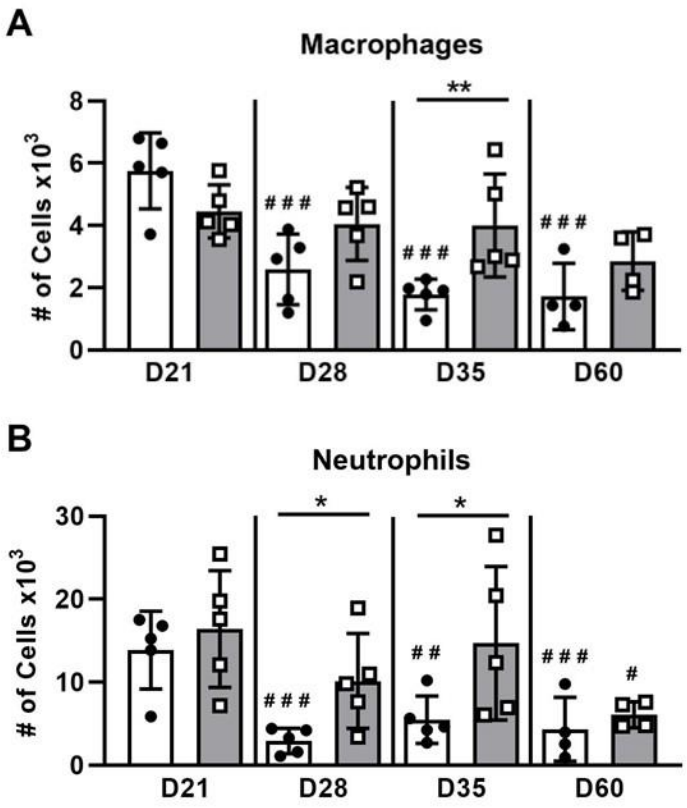

Figure 3.4. Late-phase mLA in 12/15-LO$^{-/-}$ mice is characterized by delayed clearance of innate immune cells from ankle joints.

Cells from ankle joints were isolated over the time course of mLA and (A) macrophage (CD45.2^{+}F4/80^{+}) and (B) neutrophil (CD45.2^{+}Ly-6G^{hi}) populations were quantified by flow cytometry. n=4-5/group. *p<0.05, **p<0.01 by t-test between strains per timepoint. $^{\#}$p<0.05, $^{\#\#}$p<0.01, $^{\#\#\#}$p<0.001 by one-way ANOVA with Dunnett's test compared to D21 of the respective strain.

ankle joint were maintained near peak levels, demonstrating a failure of resolution in these animals. Macrophage numbers were significantly higher in 12/15-LO$^{-/-}$ mice compared to WT mice at 35 dpi (Fig 3.4A). Similarly, neutrophil numbers were significantly higher in 12/15-LO$^{-/-}$ mice than WT mice at both 28 and 35 dpi (Fig 3.4B). By 60 dpi, macrophage and neutrophil levels in ankle joints of 12/15-LO$^{-/-}$ mice were not different from WT mice. Together, these results demonstrate a significant delay in the clearance of these innate populations in 12/15-LO$^{-/-}$ mice.

Defective efferocytosis of apoptotic 12/15-LO$^{-/-}$ neutrophils

Efferocytic clearance of apoptotic cells is a critical component of inflammation resolution via both the timely removal of apoptotic cells to prevent secondary necrosis and the reprogramming of efferocytosing macrophages toward a pro-resolving phenotype [62]. As LXA_4 and several SPM can promote efferocytosis [59, 61], we hypothesized that clearance of apoptotic neutrophils from joints in 12/15-LO$^{-/-}$ mice could be defective and contribute to the resolution defect seen in these mice. Using a reciprocal assay approach, we tested the ability of WT and 12/15-LO$^{-/-}$ BMDM to clear WT or 12/15-LO$^{-/-}$ apoptotic neutrophils (AN). Regardless of BMDM strain, a significantly smaller proportion of BMDMs were able to efferocytose 12/15-LO$^{-/-}$ versus WT AN (Fig 3.5A), suggesting there is an intrinsic difference in 12/15-LO$^{-/-}$ AN that may prevent their efficient clearance from inflammatory sites. We next determined if the lack of 12/15-LO in neutrophils altered their ability to undergo apoptosis and whether this was

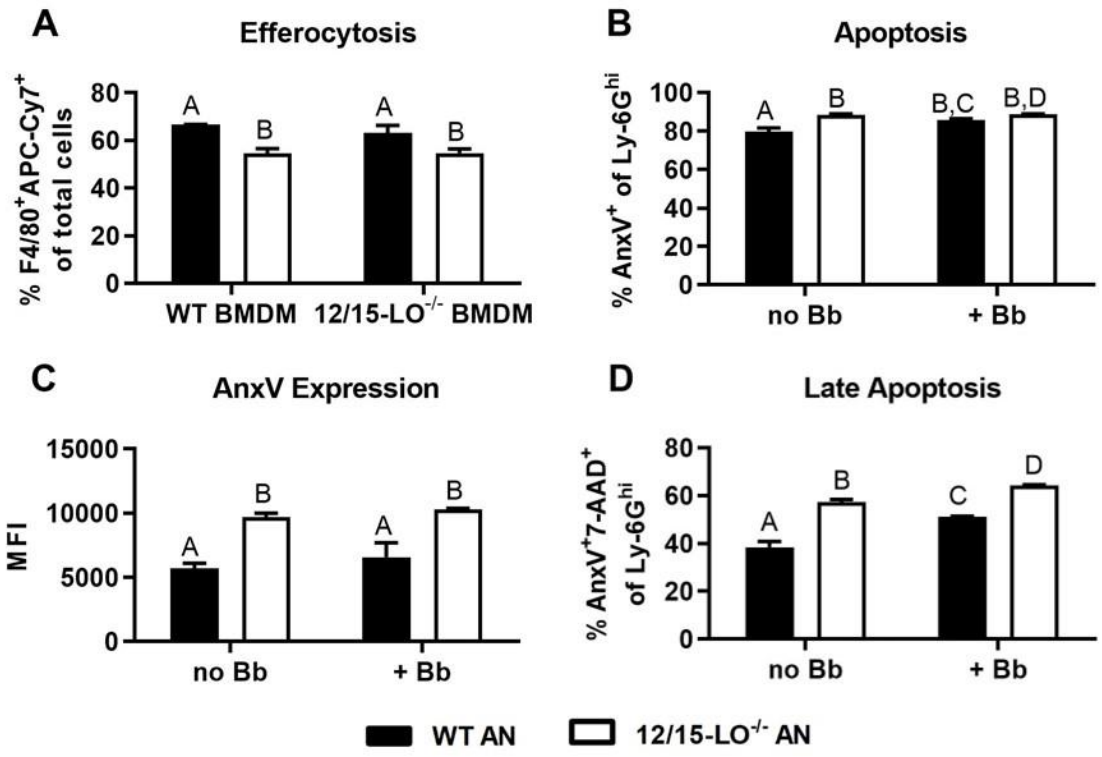

Figure 3.5. Apoptosis and efferocytosis in 12/15-LO$^{-/-}$ bone marrow neutrophils and macrophages.

Bone marrow neutrophils (BMN) were isolated and cultured for 24hr to induce apoptosis. (A) Untreated APC-Cy7-stained apoptotic BMN (AN), either WT (black bars) or 12/15-LO$^{-/-}$ (white bars), were cultured with WT or 12/15-LO$^{-/-}$ BMDM (2:1) for 4hr, and efferocytosis, defined as F4/80^{+}APC-Cy7^{+} cells, was determined by flow cytometry. Apoptosis of WT and 12/15-LO$^{-/-}$ in 24hr culture +/- *Bb* (MOI 10) was measured by proportion (B) and MFI (C) of AnxV expression. (D) Late-stage apoptosis in cultures from B&C as measured by AnxV and 7-AAD co-staining. n=3/group, assayed in duplicate. Columns with different letters are significantly different by $p<0.05$ by one-way ANOVA with Tukey's test.

impacted by the presence of *Bb* in the culture. Following 24hr in culture, BMN from 12/15-LO$^{-/-}$ mice had a significantly higher percentage of annexin V (AnxV)-expressing cells regardless of the presence of *Bb* (Fig 3.5B). In addition, 12/15-LO$^{-/-}$ BMN also expressed significantly higher levels of annexin V than WT BMN as determined by flow cytometry, again regardless of the presence of *Bb* in the cultures (Fig 3.5C). Inefficient clearance of apoptotic cells may increase the number of cells in late-stage apoptosis which may progress into secondary necrosis and prolong inflammation [97]. When WT and 12/15-LO$^{-/-}$ AN were co-stained with 7-AAD as a measure of membrane damage, a higher proportion of 12/15-LO$^{-/-}$ AN than WT AN were AnxV^{+}7-AAD^{+}, indicating necrosis (Fig 3.5D). The presence of *Bb* in the culture significantly increased the percentage of cells from both strains in apoptosis and/or post-apoptotic necrosis, indicating that the uptake of *Bb* by neutrophils may induce apoptosis. Together, these findings suggest that a failure to efficiently clear apoptotic neutrophils may contribute to the lack of arthritis resolution in 12/15-LO$^{-/-}$ mice.

B. burgdorferi *induces LXA$_4$ and mFpr2 expression by WT BMDM*

Metabolic activity by 12/15-LO results in the production of numerous pro-resolution lipid metabolites such as lipoxins, resolvins, and protectins [98]. LXA$_4$ is an AA-derived metabolite of 12/15-LO enzymatic activity that can promote resolution in other mouse models of arthritis [87, 91-93, 95]. LXA$_4$ has not previously been isolated out of mLA ankles [74] and may be technically difficult to measure out of tissue due to its rapid metabolism *in vivo* [99]. However, we have

identified high levels of its metabolic precursors, 12-HETE and 15-HETE, out of joints during mLA [74], so we sought to determine if *Bb* could stimulate LXA_4 production *in vitro*. We cultured WT BMDM with or without *Bb* (MOI 10) for 2hr and found that coculture with *Bb* induced LXA_4 production by BMDMs (Fig 3.6A). Further, transcription of the murine LXA_4 high-affinity receptor, mFpr2 [100], was significantly upregulated in WT BMDM following co-culture with *Bb* (Fig 3.6B). We also confirmed that *mFpr2* transcription is increased during mLA in C3H mice (Fig 3.6C). Together, these findings suggest that *Bb* can upregulate components of LXA_4:mFpr2 signaling, providing a rationale to investigate the ability of LXA_4:mFpr2 signaling to resolve inflammation in mLA.

Exogenous LXA_4 reduces ankle edema during mLA in WT mice

Previous studies in other murine arthritis models have had varied results when investigating the therapeutic efficacy of exogenous LXA_4. A study on zymosan-induced arthritis in mice found that LXA_4 administration ameliorated inflammation by reducing edema and leukocyte infiltration [93]. However, another study using a *S. aureus*-induced septic arthritis mouse model found that treatment with LXA_4 impaired inflammation resolution because it interfered with pathogen control [101]. Therefore, while we hypothesized that exogenous LXA_4 would ameliorate mLA in WT C3H mice, we also wanted to avoid interfering with bacterial clearance to prevent prolonged active infection and inflammation. To investigate the therapeutic capacity of exogenous LXA_4 in mLA, we infected WT C3H mice with *B. burgdorferi* to induce mLA then administered either a vehicle control (VC)

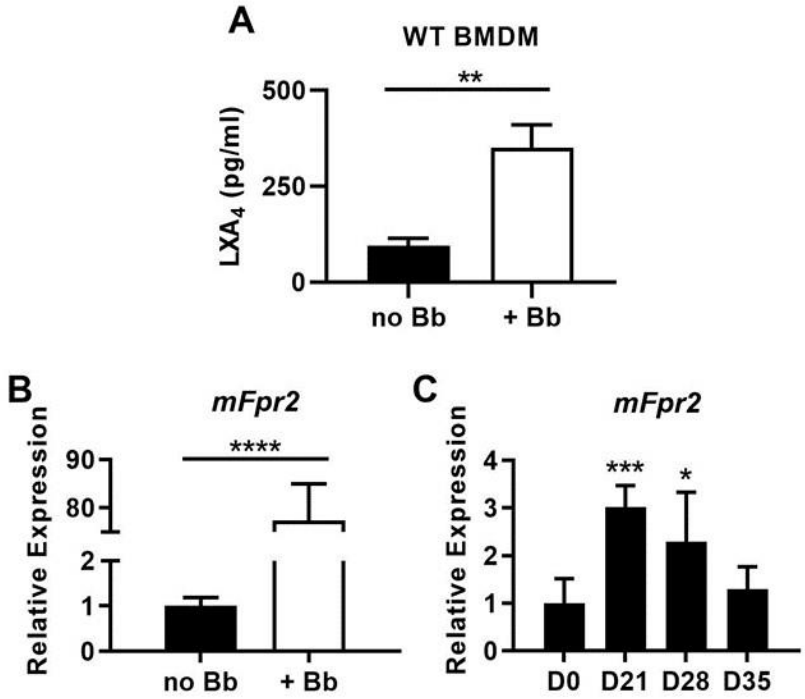

Figure 3.6. LXA_4:mFpr2 signaling axis components are upregulated in response to *B. burgdorferi*.

(A) LXA_4 production by WT BMDMs after 2hr incubation with or without *Bb* (MOI 10). (B) *mFpr2* mRNA expression by RT-qPCR after 24hr culture +/- *Bb*, normalized to *Gapdh* and relative to expression in unstimulated (no *Bb*) BMDM. (C) *mFpr2* mRNA by RT-qPCR from WT ankle joints during mLA, normalized to mouse nidogen (*Nid1*) and relative to D0 levels. (A&B) n=3/treatment, assayed in duplicate, *p<0.05, **p<0.01, ***p<0.001, ****p<0.0001 by t-test. (C) n=7-10/timepoint, one-way ANOVA with Dunnett's test, compared to D0.

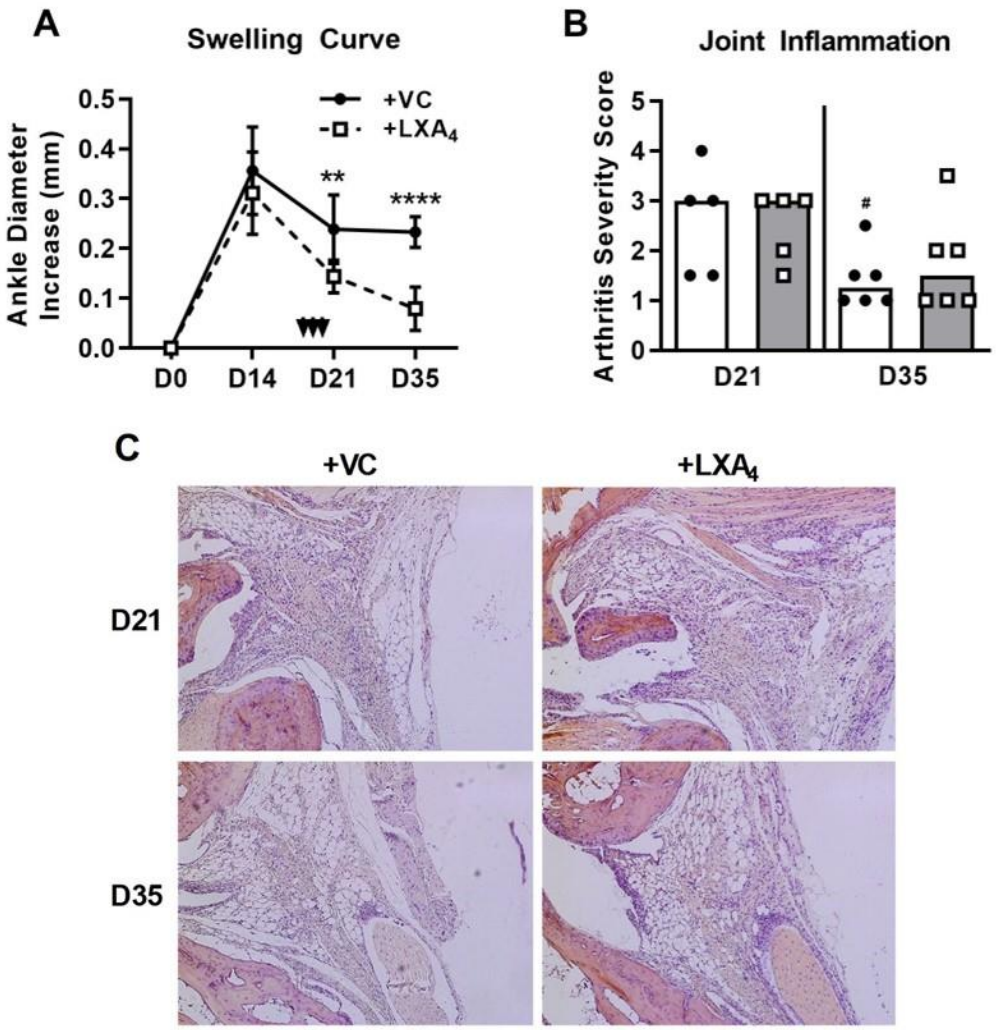

Figure 3.7. Exogenous LXA_4 treatment reduces ankle edema.

C3H WT mice were infected with *Bb* and treated with either vehicle control (VC; closed circles) or LXA_4 (open squares) i.p. on D18,19, and 20 (arrows in A). Development of mLA was followed over time. (A) Ankle diameters were measured on the days indicated. n=6/group. **p<0.01 and ****p<0.0001 by t-test between treatment groups per timepoint. (B) Arthritis severity scores of H&E-stained ankle joints from mice sacrificed on D21 and D35. Bars represent median values. n=5-6/group. $^{\#}p<0.05$ by Mann-Whitney U test between same strain on different days. Representative histology is in (C). Data from two experiments were combined to reach power in (A) and for D35 in (B).

or 1μg LXA_4 i.p. per day on 18, 19, and 20 dpi and measured resolution outcomes. As shown in Figure 3.7A, treatment with LXA_4 resulted in an acute reduction of edema compared to VC-treated mice, starting at 21 dpi and continuing through 35 dpi.

To determine if the reduction in edema in LXA_4-treated mice correlated to a decrease in inflammation at these timepoints, we performed histological scoring of ankle sections at both 21 and 35 dpi and found that VC- and LXA_4-treated mice had similar arthritis severity at both timepoints (Fig 3.7B&C). We also confirmed that LXA_4 delivery at this timepoint did not interfere with formation of an anti-*Borrelia* immune response, with both *Bb*-specific IgM and IgG successfully produced and *Bb* as efficiently cleared in VC- and LXA_4-treated mice (Fig 3.S1, Appendix I). These data demonstrate that while joint edema was significantly reduced by LXA_4 treatment, this strategy of LXA_4 delivery did not ameliorate underlying inflammatory responses by 35 dpi.

Exogenous LXA_4 alters joint cell populations towards a pro-resolving phenotype

While LXA_4 treatment did not reduce arthritis severity in WT mice, we sought to determine the effect of LXA_4 on cellular infiltrate during mLA. As before, we prepared single cell suspensions from VC- or LXA_4-treated ankles and quantified the macrophage and neutrophil populations at 21 and 35 dpi. We found no differences between the absolute number of macrophages or neutrophils in VC-

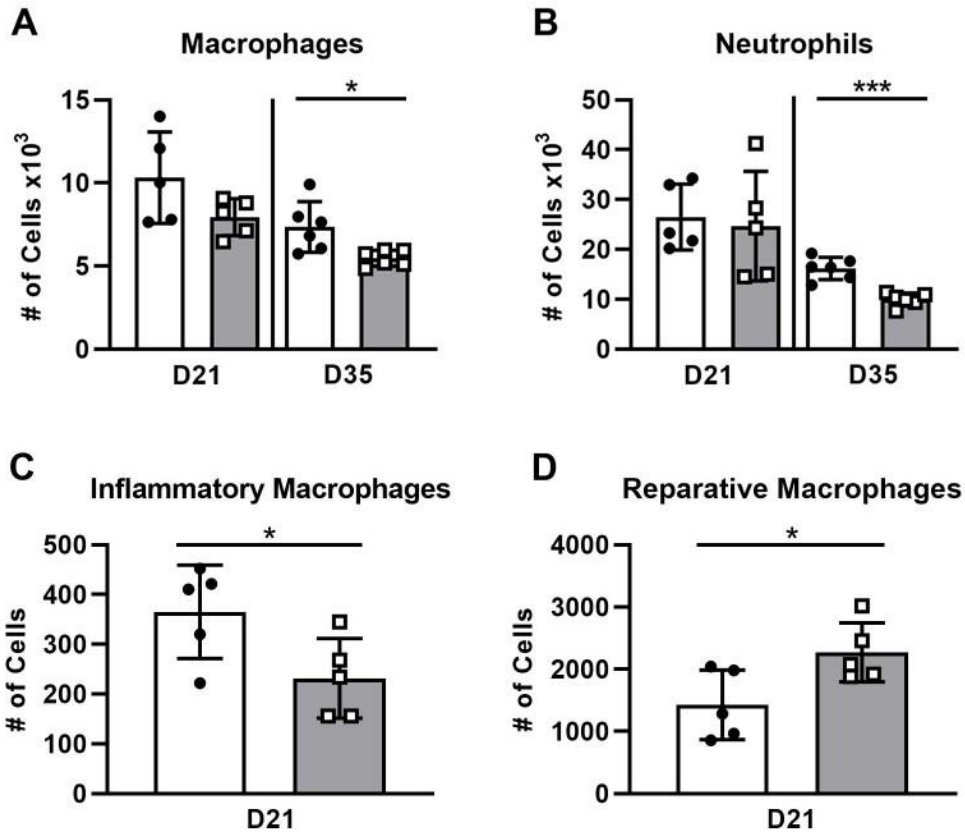

Figure 3.8. Exogenous LXA_4 treatment accelerates joint inflammatory cell removal.

C3H WT mice were infected with *Bb* and treated with either vehicle control (VC; closed circles) or LXA_4 (open squares) i.p. on D18,19, and 20. Total macrophages (A) and neutrophils (B) quantified from the ankle joints of VC- or LXA_4-treated WT mice at D21 and D35 by flow cytometry. Two macrophage subsets were further measured in D21 ankles: inflammatory macrophages (C; $CD45.2^+F4/80^+Ly\text{-}6C^{hi}$) and reparative macrophages (D; $CD45.2^+F4/80^+Ly\text{-}6C^{int/lo}$). n=5/group. *p<0.05, ***p<0.001 by t-test. Data from two experiments were combined to reach power in D35 groups (A&B).

and LXA_4-treated mice at 21 dpi, but there were significantly fewer macrophages and neutrophils in LXA_4-treated joints at 35 dpi (Fig 8A&B). Although overall macrophage numbers were not different between treatment groups at 21 dpi, we hypothesized that LXA_4 may have altered the inflammatory phenotypes of the macrophage population, since it is known to induce non-phlogistic monocyte recruitment to assist in inflammation resolution [102]. To test this hypothesis, we measured Ly-6C expression on $F4/80^+$ cells as an indication of inflammatory state, with $F4/80^+Ly\text{-}6C^{hi}$ cells categorized as inflammatory macrophages and $F4/80^+Ly\text{-}6C^{int/lo}$ cells categorized as reparative macrophages [103]. In doing so, we found that LXA_4-treated mice had significantly fewer $Ly\text{-}6C^{hi}$ inflammatory macrophages and significantly more $Ly\text{-}6C^{int/lo}$ reparative macrophages compared to VC-treated mice (Fig 3.8C&D). Together these data demonstrate that LXA_4 treatment accelerated the removal of inflammatory cells from the joints by 35 dpi and promoted a reparative macrophage phenotype.

Conclusion

To elucidate the role of 12/15-LO activity in mLA, we infected WT and $12/15\text{-}LO^{-/-}$ C3H mice with *Bb* and characterized the development and resolution of arthritis in the tibiotarsal joints. While *Bb*-infected $12/15\text{-}LO^{-/-}$ mice still developed robust arthritis, they showed a defect in efficient resolution of arthritis despite successful bacterial control. This non-resolving phenotype was characterized by persistent neutrophil and macrophage populations in the joint even as this infiltrate was cleared in WT controls. *In vitro* experiments suggested that inflammatory cell

persistence may be due to defective efferocytic removal of apoptotic 12/15-LO$^{-/-}$ neutrophils by macrophages. As *Bb* was found to upregulate components of the pro-resolving LXA_4:mFpr2 signaling axis, we sought to further investigate the contribution of 12/15-LO activity to mLA by testing the ability of 12/15-LO metabolite LXA_4 to induce arthritis resolution. Therapeutic treatment of mLA in WT C3H mice with exogenous LXA_4 around the peak of inflammation reduced edema and remodeled joint macrophage populations towards a pro-resolving phenotype. Two weeks later, macrophage and neutrophil numbers were significantly decreased in LXA_4-treated mice, though overall arthritis severity was not reduced. Together, these findings demonstrate that 12/15-LO activity is critical for efficient mLA resolution and lipoxin treatment may be efficacious to reduce joint edema without compromising bacterial clearance.

CHAPTER 4

PGE_2 IS NOT REQUIRED FOR THE DEVELOPMENT OR RESOLUTION OF MURINE LYME ARTHRITIS

Introduction

During the inflammatory response, COX-2 metabolizes AA to PGH_2, which is then converted to PGE_2 by mPGES-1. While originally described as a proinflammatory mediator, PGE_2 can play both proinflammatory and anti-inflammatory/pro-resolving roles depending on which of four G protein-coupled receptors, E prostanoid receptors EP1-4, it signals through. PGE_2 signaling through EP1 or EP3 increases intracellular calcium, a feature of the proinflammatory response [104]. PGE_2 signaling through either EP2 or EP4 increases intracellular cyclic AMP to reduce the production of proinflammatory mediators and induce the production of anti-inflammatory/pro-resolving mediators [105, 106]. PGE_2 activity, then, depends on the context of the inflammatory environment, including the prevalence and localization of its receptors.

PGE_2 has previously been characterized as predominantly proinflammatory in the context of joint inflammation during RA [107, 108]. In the collagen-induced arthritis (CIA) mouse model of RA, neither COX-$2^{-/-}$ nor mPGES-$1^{-/-}$ mice developed arthritis, demonstrating a requirement for the proinflammatory activity of mPGES-1-produced PGE_2 [109, 110]. On the other hand, one group described a potential anti-inflammatory role for PGE_2 in RA whereby PGE_2 may reduce joint

tissue damage via downregulation of MMP-1 [55]. These dual roles illustrate how the treatment of inflammation using NSAIDs to suppress COX-2 activity and PGE_2 production, while capable of reducing pain and swelling, may ultimately be detrimental to the long-term resolution of inflammation.

Contrary to findings in the CIA model of RA, we have demonstrated that COX-2 is not required for arthritis development during mLA [71]. However, pharmacological inhibition or genetic deletion of COX-2 resulted in a defect in mLA resolution out to at least 60 dpi [71, 72]. Lipidomic analysis demonstrated that PGE_2 was the most prevalent AA-derived COX-2 product during mLA, with a biphasic expression pattern peaking both early during arthritis development (7-17 dpi) and later as arthritis is resolving (28 dpi) [72]. Inhibition of COX-2 during early mLA (-1 through 14 dpi) was sufficient to prevent arthritis resolution [71], supporting a previous hypothesis that resolution programs are initiated during the development of inflammation [49]. Since PGE_2 production was at its highest during the early time period, these studies may indicate that early PGE_2 is required for successful inflammation resolution. Indeed, this was suggested by Levy et al., who demonstrated that early production of PGE_2 triggered class-switching from the 5-LO pathway to the 12/15-LO pathway and subsequent production of pro-resolving mediators like LXA_4 [49].

The purpose of this study, then, is to determine the contribution of mPGES-1-produced PGE_2 to inflammation resolution in mLA. Our overall hypothesis is that

PGE_2, due to its characterization as a potent mediator of inflammation and the finding that it is a predominant metabolite in WT ankles during mLA, is at least partially responsible for the non-resolving mLA phenotype seen in COX-$2^{-/-}$ mice. However, COX-$2^{-/-}$ mice have not only reduced PGE_2 synthesis but limited production of all prostanoids, so we will use mPGES-$1^{-/-}$ mice to delineate the specific contribution of PGE_2 to mLA pathogenesis.

Results

mPGES-$1^{-/-}$ mice resolve mLA more efficiently than WT mice

PGE_2 production during mLA is biphasic, indicating a role for PGE_2 in both development and resolution of arthritis [74]. Indeed, we found that *Bb*-infected WT mice significantly induced transcription of *Ptges*, the gene encoding mPGES-1, at 28 and 35 dpi (Fig 4.1). While successful mLA induction in COX-$2^{-/-}$ mice demonstrates that PGE_2 is dispensable for arthritis development, we hypothesize that the absence of this second, resolution-phase peak of PGE_2 may contribute to the non-resolution phenotype in COX-$2^{-/-}$ mice. Therefore, we expect that, as in COX-$2^{-/-}$ mice, mPGES-$1^{-/-}$ mice will develop mLA but will be unable to efficiently resolve their arthritis.

To test this hypothesis, we infected both WT and mPGES-$1^{-/-}$ C3H mice with *Bb* and characterized the course of mLA development and resolution. We tracked ankle diameter over time and observed that mPGES-$1^{-/-}$ mice developed significantly less ankle edema by 14 dpi as compared to WT mice, and this

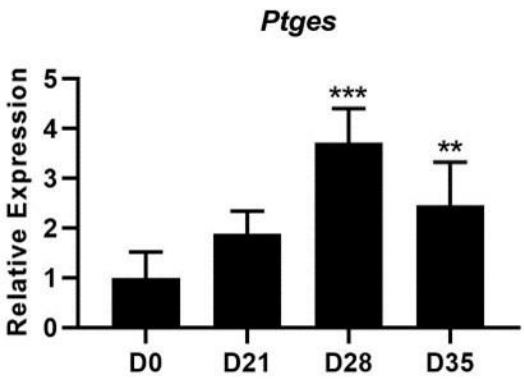

Figure 4.1. mPGES-1 transcript is upregulated at mLA resolution-phase timepoints in WT mice.

WT C3H mice were infected with *Bb* and sacrificed on the indicated days. *Ptges* transcript, encoding mPGES-1, in ankle joints was isolated, converted to cDNA, and quantified by qPCR. Data was normalized to *Nid1* and reported relative to baseline (D0) levels. n=5/group. **p<0.01, ***p<0.001 by one-way ANOVA with Dunnett's posttest, compared to D0.

difference was maintained throughout the rest of the time course (Fig 4.2A). This was not unexpected, as PGE_2 promotes edema formation by increasing vasodilation [111, 112] and vascular permeability [113]. Since swelling is not necessarily indicative of underlying pathology, we determined arthritis severity using histological scoring of H&E-stained ankle sections. At 21 dpi, arthritis severity was not different between mPGES-$1^{-/-}$ and WT mice (Fig 4.2B), confirming that PGE_2 is not required for mLA development. However, mPGES-$1^{-/-}$ mice had significantly lower arthritis severity scores when compared to WT mice at 28 and 35 dpi, indicating that the absence of PGE_2 may contribute to improved arthritis resolution (Fig 4.2B&C). Indeed, mPGES-$1^{-/-}$ mice also had significantly reduced arthritis at 35 and 60 dpi compared to the 21 dpi peak, while WT mice only had significantly reduced arthritis at 60 dpi compared to severity levels at 21 dpi (as indicated by pound signs). These findings do not support our hypothesis that PGE_2 is required for mLA resolution, but instead demonstrate that PGE_2-deficient mPGES-$1^{-/-}$ mice develop mLA and then resolve arthritic inflammation faster than WT mice.

Immune infiltrate is cleared more efficiently from the mPGES-$1^{-/-}$ joint

As shown in representative histology, mPGES-$1^{-/-}$ mice had visibly less inflammatory infiltrate in the joint than WT mice did at 35 dpi (Fig 4.2C). Therefore, we sought to determine the extent of immune infiltration into the arthritic joint in mPGES-$1^{-/-}$ mice by flow cytometry (Fig 4.3 A&B). As expected, both macrophage ($CD45.2^+F4/80^+$) and neutrophil ($CD45.2^+Ly\text{-}6G^{hi}$) populations

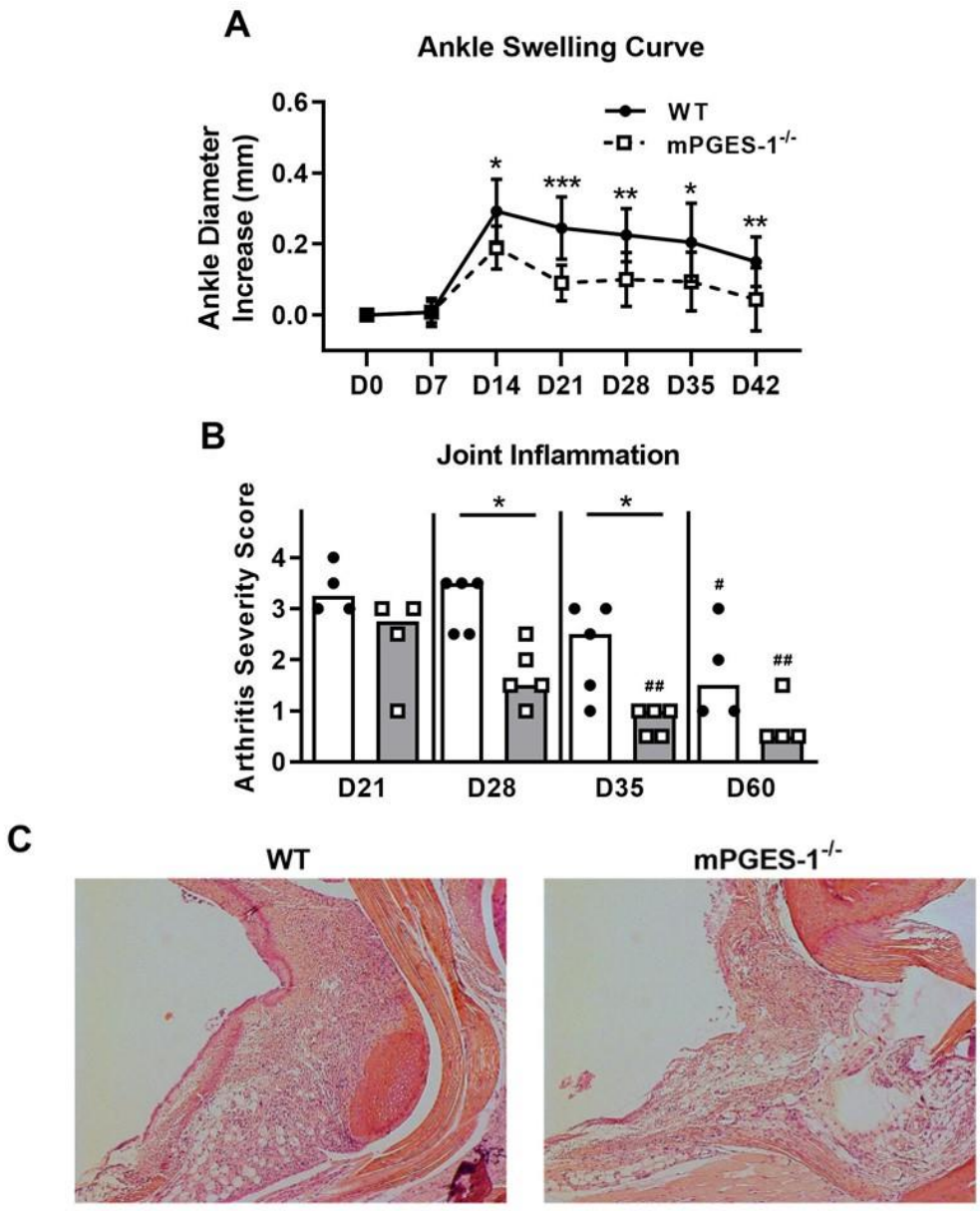

Figure 4.2. mPGES-1$^{-/-}$ mice resolve mLA more efficiently than WT mice.

WT and mPGES-1$^{-/-}$ C3H mice were infected with *Bb* and mLA progression was followed over time. (A) Ankle swelling curve throughout mLA displayed as the diameter change from baseline (D0). n=9-10/group. *p<0.05, **p<0.01, ***p<0.001 by t-test between strains per timepoint. (B) Arthritis severity scores as determined by histological scoring of H&E-stained ankle joints (scale 0-4). Closed circles represent WT and open squares represent mPGES-1$^{-/-}$ animals. Bars are at median. n=4-5/group. *p<0.05 by Mann-Whitney U test. $^{\#}$p<0.05 and $^{\#\#}$p<0.01, by Kruskal-Wallis test with Dunnett's posttest, compared to D21 of the respective strain. (C) Representative histology from WT and mPGES-1$^{-/-}$ ankles at D35. Data is representative of two independent experiments.

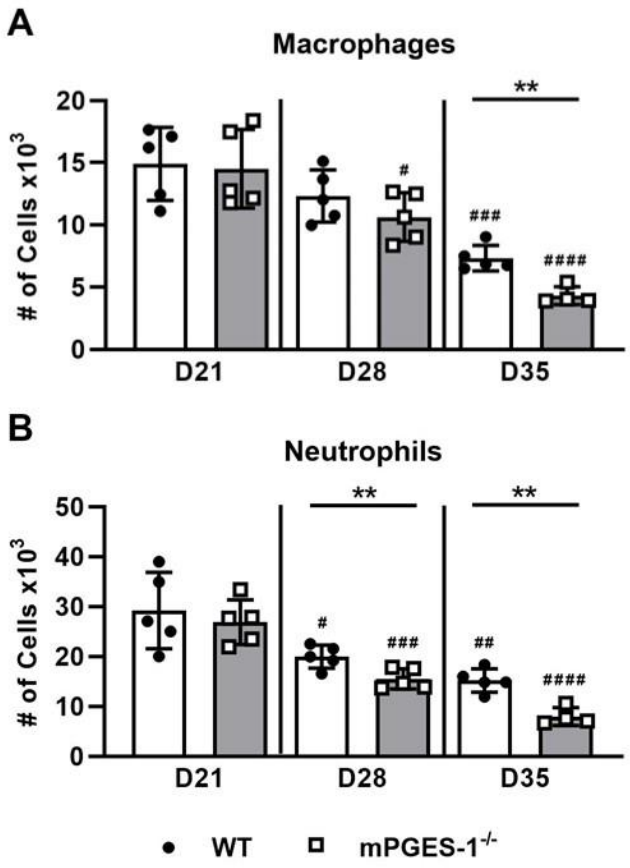

Figure 4.3. mPGES-1$^{-/-}$ mice clear inflammatory infiltrate from arthritic joints more efficiently than WT mice.

WT and mPGES-1$^{-/-}$ C3H mice were infected with *Bb* and ankles were harvested on the indicated days. (A) Macrophages (CD45.2^{+}F4/80^{+}) and (B) neutrophils (CD45.2^{+}Ly-6G^{hi}) were quantified from the joints by flow cytometry. n=4-5/group. **p<0.01 by t-test between strains per timepoint. $^{\#}$p<0.05, $^{\#\#}$p<0.01, $^{\#\#\#}$p<0.001, $^{\#\#\#\#}$p<0.0001 by one-way ANOVA with Dunnett's test compared to D21 of the respective strain. Data is representative of two independent experiments.

were highest at 21 dpi and decreased in both WT and mPGES-1$^{-/-}$ mice as arthritis resolved (as indicated by pound signs). However, while there was no significant difference between the absolute number of either macrophages or neutrophils in mPGES-1$^{-/-}$ and WT mice at 21 dpi, mPGES-1$^{-/-}$ mice had significantly fewer macrophages at 35 dpi and significantly fewer neutrophils at both 28 and 35 dpi as compared to WT controls. Anecdotally, the neutrophil population usually outnumbers the macrophage population during inflammation in our model (compare scales in Fig 4.3A&B). This trend holds even at 35 dpi in WT mice, where the ratio is approximately 2 neutrophils:1 macrophage, but in mPGES-1$^{-/-}$ mice, this ratio is closer to 1:1. This observation may indicate that infiltrating neutrophils have been more effectively cleared from the site of inflammation in mPGES-1$^{-/-}$ mice compared to WT mice. Overall, these results reflect the histological findings that mPGES-1$^{-/-}$ mice develop mLA to the same extent as WT mice, with similar levels of immune infiltrate at 21 dpi, but that mPGES-1$^{-/-}$ mice resolve arthritis more quickly, as evidenced by removal of inflammatory infiltrate from the joint.

mPGES-1$^{-/-}$ mice control B. burgdorferi *burdens more efficiently than WT mice*

mLA resolution in WT C3H mice generally coincides with the clearance of *Bb* from the arthritic joint [94], so we hypothesized that mPGES-1$^{-/-}$ mice may resolve arthritis faster because *Bb* are removed from the joint more efficiently. To test this, we measured *Bb* loads in the arthritic ankles at 35 dpi and found that

the *Bb* burden was significantly lower in mPGES-1$^{-/-}$ mice than in WT mice (Fig 4.4A). *Bb* phagocytosis is partially facilitated by anti-*Borrelia* antibody opsonization of the spirochete, which allows efficient uptake by immune cells at the infection site [114]. We characterized the development of the humoral response during mLA by quantifying anti-*Borrelia* IgM and IgG in the sera of infected WT and mPGES-1$^{-/-}$ mice and found there was no difference in the amount of *Bb*-specific IgM or IgG in the sera of mPGES-1$^{-/-}$ compared to WT mice at each time point assayed (Fig 4.4B&C). These findings suggest that improved clearance of *Bb* from arthritic joints in mPGES-1$^{-/-}$ versus WT mice is not due to altered kinetics or magnitude of anti-*Borrelia* antibody production. More studies are required to determine if *Bb* loads are lower in the joint at this timepoint due to decreased initial colonization of the joint by *Bb* or if phagocytosis of *Bb* by immune cells in the joint is enhanced in mPGES-1$^{-/-}$ mice.

***Lack of PGE_2 does not prevent LXA_4 formation and increases neutrophil apoptosis* in vitro**

We originally hypothesized that a critical part of PGE_2-mediated mLA resolution would be the ability of PGE_2 to switch eicosanoid synthesis towards the pro-resolving pathway, boosting production of SPM to aid in resolution (Chapter 3). However, after finding that PGE_2 is not required for mLA resolution, we wanted to determine to what extent PGE_2 might be required for 12/15-LO expression and LXA_4 synthesis in this model. To address this, we first measured transcription of *Alox15*, the gene encoding murine 12/15-LO, throughout mLA in WT and

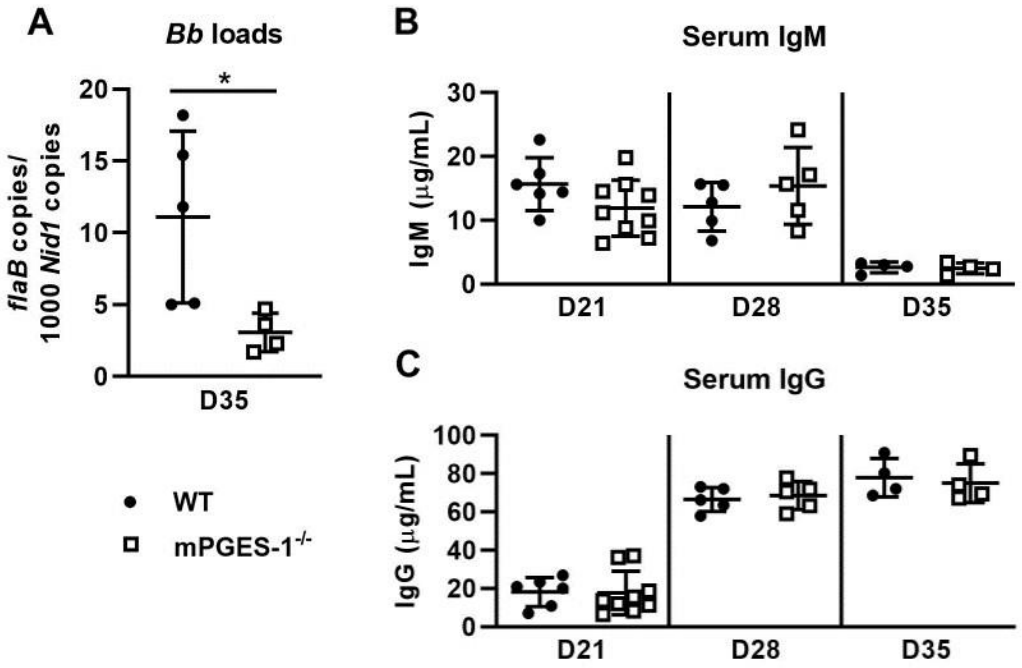

Figure 4.4. mPGES-1$^{-/-}$ mice clear *B. burgdorferi* from arthritic joints more efficiently than WT mice.

WT and mPGES-1$^{-/-}$ C3H mice infected with *Bb* were sacrificed on the indicated days. (A) *Bb* burdens in ankles at D35 by qPCR. *Bb*-specific serum IgM (B) and IgG (C) levels by ELISA. n=4-9/group. (C) n=4-5/group. *p<0.05 by t-test. Data is representative of two independent experiments.

mPGES-1$^{-/-}$ mice. We hypothesized that if PGE_2 played a significant role in inducing *Alox15* transcription, we would see a decrease in the *Alox15* transcript in mPGES-1$^{-/-}$ mice. However, we found that, as in WT mice, mPGES-1$^{-/-}$ mice significantly upregulate *Alox15* transcription at 28 dpi, and this relative expression is not different between the two strains (Fig 4.5A). There is significantly lower relative expression of *Alox15* in mPGES-1$^{-/-}$ versus WT mice at 35 dpi, but this may be because mPGES-1$^{-/-}$ mice have almost completely resolved their arthritis at this timepoint and may have no more need for 12/15-LO transcription. These results indicate that another mediator may be inducing *Alox15* transcription during mLA.

Since *Alox15* transcription is similar during mLA in WT and mPGES-1$^{-/-}$ mice, we sought to determine whether mPGES-1$^{-/-}$ BMDM could still produce LXA_4 by culturing mPGES-1$^{-/-}$ BMDM with or without *Bb* (MOI 10) for two hours and measuring LXA_4 in the supernatant. Using this approach, we observed that mPGES-1$^{-/-}$ BMDMs had significantly increased LXA_4 production following *Bb* stimulation compared to unstimulated controls (Fig 4.5B). Further, mPGES-1$^{-/-}$ BMDMs produced similar levels of LXA_4 to WT BMDM after *Bb* stimulation, and addition of exogenous PGE_2 (10nM) did not significantly increase LXA_4 synthesis in either WT or mPGES-1$^{-/-}$ BMDM, regardless of *Bb* stimulus (data not shown). Together, the data from Figures 4.5A&B suggest that 12/15-LO-mediated synthesis of LXA_4 and SPM may still be intact during mLA in mPGES-1$^{-/-}$ mice.

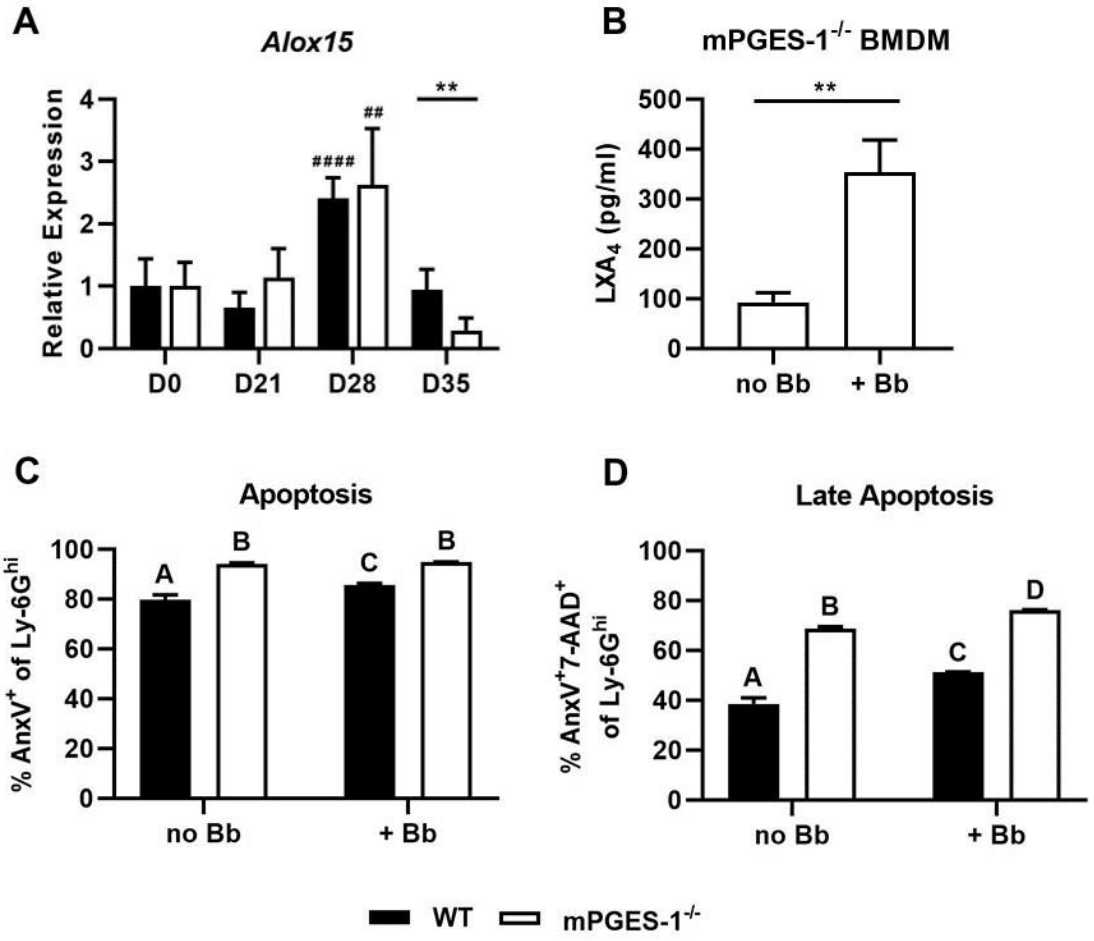

Figure 4.5. Lack of PGE_2 does not prevent LXA_4 formation and increases neutrophil apoptosis *in vitro*.

WT and mPGES-$1^{-/-}$ C3H mice were infected with *Bb* and transcription of *Alox15*, the gene encoding 12/15-LO in mice, was quantified over time by qPCR. Data was normalized to *Nid1* expression and reported relative to D0 expression of same strain. n=5/group. **p<0.01 by t-test. $^{\#\#}$p<0.01 by one-way ANOVA with Dunnett's posttest compared to D0 of the respective strain. (B) LXA_4 production by mPGES-$1^{-/-}$ BMDMs after 2hr incubation +/- *Bb* (MOI 10). n=3/group. **p<0.01 by t-test. (C) Apoptosis of WT and mPGES-$1^{-/-}$ BMN in 24hr culture +/- *Bb* (MOI 10) was measured by proportion of neutrophils expressing AnxV. (D) Late-stage apoptosis in BMN cultures from C as measured by AnxV and 7-AAD co-staining. (C&D) n=3/group. Bars with different letters are significantly different by p<0.05 using one-way ANOVA with Tukey's posttest. Data is representative of two independent experiments.

We also characterized the *in vitro* apoptosis of mPGES-1$^{-/-}$ bone marrow neutrophils (BMN). After 24 hours, a larger proportion of mPGES-1$^{-/-}$ BMN expressed AnxV compared to WT BMN (Fig 4.5C). Coculture with *Bb* increased the apoptotic proportion of the WT BMN but had no effect on apoptosis in the mPGES-1$^{-/-}$ culture. We also measured necrosis using 7-AAD as a measure of membrane damage. After 24 hours, a higher proportion of the mPGES-1$^{-/-}$ BMN culture was necrotic than in the WT culture (Fig 4.5D). Coculture with *Bb* further increase the necrotic proportions regardless of strain, but this proportion was still higher in mPGES-1$^{-/-}$ than WT BMN. More work needs to be done to uncover the mechanism behind the increased apoptosis in mPGES-1$^{-/-}$ BMN, as this may contribute to the faster mLA resolution in mPGES-1$^{-/-}$ mice.

PGE_2 addback near the arthritic peak does not affect mLA outcomes in mPGES-1$^{-/-}$ mice

Our findings in Fig 4.2B demonstrate that PGE_2 is not required for either development or resolution of mLA in C3H mice, indicating the presence of a compensatory mechanism for PGE_2 activity in this inflammation. As PGE_2 may be proinflammatory or pro-resolving depending on the context in which it is produced, we sought to investigate the effect of PGE_2 addback near the inflammatory peak of mLA in mPGES-1$^{-/-}$ mice. We infected mPGES-1$^{-/-}$ mice with *Bb* and allowed mLA to develop before treating mice with either vehicle control (VC) or 100μg PGE_2 i.p. on 18, 19, and 20 dpi. Administration of PGE_2 at this timepoint further reduced the ankle swelling seen in mPGES-1$^{-/-}$ mice at 21

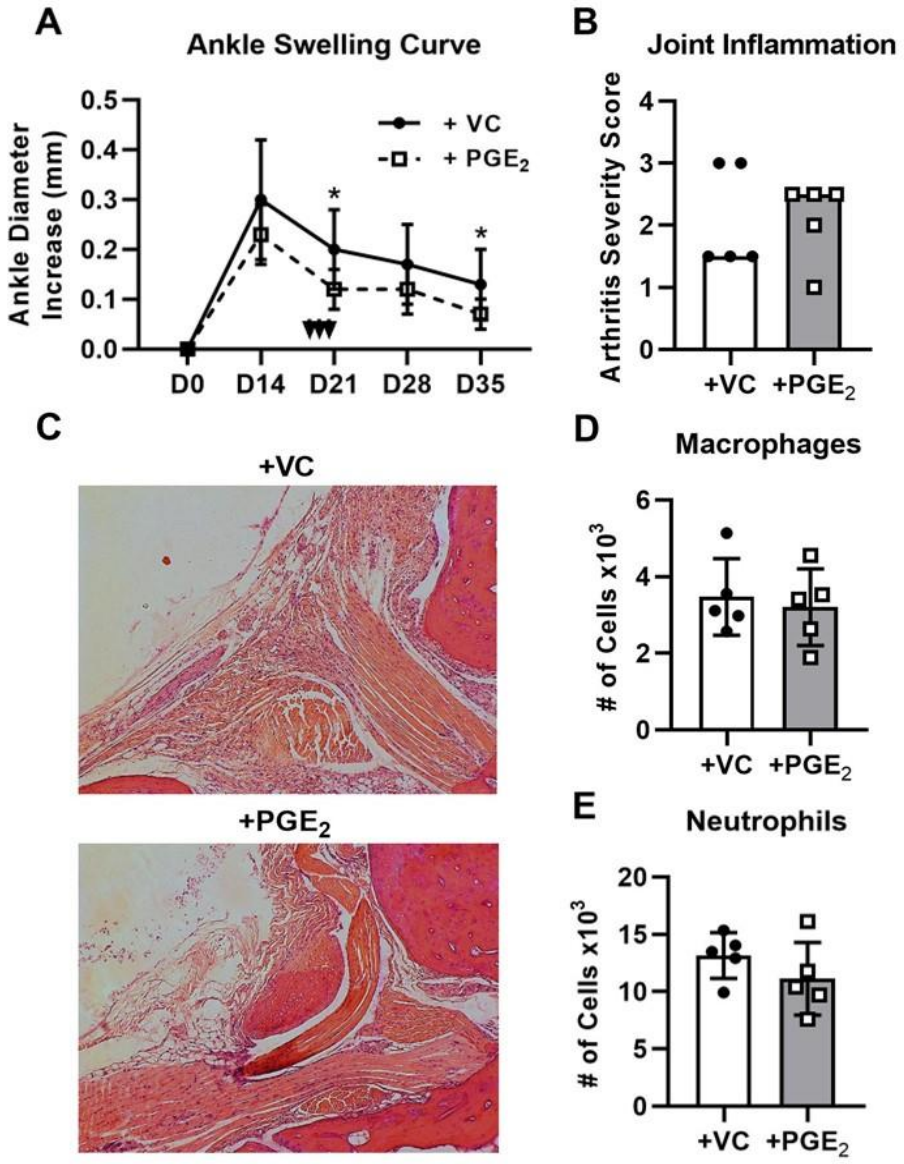

Figure 4.6. Exogenous PGE_2 delivered near the peak of mLA inflammation reduces ankle edema but does not significantly alter mLA resolution outcomes.

Bb-infected mPGES-$1^{-/-}$ mice received either vehicle control (VC; 10% EtOH in PBS) or PGE_2 (100µg in PBS) i.p. on D18,19,20, as shown by arrows in A. (A) Ankle swelling curve displayed as diameter increase from D0 (uninfected). n=5/group. *$p<0.05$ by t-test between strains per timepoint. (B) Arthritis severity scoring of H&E-stained ankle joints from treated mice at D35, with representative histology in (C). n=5/group. Bar is median. Macrophages (D) and neutrophils (E) quantified from ankle joints via flow cytometry. n=5/group. Data is representative of two independent experiments.

and 35 dpi (Fig 4.6A). Despite this decrease in ankle edema with PGE_2 treatment, there was no difference between the severity of mLA in VC- or PGE_2-treated ankles at 35 dpi (Fig 4.6B&C) or in the absolute numbers of macrophages and neutrophils in VC- or PGE_2-treated joints by flow cytometry at the same timepoint (Fig 4.6D&E). We also determined that there was no difference between either the amount of *Bb*-specific IgM and IgG in serum or the spirochete burdens in the ankle joints at this timepoint (Fig 4.S1). Together, these findings demonstrate that PGE_2 addback near the peak of inflammation further reduces ankle edema of mPGES-$1^{-/-}$ mice, but we cannot conclusively determine if PGE_2 addback affects overall arthritis outcomes.

Early PGE_2 addback to mPGES-$1^{-/-}$ mice delays mLA resolution

Inhibition of COX-2 during early mLA development was shown to prevent efficient arthritis resolution, demonstrating the importance of early inflammation mechanics in initiating pro-resolution programs [71]. Although PGE_2 is dispensable for the development or resolution of mLA (Figure 4.2), we hypothesized that exogenous PGE_2 would disrupt or augment early inflammation mechanics in mPGES-$1^{-/-}$ mice and what the overall outcomes would be. As the joint during early mLA is an inflammatory environment, we hypothesized that addback of exogenous PGE_2 during this time would further amplify the inflammatory environment and exacerbate arthritis, potentially delaying inflammation resolution. To test this hypothesis, we infected mPGES-$1^{-/-}$ mice with *Bb* before treating them i.p. with either vehicle control (VC) or 100μg PGE_2

on 7, 8, and 9 dpi and measuring arthritis outcomes at 35 dpi. As in Fig 4.6, early administration of PGE_2 also significantly reduced ankle swelling, starting after treatment at 14 dpi and continuing through 28 dpi (Fig 4.7A). However, unlike the later addback, early PGE_2 addback significantly exacerbated arthritis severity at 35 dpi compared to VC controls (Fig 4.7B). Increased inflammatory infiltrate in the PGE_2-treated joint is clearly visualized in Fig 4.7C. We quantified this joint infiltrate by flow cytometry and found no difference in the number of macrophages between treatment groups, but the absolute number of neutrophils was significantly increased in PGE_2-treated versus VC-treated animals (Fig 4.7D&E). We confirmed that the arthritis was not due to an impaired anti-*Borrelia* host response, with similar levels of *Bb*-specific IgM and IgG in sera and *Bb* burdens in the joint at 35 dpi between treatment groups (Fig 4.S2). Further studies should be performed to determine the immediate effect of this early PGE_2 addback on the inflammatory joint environment and the kinetics of arthritis development and infection control should be characterized more completely.

Conclusions

Based on previous findings that (1) COX-2 deficiency did not affect development of mLA but instead prevented its timely resolution in C3H mice [71], and, (2) that PGE_2 production is significantly increased during mLA [74], we hypothesized that PGE_2 would be required for efficient mLA resolution. To test this hypothesis, we infected WT and mPGES-$1^{-/-}$ mice with *Bb* and tracked mLA progression, expecting to find that the mPGES-$1^{-/-}$ mice incapable of synthesizing PGE_2 would

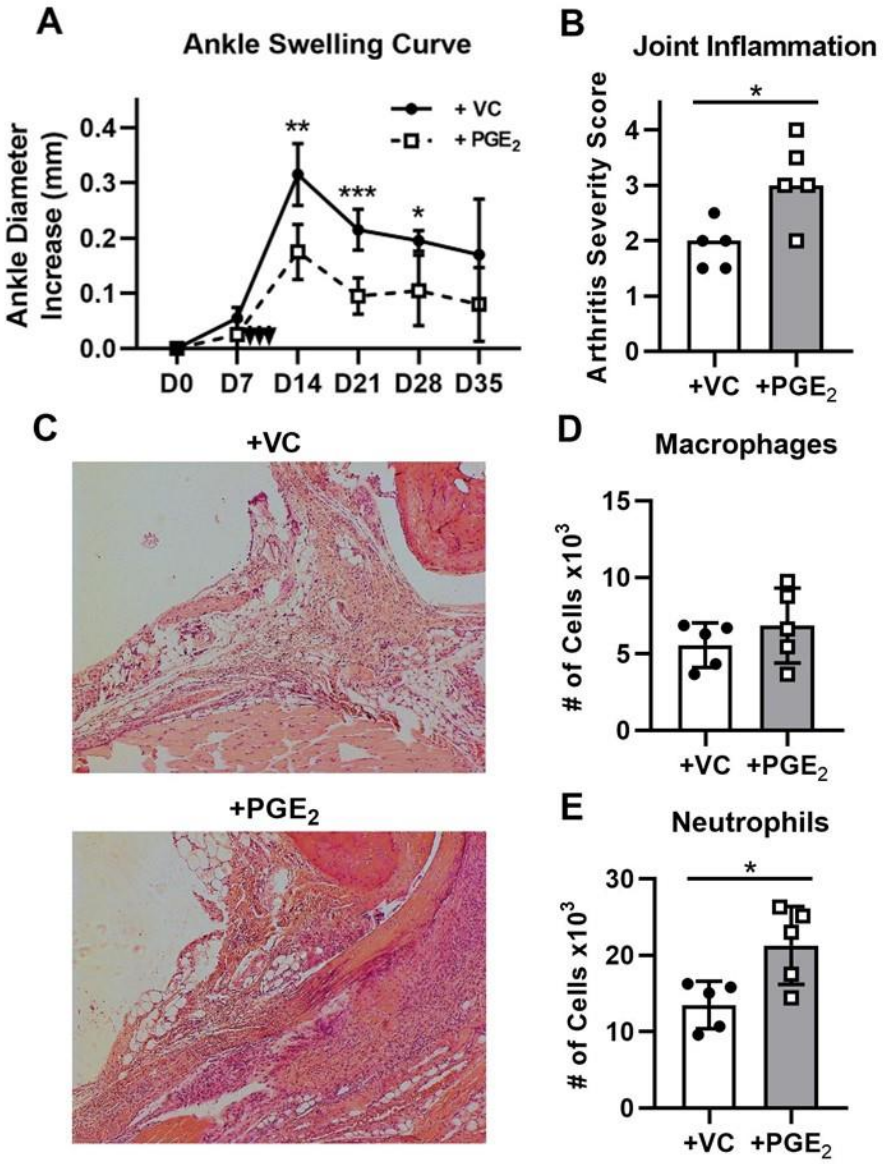

Figure 4.7. Exogenous PGE_2 delivered during early mLA development reduces ankle edema but exacerbates arthritis severity.

Bb-infected mPGES-$1^{-/-}$ mice received either vehicle control (VC; 10% EtOH in PBS) or PGE_2 (100µg in PBS) i.p. on D7,8,9, as shown by arrows in A. (A) Ankle swelling curve displayed as diameter increase from D0 (uninfected). n=5/group. *p<0.05, **p<0.01, ***p<0.001 by t-test between strains per timepoint. (B) Arthritis severity scoring of H&E-stained ankle joints from treated mice at D35, with representative histology in (C). n=5/group. *p<0.05 by Mann-Whitney test. Bar is median. Macrophages (D) and neutrophils (E) quantified from ankle joints via flow cytometry. n=5/group. *p<0.05 by t-test.

have a resolution defect similar to COX-2$^{-/-}$ mice. As in COX-2$^{-/-}$ mice, we found that mPGES-1$^{-/-}$ mice developed arthritis to a similar extent as WT mice; however, mPGES-1$^{-/-}$ mice did not have a resolution defect as seen in COX-2$^{-/-}$ mice, but instead resolved mLA more efficiently than WT mice. This was reflected not only in reduced edema in mPGES-1$^{-/-}$ mice, but also in lower arthritis severity scores and fewer neutrophils and macrophages at resolution timepoints. This shortened resolution timeline in mPGES-1$^{-/-}$ mice may be due in part to enhanced control of *Bb* burdens in the joint, but more work is needed to determine why *Bb* burdens are lower in the joint by 35 dpi. PGE_2 addback in mPGES-1$^{-/-}$ mice near the peak of inflammation reduced joint edema but did not significantly affect mLA outcomes or the anti-*Borrelia* host response. In contrast, early PGE_2 addback significantly reduced the extent to which edema formed while also hampering arthritis resolution by 35 dpi. Overall, these findings demonstrate that PGE_2 is not required for the development or resolution of mLA and that, as in COX-2-inhibited WT mice, early disruption of inflammation mechanics is deleterious to arthritis resolution.

CHAPTER 5

THE DEVELOPMENT OF AN *IN VIVO* STAINING TECHNIQUE TO MEASURE REVERSE TRANSENDOTHELIAL MIGRATION OF NEUTROPHILS FROM THE ARTHRITIC JOINT

Introduction

The current paradigm for inflammation resolution in mLA involves the phagocytosis of *B. burgdorferi* by infiltrating neutrophils, which will subsequently undergo apoptosis and be cleared by macrophages via efferocytosis (Fig 1.2). This process promotes resolution in the following ways: (1) removing the inflammatory stimulus (i.e., *Bb*); (2) removing apoptotic cells before they progress into secondary necrosis, at which point they may burst and their components may act as DAMPs to augment inflammation [97]; and (3), by reprogramming macrophages towards a pro-resolving phenotype [62]. Dysregulation of apoptosis or efferocytosis, therefore, can lead to a prolonged inflammatory state, delaying or preventing inflammation resolution.

Using this model, we have previously presumed that all infiltrating neutrophils, even those which do not phagocytose *Bb*, will die at the site of inflammation and be cleared via efferocytosis. However, recent studies suggest an alternative mechanism by which neutrophils may be cleared from the site of inflammation, termed reverse transendothelial migration (rTEM). In rTEM, neutrophils responding to inflammation or injury perform their task and then, instead of

undergoing apoptosis at the site, re-enter circulation. In two studies using different models of sterile inflammation, neutrophils which had undergone rTEM were tracked to the lung, where they were transiently retained while they upregulated CXCR4 expression before returning to the bone marrow [84, 115]. In our model, rTEM could serve as an additional mechanism of neutrophil clearance from the joint, especially during inflammation resolution.

Thus far, neutrophil rTEM has been investigated only in the context of sterile injury [115, 116] and inflammation [84, 117, 118], so it is yet unknown whether neutrophil rTEM occurs during infectious insult and if it may play a role in the host response to infection. Further, one of these studies described a role for 5-LO metabolite LTB_4 in mediating rTEM, whereby the LTB_4:neutrophil elastase axis was shown to potentiate rTEM by increasing vascular permeability [117]. In our mLA model, genetic deletion of 5-LO resulted in a resolution defect in C3H mice with persistent immune infiltrate [72]. If rTEM does provide a partial mechanism for neutrophil clearance, it may follow that a lack of LTB_4 in 5-$LO^{-/-}$ mice could prevent rTEM in these mice, exacerbating the amount of neutrophil infiltrate remaining in the joint. There is, therefore, a question of whether rTEM is involved in infectious inflammation, and murine Lyme arthritis is a prime model in which to address this gap.

We propose that rTEM could be a mechanism by which infiltrating neutrophils that do not encounter PAMPs are cleared from the joint. *Bb* phagocytosis

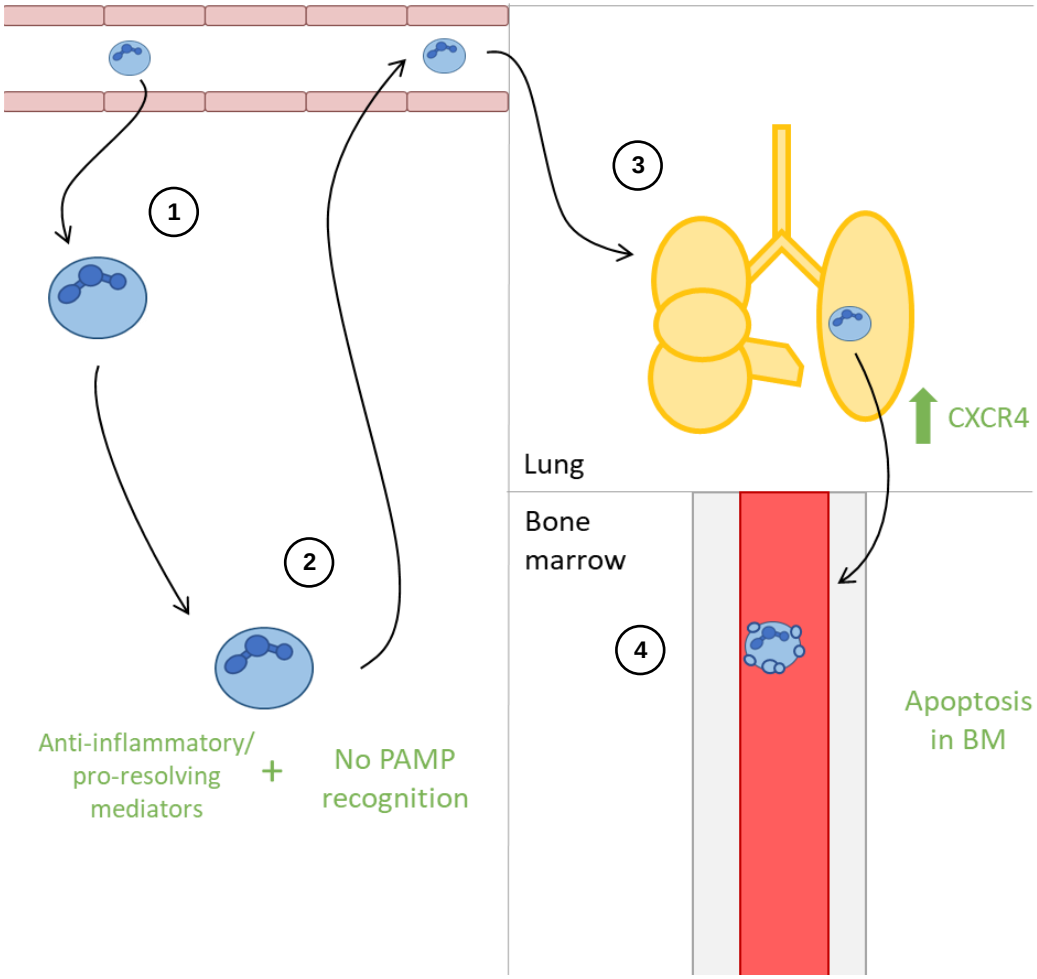

Figure 5.1. Proposed model for rTEM during mLA.

In this model, we hypothesize that neutrophils which extravasate into the site of inflammation will undergo rTEM if they do not encounter PAMPs. (1) Circulating neutrophils will leave the vasculature in response to *Bb* infection and/or mLA inflammation. (2) If they do not encounter PAMPs, neutrophils may undergo rTEM instead of dying of apoptosis at the site of inflammation. (3) rTEM neutrophils will traffic to the lungs, where they will upregulate surface CXCR4. (4) CXCR4:CXCL12 signaling facilitates rTEM neutrophil homing to the bone marrow where they undergo apoptosis.

induces neutrophil apoptosis (Figure 3.4), so we would expect those cells to remain at the site of infection. It would also be reasonably detrimental for neutrophils which have phagocytosed *Bb* to leave the site of infection as they may initiate inflammation at distal sites. Further, neutrophil apoptosis and efferocytosis is a critical component of the pro-resolution program, so we expect neutrophil apoptosis would still be the primary way that infiltrating neutrophils are cleared. However, if some of the infiltrating neutrophils undergo rTEM instead of dying at the site of infection/inflammation, it may reduce the burden of efferocytosis on phagocytes, allowing them to more effectively clear apoptotic cells and debris.

Overall, we hypothesize that neutrophils which respond to joint inflammation in mLA but do not come into contact with PAMPs will undergo rTEM and ultimately traffic back to the bone marrow to die (Figure 5.1). This chapter describes the technical design of an *in vivo* staining method to measure rTEM and preliminary findings characterizing neutrophil rTEM and trafficking to other organs.

Results

Setup and methodology design

Several studies have reported that neutrophils responding to sterile inflammation trafficked to the lung after rTEM [84, 115, 117, 118], so we ran a pilot experiment to determine if the number of neutrophils in the lung was increased during *Bb* infection. Lungs were perfused of blood and harvested from infected (28 dpi) and

uninfected WT C3H mice and homogenized to create a single cell suspension. Cells were then stained and neutrophils quantified by flow cytometry. We found that >15% of CD45.2^{+} cells in the lungs of *Bb*-infected WT mice were neutrophils as compared to <5% in uninfected lungs (data not shown). The n value for the "infected" group in this pilot was too low to run statistical analysis (n=2), but we felt confident that, wherever they were coming from, neutrophils were indeed ending up in the lung during *Bb* infection, and that it would be worth pursuing this line of inquiry.

A study by Owen-Woods et al. visualized neutrophil rTEM in the cremaster muscle by applying a method that took advantage of the high-affinity bonding between biotin and streptavidin. They injected a biotinylated anti-Ly-6G (αLy-6G) mAb (2μg) via tail vein and then, after inflammatory stimulation and exteriorization, superfused the cremaster muscle with AlexaFluor647-tagged streptavidin (AF647-SA) [84]. By this approach, circulating neutrophils would be tagged with the biotinylated antibody and then any neutrophils which responded to the inflammatory stimulus would pick up the fluorescently-tagged streptavidin, allowing the cell to be visualized via intravital microscopy (IVM). This provided the template for our approach, which we modified by delivering the AF647-SA (0.1μg in10μl sterile PBS) into the knee synovium through the patellar tendon. As we have observed that mLA also presents in knee joints, though to a lesser extent than in ankles (data not shown), we chose to inject knees instead of ankles because we could more reliably deliver AF647-SA into the knee

synovium. Because the inflammation we are studying lasts weeks, not hours as in [84], we decided to deliver the biotinylated mAb and AF647-SA at the same time. Further, as we were initially unable to perform IVM, we opted to wait until a few hours post-staining (hps) and harvest the knee and other tissues for flow cytometry. This would allow us to both check that we were successfully staining knee-infiltrating neutrophils and to see if those neutrophils were exiting the knee and reentering the vasculature to travel to other tissues, particularly the lung.

Neutrophils can be successfully stained* in vivo *using this approach

Figure 5.2 shows sample results of *in vivo* neutrophil staining in uninfected mice at 6 hps. After gating out doublets and $SSC^{lo}FSC^{lo}$ debris, cells were gated on CD45.2 PE and AF647 (top right plot). The circled population is comprised of neutrophils which were successfully tagged with the biotinylated αLy-6G mAb, infiltrated into the knee in response to the sterile trauma of the needle injection where they picked up the AF647-SA, then subsequently exited the knee and trafficked to the lung.

Notably, while our standard practice is to count only Ly-$6G^{hi}$ cells as neutrophils, these cells predominantly stained as Ly-$6G^{int/lo}$ by our method. However, we hypothesized that this discrepancy could be due to only a low-to-intermediate coverage of surface Ly-6G by the biotin-streptavidin complex. The panel on the bottom left shows these same *in vivo*-stained cells stained *in vitro* with an additional αLy-6G PE-Cy7 mAb. There were two clear populations in this plot:

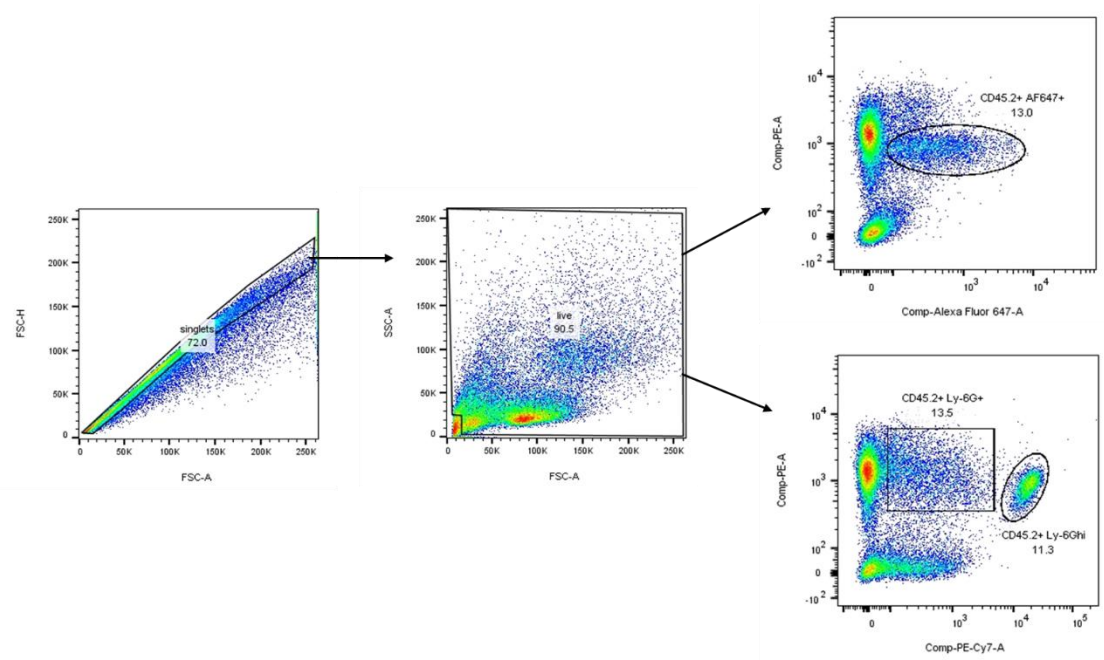

Figure 5.2. Infiltrating neutrophils were successfully stained *in vivo* and trafficked to the lung.

An uninfected WT mouse was injected with biotinylated αLy-6G mAb (2μg in 100μl sterile PBS) i.v. and then with AF647-SA (0.1μg in 10μl sterile PBS) in the left knee synovium. Single cell suspensions from lungs harvested at 6hps were stained for flow cytometry. Doublets and debris were gated out. The top right panel shows the *in vivo*-stained population ($CD45.2^+AF647^+$). The bottom right panel shows a staining control from the same samples that was stained *ex vivo* using our usual anti-Ly-6G PE-Cy7 mAb.

one that was CD45.2^{+}Ly-6G$^{+/lo/int}$ and one that was CD45.2 Ly-6G^{hi}. The Ly-6G^{hi} population is presumably comprised of cells which were either unstained by our *in vivo* staining method or which had low-coverage staining, leaving more surface Ly-6G available for *in vitro* staining. The CD45.2^{+}PE-Cy7$^{+/int/lo}$ population seen in this plot may then be cells that are already partially stained with AF647, so fewer surface Ly-6G are available for staining with the PE-Cy7 mAb. This may be supported by the observation that the proportion of PE-Cy7$^{+/int/lo}$ in this plot and AF647$^{+/int/lo}$ in the plot above are very similar (13.5% versus 13.0%). Further, this population was not present in the pilot study, where nearly all Ly-6G-expressing cells were Ly-6G^{hi} (data not shown). This supports the idea that the low-to-intermediate Ly-6G staining seen in either the top or bottom right panels of Figure 5.2 may be due to partial coverage of the surface Ly-6G on each cell by the *in vivo* staining method employed.

AF647-SA does not leak out from the knee into the vasculature

The primary concern having seen that stained neutrophils were indeed showing up in the lung was that the AF647-SA was leaking out of the knee and into the vasculature, staining the neutrophils there. To address this concern, we performed *in vivo* staining, this time using a biotinylated αCD4 mAb. Unlike neutrophils, we would not expect circulating CD4^{+} T cells to extravasate into the knee in response to needle injury. Therefore, there would be no reason that biotinylated CD4^{+} T cells would show up as AF647^{+} unless AF647-SA was leaking into the vasculature.

To test this, we injected an uninfected mouse with the biotinylated αCD4 mAb i.v. and then AF647-SA in the knee. We reasoned that if AF647-SA was indeed leaking out of the joint, it would be during the acute response to the needle injury, when vascular permeability would be at its highest. We therefore sacrificed mice at 2 hps and collected blood via cardiac puncture. RBC lysis was performed and white blood cells were prepared for flow cytometry. An excess of biotinylated αCD4 mAb and AF647-SA were added to some samples for *in vitro* staining as a positive control (i.e., total $CD4^+$ T cells in blood). Little to no *in vivo*-stained CD4 T cells were $AF647^+$ via flow cytometry (Fig 5.3), indicating that AF647-SA did not leak into the vasculature. We confirmed that circulating $CD4^+$ T cells had been tagged with the biotinylated mAb *in vivo* with good coverage both per cell (Fig 5.S1A) and as a population (Fig 5.S1B). These findings validate the injection of AF647-SA through the patellar tendon and into the knee synovium. However, as technical injection accuracy may vary, it may still be a good idea to regularly run this check to ensure that poor injecting technique is not causing AF647-SA leakage into the vasculature.

Characterizing the staining and localization of infiltrating neutrophils

After validating our *in vivo* staining method, we performed an experiment to investigate the staining of neutrophils in the knee and subsequent trafficking to the lung and bone marrow, as described [84, 115]. As shown in Figure 2, we knew that needle injury alone was enough to recruit neutrophils to the knee for staining, and that some of these stained neutrophils also ended up in the lung.

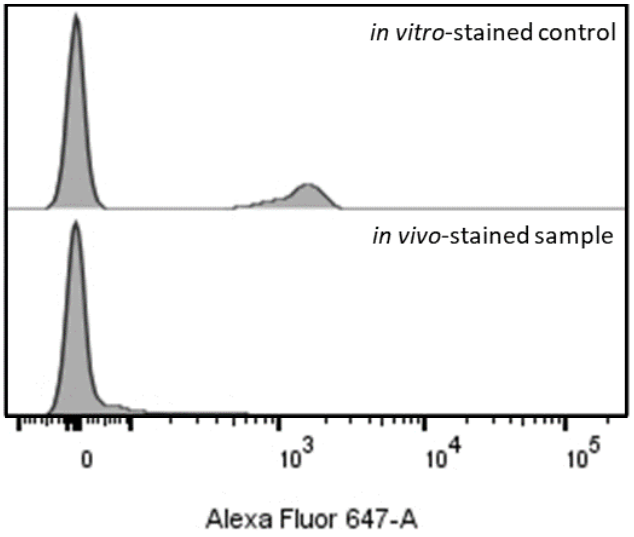

Figure 5.3. AF647-SA does not leak into the vasculature from the knee synovium.

An uninfected mouse was injected with biotinylated αCD4 mAb (2μg in 100μl sterile PBS) i.v. and then with AF647-SA (0.1μg in 10μl sterile PBS) in the left knee synovium. Blood was collected at 2 hps, RBCs were lysed, and white blood cells were stained for flow cytometry. The top graph shows AF647 expression on blood cells stained with biotinylated αCD4 and AF647-SA *in vitro* (positive control), while the bottom graph shows the *in vivo*-stained population.

This needle injury is unavoidable and may confound rTEM experiments in *Bb*-infected mice with arthritis. Therefore, this experiment included staining in both uninfected and *Bb*-infected C3H WT mice (24 dpi) in an attempt to parse out the differences between sterile injury alone and sterile injury on top of the inflammatory environment of the arthritic joint.

In this experiment, a set of WT C3H mice were infected with *B. burgdorferi* and left to develop mLA. At 24 dpi, half the infected mice and an equal number of uninfected mice were injected i.v. with biotinylated αLy-6G mAb and in the knee with AF647-SA. The other half of the infected mice and an equal number of uninfected mice were sacrificed to collect baseline (unstained) samples. At 6 hps, half of the stained mice, infected and uninfected, were sacrificed and perfused of blood, and the injected knee and lungs were collected. The other half of the stained mice were sacrificed at 20 hps and bone marrow was collected.

Staining of infiltrating neutrophils in the knee

Knees harvested from infected and uninfected mice, both with and without *in vivo* staining, were homogenized and cells were stained for flow cytometry. We observed that the total number of infiltrating neutrophils in the knee was increased at 6 hps as compared to baseline in both uninfected and *Bb*-infected mice (Fig 5.4A), again confirming that the needle injury sustained during AF647-SA injection increased recruitment of neutrophils to the knee. Further, while baseline neutrophil numbers were not different, there were significantly more

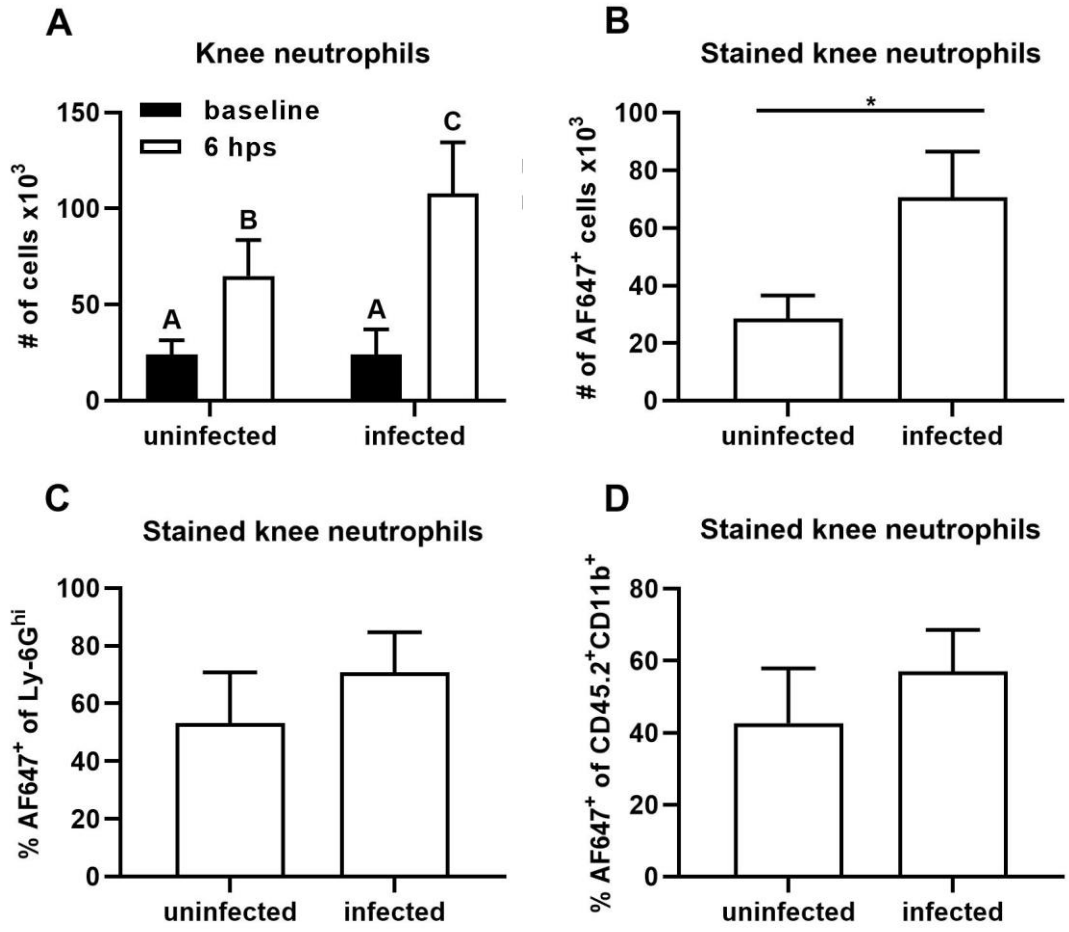

Figure 5.4. Needle injury recruits neutrophils to the knee.

Uninfected and *Bb*-infected WT C3H mice (24 dpi) were injected with biotinylated αLy-6G and AF647-SA and injected knees were harvested 6 hps. Single cell suspensions from knees were stained for flow cytometry. (A) The number of neutrophils in uninfected control and infected knees at both baseline (no injection) and at 6hps. Bars with different letters are significantly different by one-way ANOVA with Tukey's test at $p<0.05$. (B) The absolute number of $AF647^+$ cells in infected and uninfected knees at 6hps. (C) The proportion of $AF647^+$ cells of neutrophils in uninfected and infected knees. (D) The proportion of $AF647^+$ cells of inflammatory infiltrate in uninfected and infected knees. n=4/group. *$p<0.05$ by t-test.

neutrophils in the infected versus uninfected knees at 6 hps (Fig 5.4A). It is possible that the combination of needle injury and inflammatory arthritis in the joint recruited more neutrophils to the site as compared to needle injury alone. Alternatively, neutrophils may be retained for longer in the arthritic joint after being recruited by needle injury, while neutrophils responding to needle injury alone come and go more easily. Significantly more $AF647^{+}$ cells were found in the knees of infected versus uninfected mice (Fig 5.4B), though this is not unexpected if total neutrophil numbers are higher in infected mice (Fig 5.4A). However, the proportion of $AF647^{+}$ cells among Ly-$6G^{hi}$ neutrophils (Fig 5.4C) or immune infiltrate (Fig 5.4D) in the joint was not different between uninfected and infected animals. In both groups, only about 50% of neutrophils were $AF647^{+}$, which could mean that cells are being inefficiently stained in the joint or that there is not enough AF647-SA left to stain all the neutrophil infiltrate at this timepoint.

Trafficking of stained neutrophils to the lung

Lungs were also harvested from uninfected and infected mice at both baseline and at 6 hps. To prevent contamination of lung-infiltrating neutrophil populations by circulating neutrophils in the lung vasculature, mice were perfused of blood before all right lung lobes were harvested. Lung lobes were homogenized and isolated cells were stained for flow cytometry. In line with our preliminary findings (data not shown), there were significantly more neutrophils in the lungs of infected mice compared to uninfected mice at baseline (Fig 5.5A). However, the absolute number of neutrophils in the lungs of uninfected or infected mice were

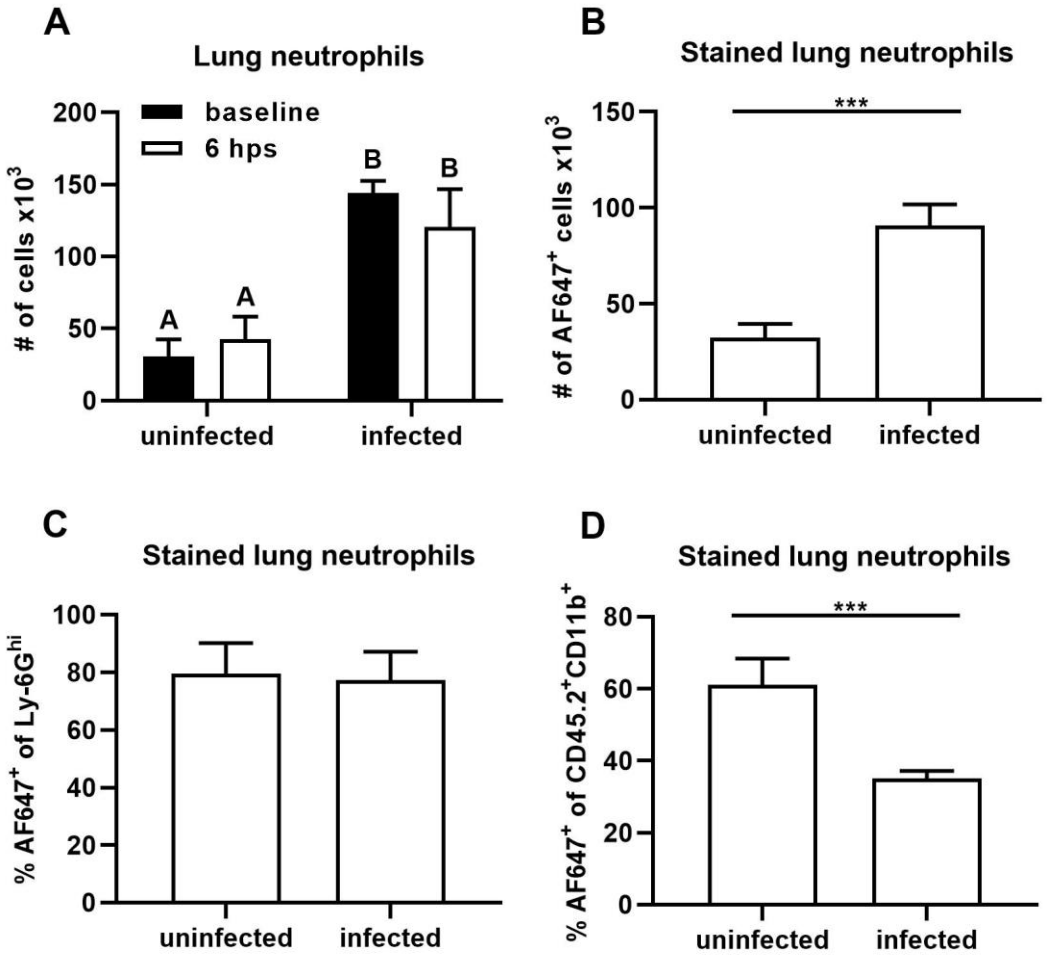

Figure 5.5. AF647⁺ neutrophils traffic to the lung.

Uninfected and *Bb*-infected WT C3H mice (24 dpi) were injected with biotinylated αLy-6G and AF647-SA and lungs were harvested 6 hps. Lungs were homogenized and stained for flow cytometry. (A) The number of neutrophils in uninfected control and infected lungs at both baseline (no injection) and at 6hps. Bars with different letters are significantly different by one-way ANOVA with Tukey's test at $p<0.05$. (B) The absolute number of AF647⁺ cells in infected and uninfected lungs at 6hps. (C) The proportion of AF647⁺ cells of neutrophils in uninfected and infected lungs. (D) The proportion of AF647⁺ cells of total inflammatory infiltrate in uninfected and infected lungs. n=4/group. ***$p<0.001$ by t-test.

not significantly altered after staining. The number of AF647$^+$ cells was significantly higher in infected versus uninfected lungs (Fig 5.5B), but the proportion of neutrophils (Fig 5.5C) that were AF647$^+$ was not different between the two groups. The presence of AF647$^+$ neutrophils in the lung demonstrates that rTEM is indeed occurring in both uninfected and infected mice and that these cells are trafficking to the lung. The combined data from Figures 5.5B&C suggest that instead of accumulating alongside other neutrophils in the lung, AF647$^+$ rTEM neutrophils are replacing the other neutrophils in the lung. This may be in line with the findings from Wang et al. [115], where rTEM neutrophils trafficked to the lung to upregulate CXCR4 before travelling to the bone marrow. Further, the similar proportion of AF647$^+$ neutrophils in uninfected and *Bb*-infected lungs despite the larger population of neutrophils in the infected lungs demonstrates that more cells are undergoing rTEM from the infected joint. Whether this is because there are more cells involved in the response in the first place or whether increased vascular permeability permits more rTEM in the infected joint requires further investigation. Lastly, Figure 5.5D shows that AF647$^+$ cells make up a much smaller proportion of immune infiltrate in the lungs of infected versus uninfected mice, which likely means that there is more general immune infiltrate in the lungs during infection. As it appears that neutrophils are undergoing rTEM and trafficking from the knee to the lung after needle injury, CXCR4 expression on AF647$^+$ neutrophils in the lung should be determined to see if the rTEM neutrophils in our model are following a similar path to neutrophils in the Wang et al. study [115].

Trafficking of stained neutrophils to the bone marrow

Lastly, we determined if AF647$^+$ neutrophils would traffic to the bone marrow. We waited until 20 hps to harvest BMDM from stained mice because we did not know how long it might take for the neutrophils to end up in the bone marrow. Figure 5.6A shows that there are more neutrophils in the bone marrow of infected mice as compared to uninfected mice as baseline. This may be expected as granulopoiesis is increased during infection to keep up with the demand for innate immune effector cells [119]. The number of neutrophils in the bone marrow was significantly higher at 20 hps compared to baseline in both the uninfected and infected mice (Fig 5.6A), which may be due to either increased granulopoiesis or trafficking of rTEM (and other) neutrophils back to the bone marrow for apoptosis. The proportion of neutrophils of total CD45.2$^+$CD11b$^+$ cells in the bone marrow was higher in infected mice at baseline but evened out between uninfected and infected mice at 20 hps (Fig 5.6B). There may be a maximum capacity for Ly-6G^{hi} cells in this compartment, so cells are killed off at a certain threshold. There are significantly more AF647$^+$ neutrophils in the bone marrow of infected versus uninfected mice (Fig 5.6C), but again the proportion of Ly-6G^{hi} cells that are AF647$^+$ is not different between the groups (Fig 5.6D). Indeed, approximately 60% of neutrophils are AF647$^+$ in bone marrow from both groups, confirming that rTEM neutrophils are ultimately trafficking back to the bone marrow, where they presumably undergo apoptosis [115].

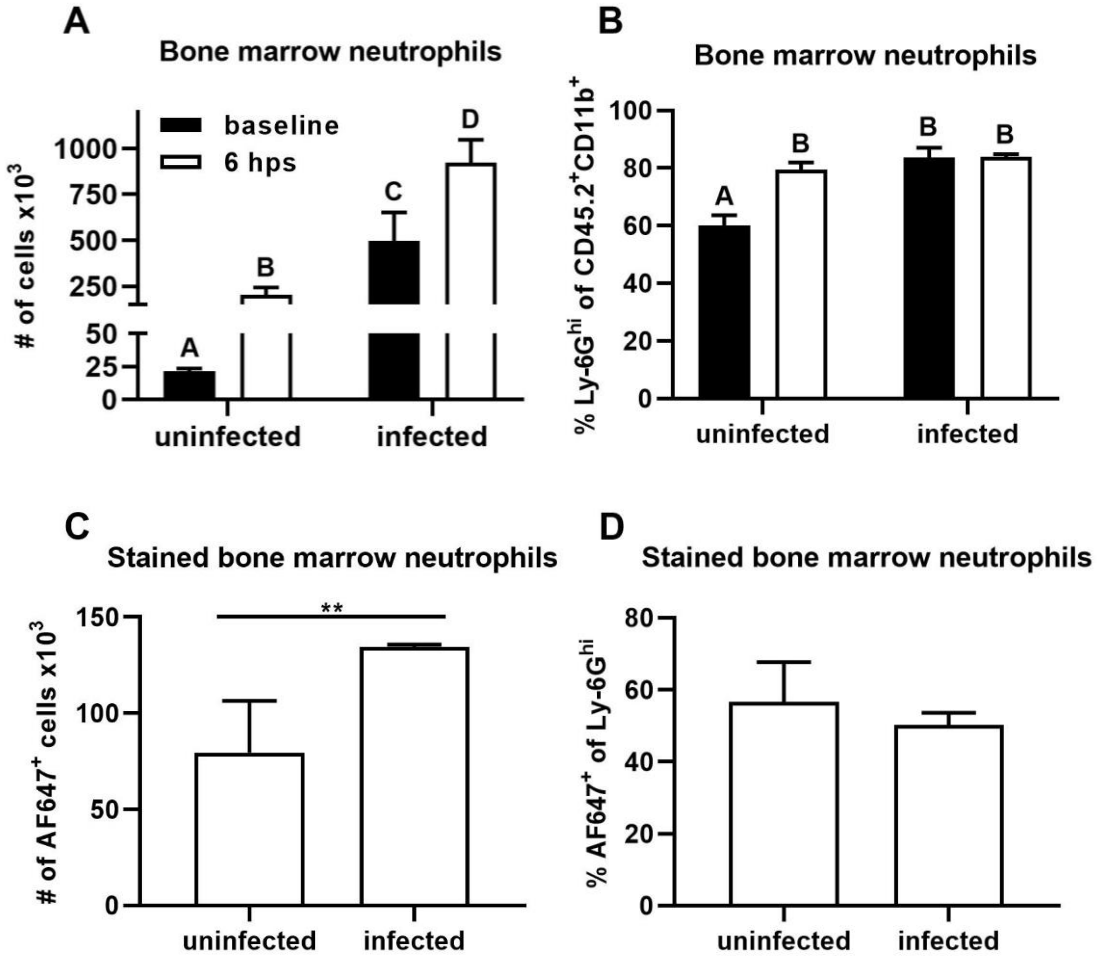

Figure 5.6. AF647$^+$ neutrophils traffic to the bone marrow.

Uninfected and *Bb*-infected WT C3H mice (24 dpi) were injected with biotinylated αLy-6G and AF647-SA and bone marrow was harvested 20 hps. RBCs were lysed and cells were stained for flow cytometry. (A) The number of neutrophils in uninfected control and infected knees at both baseline (no injection) and at 20 hps. (B) The proportion of neutrophils in the bone marrow at baseline and 20 hps was measured in both uninfected and infected mice. (C) The absolute number of AF647$^+$ cells in infected and uninfected knees at 20 hps. (C) The proportion of AF647$^+$ cells of neutrophils in uninfected and infected knees. n=4/group. **p<0.01 by t-test. Bars with different letters are significantly different by one-way ANOVA with Tukey's test at p<0.05.

Intravital microscopy of in vivo*-stained neutrophils*

In collaboration with Steven Segal, Ph.D., at the University of Missouri School of Medicine, we are currently investigating the potential of our *in vivo* staining method to visualize neutrophils via IVM. As opposed to flow cytometry which allows us to characterize the distribution of $AF647^+$ cells at any given time, we hope that IVM will allow us to visualize rTEM in real time. For our first trial, we injected an uninfected mouse with the staining components as usual and waited until 2 hps to attempt imaging. The mouse was anesthetized with ketamine/xylazine and re-dosed as needed. The skin was resected from the AF647-SA-injected knee and the mouse was positioned so that the knee could be held in place, with the camera focused on the tissue medial to the patella. The $AF647^+$ cells were readily seen under the fluorescent microscope. We perused different planes and regions of the knee and found $AF647^+$ cells in both large vessels and microvasculature snaking between adipocytes. Figure 5.7 is a sample image of this IVM in which the convergence site of two vessels (outlined in red) with several $AF647^+$ cells (green arrows) is visible. In a video taken at the same time as the image, we were able to see neutrophils in various states of taxis: free flowing in the vasculature, rolling along the endothelial wall, and anchored to the endothelium. Although we did not observe $AF647^+$ cells outside of the vasculature or straddling the endothelium indicating either TEM or rTEM, this was a proof-of-concept trial and we plan to spend more time looking for evidence of TEM & rTEM in future experiments.

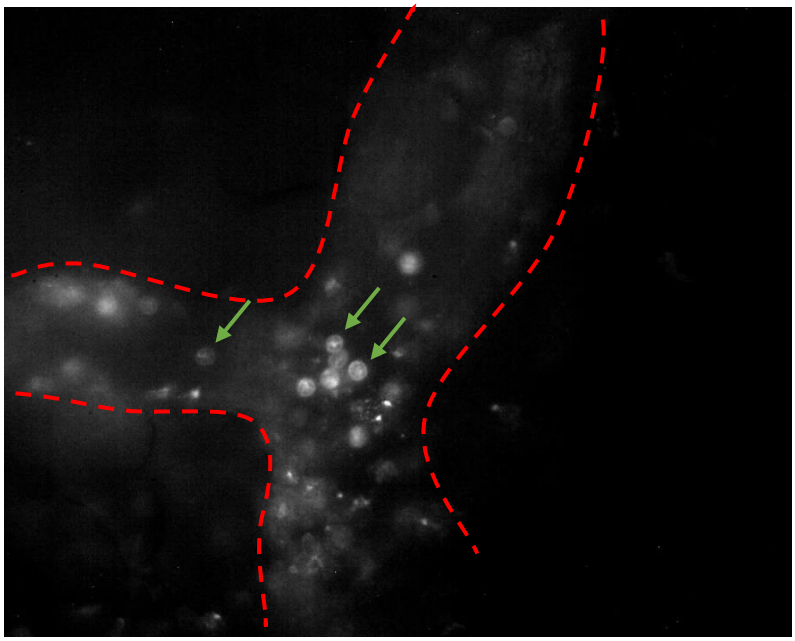

Figure 5.7. AF647^{+} neutrophils can be visualized using intravital microscopy.

In this representative IVM image, several *in vivo*-stained neutrophils (green arrows) can be seen in the vasculature (outlined in red). The direction of traffic is from the bottom left to the top right, with neutrophils starting in each of the vessel prongs, flowing towards the convergence point and onwards in the single vessel.

Conclusion

Although neutrophil apoptosis and subsequent efferocytosis by macrophages is a key component of inflammation resolution, neutrophils have also been shown to exit the site of inflammation and re-enter the vasculature in a process called reverse transendothelial migration. In models of sterile inflammation, rTEM neutrophils have been shown to traffic first to the lung and ultimately to the bone marrow [115, 116], where they undergo apoptosis [115]. To determine if rTEM contributes to removal of neutrophils from the site of inflammation in mLA, we modified an existing method of staining neutrophils *in vivo* in which neutrophils which have entered the site of inflammation are fluorescently tagged, allowing us to track them wherever they go. We first demonstrated that we could, indeed, stain neutrophils *in vivo* using this method. We also observed that these stained neutrophils showed up as Ly-6G$^{int/lo}$ via flow cytometry instead of Ly-6G^{hi}, but this is likely due to incomplete coverage of surface Ly-6G per cell by the biotin-streptavidin complex. We briefly characterized the presence of AF647^{+} cells in the knee and lung of *Bb*-infected (24 dpi) and uninfected mice at 6 hps and in the bone marrow at 20 hps. The number and proportion of neutrophils were already higher at baseline in infected lungs and bone marrow, respectively, than in these organs in uninfected mice. Needle injury increased the number of neutrophils in uninfected and infected knees and the proportion of neutrophils in uninfected bone marrow. The proportion of CD45.2^{+}CD11b^{+} cells or neutrophils that stained AF647^{+} was not different between uninfected and infected mice in knees, lungs, or bone marrow at the timepoints investigated. Together these findings

demonstrate that needle injury initiates an inflammatory response that eventually results in rTEM of neutrophils at the site of injection. Arthritic inflammation in infected knees appears to have increased the neutrophil population in the joint, potentially by retaining the needle injury-recruited neutrophils to fight the infection in the knee. The similar proportion of $AF647^+$ cells in infected versus uninfected tissues and organs may indicate that the process of rTEM is happening at a similar rate regardless of underlying infectious inflammation. Much more work will be required to characterize the kinetics of neutrophil recruitment, rTEM, and subsequent trafficking during mLA. While a major limitation of this *in vivo* staining method is the inflammatory response caused by injection of AF647-SA, the use of proper controls still allows for inferences to be made about the involvement of rTEM in mLA resolution and the mechanisms which mediate it. Further, as our current evidence of rTEM is based on the presence of $AF647^+$ cells in distal organs, the use of IVM would allow us to visually confirm on a cellular level if rTEM is occurring in our model, and it will be a useful technique in future studies into the mechanics governing rTEM in mLA.

Overall, we designed a novel method of staining infiltrating neutrophils *in vivo* and used this technique to demonstrate that not all neutrophils infiltrating into the arthritic joint during mLA will die at the site of infection/inflammation. Ultimately, whether the neutrophils are responding to the inflammation from mLA or from needle injury, a percentage of neutrophils infiltrating the site of inflammation will undergo rTEM and traffic to the lung for a time before returning to the bone

marrow. This finding opens the door for many future studies on what allows, or disallows, neutrophils to undergo rTEM in an infectious model, especially if it has to do with PAMP recognition or not.

CHAPTER 6

EXPERIMENTAL SLEEP FRAGMENTATION DISRUPTS LYME ARTHRITIS RESOLUTION IN MICE

Introduction

Sleep is a critical, if poorly understood, component of the host response to infection, inflammation, and disease [120, 121]. Indeed, sleep structure is often altered during the acute response to infection and disease as a part of the healing process [122]. In addition, sleep may conversely be disrupted by symptoms of these conditions, including pain, and the resulting poor sleep may exacerbate daytime somnolence and fatigue as well as worsen symptomology and disease pathology. In this manner, sleep and infection/inflammation/disease may be reciprocally regulated [123], and this interplay must be understood from both directions in order to improve sleep and sleep-related outcomes in patients.

The effect of LD and associated symptoms on the quality of sleep has been well-described. Several clinical studies report that patients with LD or post-treatment Lyme disease symptoms (PTLDS) have increased sleep difficulty and/or experience greater sleep disturbance when compared to healthy controls, and this was often correlated with greater self-reported fatigue and pain [124-126]. One study sought to distinguish between the sleep-infection relationship during early LD and the sleep-inflammation relationship in those experiencing PTLDS [127]. These researchers found that sleep disruption is highest in patients with active infection and decreases after receiving antibiotic treatment, with sleep

quality improving at subsequent assessments up to at least one year post-treatment. This is in line with previous findings that altered sleep during the acute response to a number of infections may support recovery [122]. Weinstein et al. also tracked a subset of patients who developed PTLDS, reporting that these patients had poorer sleep compared to controls, with frequent sleep disturbances often related to pain [127]. While these studies relied on patient self-reporting, a 1995 study measured several sleep parameters both subjectively via questionnaires and objectively via polysomnography in a small cohort with confirmed LD and LA [128]. This study found that LD/LA patients had poorer sleep efficiency, with prolonged sleep latency and greater REM fragmentation compared to controls. Notably, while these patients had all experienced LA in one or more joint, they did not have active arthritis at the time of the study, implying that their poorer sleep outcomes were not due to arthritis-related pain.

These previous studies have focused on the ways in which *Bb* infection and LD inflammation affect sleep. However, as the relationship between sleep and infection or inflammation is likely bidirectional, it is important to examine the extent to which poor sleep may contribute to LD pathology. This study attempts to address this gap in mLA by experimentally fragmenting the sleep of mice infected with *B. burgdorferi* and tracking mLA development and resolution.

Results

Sleep fragmentation during mLA development does not exacerbate the arthritic peak

Experimental sleep fragmentation (SF) in mice increases proinflammatory cytokine production [129], disrupts hematopoiesis, and increases the inflammatory output of hematopoietic cells [130]. We therefore hypothesized that sleep fragmentation during mLA development would exacerbate arthritic inflammation. To test this hypothesis, we infected WT C3H mice with *Bb* and either kept the mice in normal housing conditions or transferred them to a sleep fragmentation housing unit. Both groups of mice were kept in these conditions for 21 days before sacrifice to measure arthritis development (Fig 6.1A). After 21 days, SF group mice had similar ankle edema to control mice (Fig 6.1B) and did not have altered arthritis severity (Fig 6.1C). In human [131] and mouse [132] influenza vaccination studies, experimentally-disrupted or restricted sleep reduced antigen-specific antibody titers, resulting in an increased susceptibility to infection upon challenge in mice. As formation of a *Bb*-specific antibody response boosts phagocytic removal of the pathogen [94], we hypothesized that sleep fragmentation during early infection would be detrimental to the anti-*Bb* humoral response. However, sleep fragmentation during early *Bb* infection in C3H mice did not alter the production of *Bb*-specific IgM or subsequent class-switching to IgG by 21 dpi (Fig 6.1D-E). Spirochete burdens in arthritic joints are also not different in SF group mice as compared to control mice (Fig 6.1F). These data

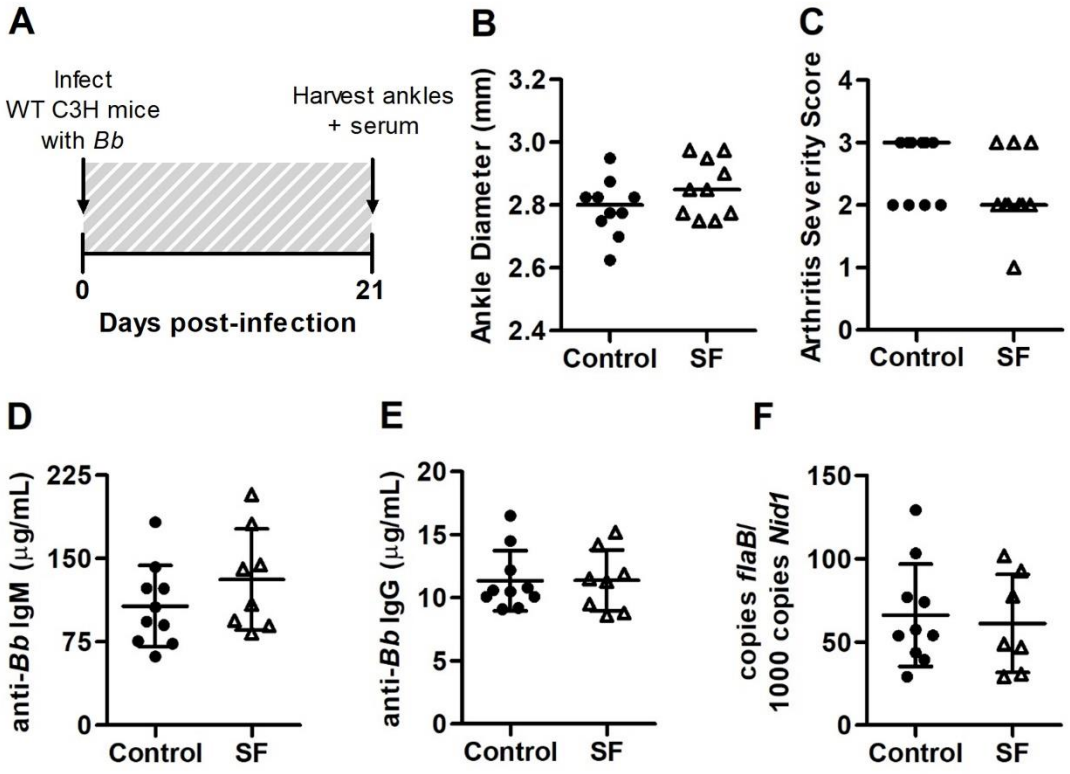

Figure 6.1. Experimental sleep fragmentation does not affect the development of mLA in WT mice.

(A) C3H mice were infected with *B. burgdorferi* and housed either normally or in a sleep fragmentation housing unit for 21 days before sacrifice and sample harvest. Shaded area represents time spent in sleep conditions. (B) Ankle diameter was measured at D21 in both the control and SF groups. n=10/group. (C) Ankle joint sections were histologically scored to determine arthritis severity (scale 0-4). n=10/group. *B. burgdorferi*-specific IgM (D) and IgG (E) were measured from D21 serum by ELISA. n=8-10/group. (F) *B. burgdorferi* levels were quantified in ankles at D21 by qPCR. n=7-10/group. Bar is median in B&C. No significance found by t-test (or Mann-Whitney test for panel C) where significance is defined as $p<0.05$. (Mice were infected and data from panels B&C were collected and graphed by C. R. Brown.)

demonstrate that sleep fragmentation does not exacerbate arthritis development or affect clearance of *Bb* from ankles by 21 dpi in C3H mice.

Sleep fragmentation starting prior to mLA induction does not affect arthritis development

As starting sleep fragmentation simultaneously with *Bb* infection did not exacerbate arthritis, we wondered if priming the mice by beginning sleep fragmentation prior to infection would affect arthritis development. We hypothesized that initiating SF before infection could weaken the mouse immune system and increase the extent to which infection and arthritis progress. Therefore, we started sleep fragmentation with a set of mice for one week prior to infection with *Bb*. These mice were then returned to the sleep fragmentation apparatus and left to develop arthritis for 21 days (Fig 6.2A). Control mice were infected and kept in normal housing conditions for 21 days, as in Fig 6.1. However, subjecting mice to SF both prior to infection and after did not alter ankle edema (Fig 6.2B) or arthritis severity scores (Fig 6.2C) as compared to control mice. Starting sleep fragmentation prior to infection also did not impact the anti-*Borrelia* immune response, with robust *Bb*-specific IgM production (Fig 6.2D), successful class-switching to IgG (Fig 6.2E), and spirochete clearance from the joint (Fig 6.2F) similar to that seen in control mice. As in Figure 6.1, these data demonstrate that sleep fragmentation does not alter arthritis development by 21 dpi or interfere with the formation of an effective anti-*Borrelia* immune response.

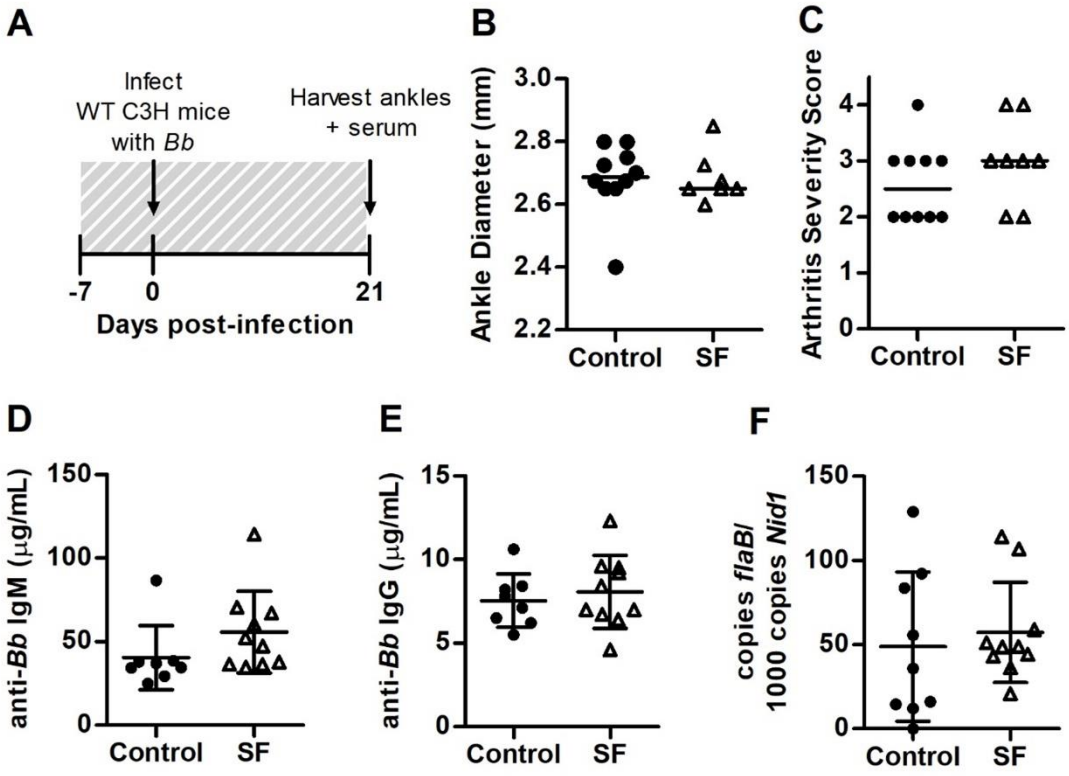

Figure 6.2. Priming with sleep fragmentation does not affect mLA severity in WT mice.

(A) A group of C3H mice were placed in a SF housing unit for 7 days prior to infection with *Bb* and then returned to the SF unit for 21 more days before sacrifice and sample harvest. Control mice were infected with *Bb* and housed in normal housing before sacrifice on D21. Shaded area represents time spent in sleep conditions. (B) Ankle diameter was measured on D21 in both the control and SF groups. n=7-10/group. (C) Ankle joint sections were histologically scored to determine arthritis severity (scale 0-4). n=8-10/group. *Bb*-specific IgM (D) and IgG (E) were measured from D21 serum by ELISA. n=8-10/group. (F) *Bb* levels were quantified in ankles at D21 by qPCR. n=9-10/group. Bar is median in B&C. No significance found by t-test (B, D-F) or Mann-Whitney test (C) where significance is defined as $p<0.05$. (Mice were infected and data from panels B&C were collected and graphed by C. R. Brown.)

Sleep fragmentation impairs mLA resolution in WT C3H mice

As we did not find that SF worsened mLA development by 21 dpi, we sought to determine if SF would instead have an impact on mLA resolution. We hypothesized that the proinflammatory effects of SF could inhibit or outweigh the anti-inflammatory and pro-resolving mechanisms required for arthritis resolution, delaying or preventing efficient resolution of mLA. To test this hypothesis, WT C3H mice were infected with *B. burgdorferi* as before and Lyme arthritis was allowed to develop for 21 days, after which one group of mice was subjected to SF for four weeks and a control group was left alone. Mice were sacrificed at 49 dpi and mLA parameters were measured (Fig 6.3A). Ankle swelling was measured at baseline (0 dpi, uninfected), at 21 dpi for the peak of edema, and at 49 dpi to measure edema resolution. While control mice had nearly cleared their edema by 49 dpi, SF mice maintained elevated ankle swelling at this time point (Fig 6.3B). This failure to resolve edema in SF mice was mirrored by a failure to resolve arthritis as efficiently as controls by 49 dpi, with some sleep-fragmented mice still exhibiting robust arthritis even as control mice were resolving (Fig 6.3C). While starting experimental SF after 21 dpi should not interfere with the formation of an anti-*Borrelia* host response (Fig 6.1&6.2 controls), we checked if sleep fragmentation during the mLA resolution phase could still affect the clearance of bacteria from the joint. As expected, *B. burgdorferi*-specific IgM and IgG from serum were not different from control mice at 49 dpi (Fig 6.3D&E). Indeed, the total amount of circulating IgM dropped as expected at this late infection time point, and the total amount of IgG increased in

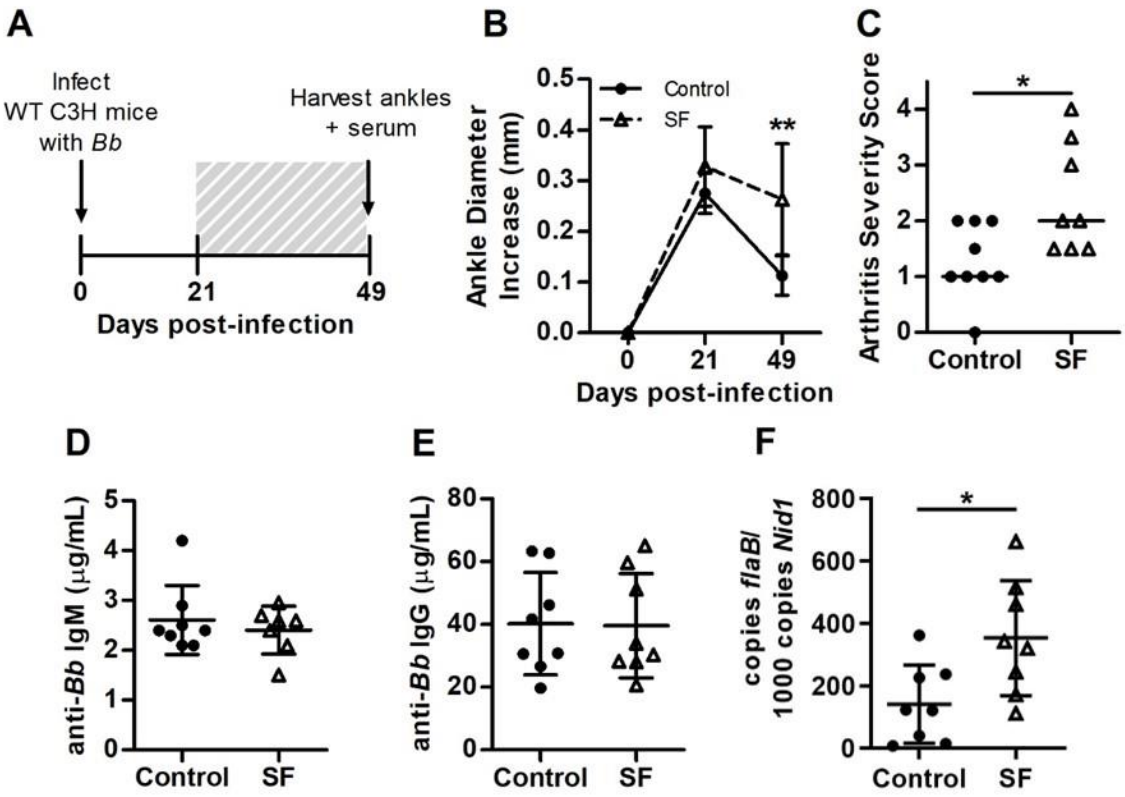

Figure 6.3. Experimental sleep fragmentation disrupts mLA resolution in WT mice.

(A) C3H mice were infected with *Bb* and left in normal housing for 21 days, after which one group of mice were transferred to a SF housing unit for 28 days while the control mice remained in normal housing. On D49, all mice were sacrificed and samples were collected for analysis. Shaded area represents time spent in sleep conditions. (B) Ankle diameter was measured at baseline (D0), on D21 before SF began, and at sacrifice on D49. Ankle swelling curve displayed as diameter change from baseline (D0). n=8/group. (C) Ankle joint sections were histologically scored to determine arthritis severity (scale 0-4). n=8/group. *p<0.05 by Mann-Whitney test and the bar is the median. *Bb*-specific IgM (D) and IgG (E) were measured from D49 serum by ELISA. n=8/group. (F) *B. burgdorferi* levels were quantified in ankles at D49 by qPCR. n=8/group. *p<0.05, **p<0.01 by t-test between strains/timepoint in B&F.

Table 6.1. Altered transcriptional regulation of inflammatory cytokines and receptors in the arthritic ankles of SF mice at 49 dpi.
Relative transcript expression in SF mice was calculated by -ΔΔCt of each gene normalized to housekeeping gene *Gapdh* and relative to control mice. Genes ordered from highest to lowest relative expression.

Gene symbol	*Gene name*	*Relative expression*
Cxcr5	Chemokine (C-X-C motif) receptor 5	6.50
Cxcl13	Chemokine (C-X-C motif) ligand 13	3.07
Tnf	Tumor necrosis factor	2.83
Ccr1	Chemokine (C-C motif) receptor 1	2.50
Ccl8	Chemokine (C-C motif) ligand 8	2.39
Tnfrsf11b	TNF receptor superfamily, member 11b	2.04
Il1rn	Interleukin 1 receptor antagonist	2.02
Ccl22	Chemokine (C-C motif) ligand 22	0.47
Cxcl15	Chemokine (C-X-C motif) ligand 15	0.46
Ccl9	Chemokine (C-C motif) ligand 9	0.45
Il4	Interleukin 4	0.45
Ccl19	Chemokine (C-C motif) ligand 19	0.44
Ccr4	Chemokine (C-C motif) receptor 4	0.39
Il1a	Interleukin 1 alpha	0.37
Osm	Oncostatin M	0.37
Il21	Interleukin 21	0.31
Csf3	Colony stimulating factor 3 (granulocyte)	0.30
Fasl	Fas ligand (TNF superfamily, member 6)	0.22
Tnfsf4	TNF (ligand) superfamily, member 4	0.21
Il7	Interleukin 7	0.19
Il2rb	Interleukin 2 receptor, beta chain	0.16
Ccr8	Chemokine (C-C motif) receptor 8	0.12
Ifng	Interferon gamma	0.07

comparison to 21 dpi controls from Fig 6.1&6.2, indicating that antibody response kinetics were still intact. However, though the antibody levels were similar between groups, mice which underwent SF had a higher bacterial burden in the ankle joint at 49 dpi, indicating a defect in antibody-mediated clearance of the spirochete from the joint (Fig 6.3F). Certainly, it can be expected that inefficient removal of *Bb* from the site of infection would require a continued proinflammatory response and contribute to the delayed mLA resolution seen in SF group mice.

Cytokines and chemokines play critical roles in regulating sleep, host response to infection, and inflammation (as rev. in [122]), so we measured the differential transcription of cytokines and chemokines in the arthritic ankles of poorly-resolving SF mice as compared to control mice at 49 dpi (Appendix II). Of the genes tested, 23 were significantly altered in SF mice (Table 6.1). Among these, tumor necrosis factor (TNF) transcript was significantly upregulated and Fas ligand (FasL) transcript was significantly downregulated in SF mice. *Bb* infection induces TNF-alpha production both *in vitro* in human PBMCs and murine BMDMs [77, 133] and *in vivo* in mice [134]. Thus, it is unsurprising that TNF transcript would be upregulated in SF ankles considering spirochete burdens were higher in these mice. Therefore, an increase in TNF, a canonically proinflammatory cytokine, could contribute to the maintenance of an inflammatory state. Similarly, a decrease in FasL transcript may also contribute to a proinflammatory environment. While it has not been specifically studied in

this mLA model, Fas:FasL interactions may induce apoptosis of infiltrating inflammatory cells. Apoptosis of inflammatory infiltrate is a critical component of inflammation resolution in mLA [77]. If SF indeed suppresses FasL expression, the infiltrating inflammatory cells may persist at the site of inflammation, preventing efficient mLA resolution as seen in these experiments. Further work is required to investigate the mechanism of SF-impaired clearance of *Bb* from arthritic joints in WT C3H mice.

Sleep fragmentation does not affect arthritis resolution in BLT1/2$^{-/-}$ C3H mice

In C3H mice, mLA is self-limiting, with arthritis resolution correlated with bacterial clearance from the joint [94]. However, it has been previously demonstrated that disruption of bioactive lipid mediator synthesis or signaling has a negative impact on inflammation control, leading to a defect in arthritis resolution in these mice [71-73]. As SF interfered with the timely resolution of mLA in WT C3H mice by hampering spirochete clearance, we wanted to determine if SF would have a similar, compounding effect on inflammation in mice with non-resolving arthritis. We had preliminarily characterized a mLA resolution defect in C3H mice deficient in both BLT1 and BLT2 (BLT1/2$^{-/-}$), the high- and low-affinity receptors for bioactive lipid mediator leukotriene B_4 (LTB_4) (data not shown; similar phenotype to BLT1$^{-/-}$ as described in [73]). Therefore, we tested whether SF would affect mLA resolution in non-resolving BLT1/2$^{-/-}$ C3H mice by infecting these mice with *B. burgdorferi* and allowing arthritis to develop

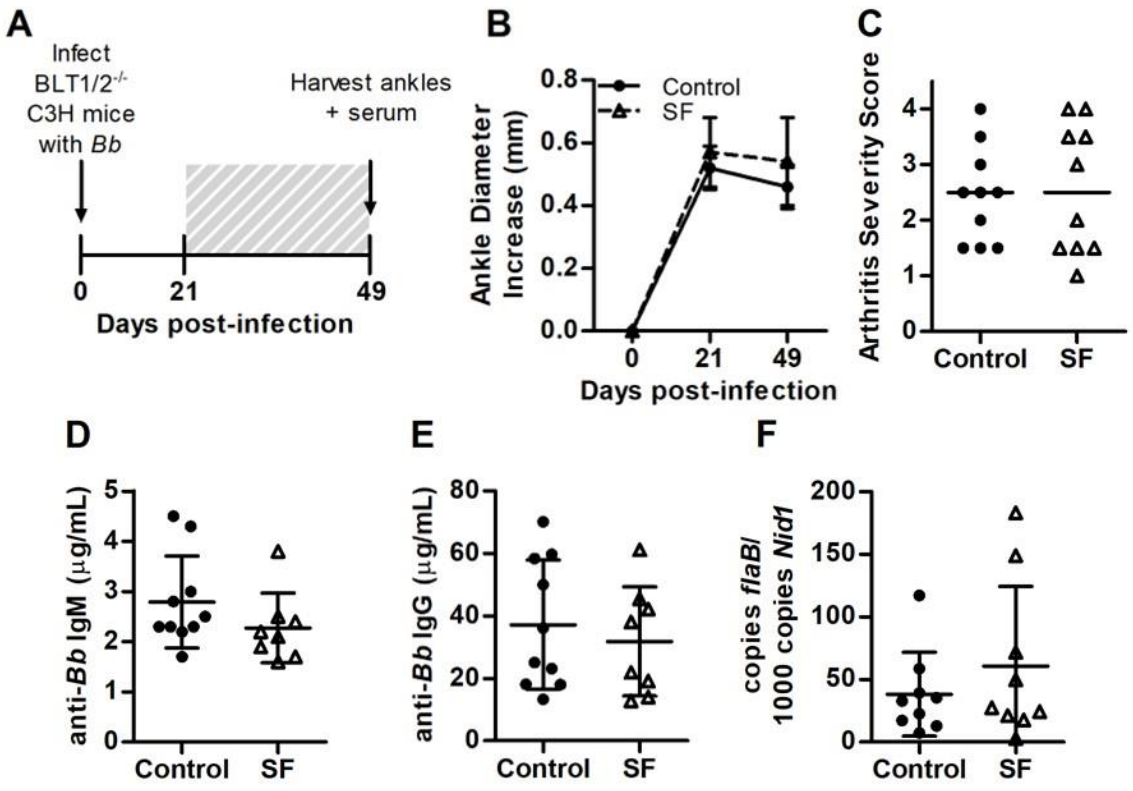

Figure 6.4. Experimental sleep fragmentation does not affect mLA outcomes in BLT1/2$^{-/-}$ mice.

(A) BLT1/2$^{-/-}$ C3H mice were infected with *Bb* and left in normal housing for 21 days, after which one group of mice were transferred to a SF housing unit for 28 days while the control mice remained in normal housing. On D49, all mice were sacrificed and samples were collected for analysis. Shaded area represents time spent in sleep conditions. (B) Ankle swelling curve displayed as diameter change from baseline (D0). n=10/group. (C) Ankle joint sections were histologically scored to determine arthritis severity (scale 0-4). n=10/group. Bar is median. *Bb*-specific IgM (D) and IgG (E) were measured from D49 serum by ELISA. n=8-10/group. (F) *B. burgdorferi* levels were quantified in ankles at D49 by qPCR. n=9/group. No significance found by t-test (B, D-F) or Mann-Whitney U test (C) where significance is defined as $p<0.05$.

for 21 days. We then transferred one group to SF housing for four weeks and left the other group alone before sacrificing at 49 dpi and measuring mLA resolution (Fig 6.4A). We confirmed that, contrary to WT C3H mice, BLT1/2$^{-/-}$ mice do not readily resolve edema or arthritis severity by 49 dpi, but this phenotype was not altered by SF (Fig 6.4B&C). However, despite defective arthritis resolution, both control and sleep-fragmented BLT1/2$^{-/-}$ mice had similar serum IgM and IgG, as well as similar *Bb* burdens in the joint (Fig 6.4D-F). More experiments are needed to determine why bacterial control was not affected in SF group BLT1/2$^{-/-}$ mice as it was in SF group WT mice. These data indicate that sleep fragmentation during mLA resolution phase does not have an additive effect in a model that already has defective arthritis resolution.

Conclusion

In this study, we investigated the effect of SF on both the development and resolution of Lyme arthritis in C3H/HeJ mice infected with *Bb*. SF during arthritis development (0-21 dpi) had no effect on arthritis development or the formation of an anti-*Borrelia* immune response. Further, extending SF to seven days prior to infection (-7 through 21 dpi) likewise had no effect on mLA development or spirochete clearance from the joint, suggesting that SF does not exacerbate ankle edema or arthritis severity in these mice. However, SF during resolution-phase mLA (21-49 dpi) did interfere with efficient inflammation resolution in WT C3H mice, as shown by increased ankle edema and joint inflammation by 49 dpi in sleep-fragmented mice compared to controls. This exacerbated arthritis in SF

mice may be partially due to ineffective bacterial control, as SF mice had significantly elevated *Bb* burdens in the arthritic joints. Further, transcript for several cytokines and chemokines were alternatively regulated in SF mice, which may contribute to increased inflammation and delayed arthritis resolution. Lastly, we determined whether SF during WT resolution-phase timepoints (21-49 dpi) would have a confounding or compounding effect on arthritis in non-resolving BLT1/2$^{-/-}$ mice and found no difference between mice with SF versus control mice. Overall, these findings demonstrate the importance of sleep in the proper clearance of *Bb* and timely resolution of mLA in C3H mice.

CHAPTER 7

DISCUSSION

Eicosanoids regulate inflammation resolution

The role of 12/15-LO and LXA_4 in mLA resolution

In the studies outlined in Chapter 3, we sought to determine the role of 12/15-LO and downstream metabolites in the development and resolution of mLA. Although we presumed that 12/15-LO would contribute to resolution via LXA_4 and SPM production, several 12/15-LO metabolites have been measured out of joints throughout mLA in C3H mice, including proinflammatory lipids 12- and 15-hydroxyeicosatetranoic acid (HETE) [135, 136]. Despite this, 12/15-$LO^{-/-}$ C3H mice were capable of developing mLA to a similar extent as WT C3H mice, indicating that proinflammatory metabolites downstream of 12/15-LO are not required for mLA development. On the other hand, 12/15-$LO^{-/-}$ mice did not readily resolve mLA, retaining significant ankle edema and inflammatory infiltrate even as WT mLA resolved (Fig 3.2&4). These results appear to confirm our hypothesis that pro-resolving lipids downstream of 12/15-LO activity are required for mLA resolution.

We have previously demonstrated that neither COX-$2^{-/-}$ nor 5-$LO^{-/-}$ mice resolve mLA despite equivalent bacterial control to WT mice, indicating a critical role for metabolites downstream of both COX-2 and 5-LO in mLA resolution [71, 72]. Here we report a similar finding in 12/15-$LO^{-/-}$ mice, where joint bacterial burdens are controlled to the same extent as in WT mice, but arthritis is not resolved (Fig

3.3). As COX-2 products, 5-LO, and 12/15-LO can cooperate in lipoxin and SPM synthesis [49, 57, 96], the non-resolution phenotype seen in COX-2$^{-/-}$, 5-LO$^{-/-}$, and 12/15-LO$^{-/-}$ mice despite spirochete clearance from the joint may be due to a shared defect of LXA_4 and SPM production. Further, as 12/15-LO$^{-/-}$ mice fail to efficiently resolve arthritis despite efficient bacterial control, these findings implicate 12/15-LO as a therapeutic target to reduce inflammation in human pLA.

LXA_4 and SPM can promote macrophage clearance of apoptotic cells in the inflamed site, during which macrophages can be remodeled towards a pro-resolution phenotype through a positive feedback loop [59, 61, 63]. This key step in inflammation resolution also ensures that apoptotic cells do not progress towards necrosis, during which they would release their cellular components as DAMPs and thereby amplify inflammation [62]. Here we report that 12/15-LO$^{-/-}$ ankle joints had persistent macrophage and neutrophil infiltration at 28 and 35 dpi, despite clearance of these populations in WT mice.

Subsequent *in vitro* experiments suggested that the prolonged presence of inflammatory cells in 12/15-LO$^{-/-}$ ankles could be due to a defect in the efferocytic clearance of 12/15-LO$^{-/-}$ AN by macrophages. Apoptotic cells promote their own efferocytosis via the secretion of “find me” signals and the surface expression of “eat me” signals [62], so a defect in the production of these signaling molecules could be responsible for poor efferocytosis. Therefore, we measured the expression levels of key “eat me” signal phosphatidylserine on the surface of

apoptotic BMN. This experiment also served as a control to determine if the suboptimal phagocytosis of 12/15-LO AN seen *in vitro* was due to a defect in the induction of apoptosis in the BMN culture. However, after 24 hours in culture, a larger proportion of 12/15-LO$^{-/-}$ AN in the culture were undergoing apoptosis, expressing higher levels of phosphatidylserine by both proportion of culture and MFI, than did WT AN under similar conditions. Further, a higher proportion of cells in these 12/15-LO AN cultures were also expressing 7-AAD (Fig 3.5D), a molecule which selectively intercalates into GC-rich DNA regions, demonstrating that these cells had increased membrane permeability/damage. AnxV^{+}7-AAD^{+} cells are sometimes called “late apoptotic,” but these are cells which have passed through stages of apoptosis and are now undergoing secondary necrosis [137]. This means that in our experiment, not only was a higher proportion of the 12/15-LO$^{-/-}$ AN culture undergoing apoptosis, but a higher proportion of these cells versus WT AN had progressed to secondary necrosis by 24 hpi. At the very least, these results indicate that the defective uptake of 12/15-LO$^{-/-}$ AN cells cocultured with BMDM was not due to decreased frequency of apoptotic cells in 12/15-LO$^{-/-}$ versus WT AN cultures. However, these findings suggest that 12/15-LO$^{-/-}$ AN may have an intrinsic defect hampering their efferocytosis that could make them more difficult to clear *in vivo*, which may explain persistent neutrophil presence in these mice late during the mLA time course. Further studies should attempt to identify the surface or soluble mediator(s), or lack thereof, that may contribute to the decreased efferocytosis of 12/15-LO$^{-/-}$ AN and determine if these *in vitro* findings reflect what is happening *in vivo*.

An alternative explanation for the persistent infiltrate seen in 12/15-LO$^{-/-}$ mice is that LXA_4 and several resolvins are known for their ability to inhibit neutrophil extravasation into the site of inflammation [138, 139]. Thus, it may be possible that 12/15-LO$^{-/-}$ mice lacking these mediators could have unchecked neutrophil extravasation into the site of inflammation, making it difficult for arthritis to resolve. However, LXA_4 inhibition of neutrophil trafficking is largely antagonistic of LTB_4- and fMLP-mediated trafficking [58], while the dominant mediator of neutrophil chemotaxis in our model is CXCL1/KC, without which arthritis does not develop [79]. To my knowledge, there is currently only one study that has investigated the interaction between LXA_4 and CXCL1, and it demonstrates that treatment of zymosan-induced arthritis with exogenous LXA_4 significantly reduces the levels of CXCL1 in the joint [93]. Therefore, while LXA_4 treatment may ultimately hamper CXCL1-mediated neutrophil chemotaxis by reducing available CXCL1, it has not been shown to directly counter CXCL1 signaling. Future studies could delineate neutrophil recruitment kinetics in 12/15-LO$^{-/-}$ mice to determine if persistent neutrophil infiltrate in the joint at 35 dpi is being freshly recruited, is being ineffectively efferocytosed, or some combination of the two.

Studies in a variety of inflammatory disease models have investigated the therapeutic efficacy of LXA_4 and SPM, alone and in combination with other treatments [64, 65]. Here we sought to determine if exogenous LXA_4 alone could hasten mLA resolution in WT mice if delivered near the peak of inflammation. In agreement with previous studies [140, 141], we saw that LXA_4 reduced ankle

edema within days of its administration, and this decrease was maintained for at least the next two weeks (Fig 3.7). LXA_4 treatment also acutely increased the number of reparative macrophages and reduced the number of inflammatory macrophages in the joint compared to control mice (Fig 3.8). This is in line with known effects of LXA_4 signaling through mFpr2 in mice to reprogram macrophages towards a pro-resolution phenotype [142]. Further, as exogenous LXA_4 can either impair or enhance bacterial control depending on the sepsis model [101, 143], we confirmed that exogenous LXA_4 did not interfere with the formation of an anti-*Borrelia* antibody response and control of spirochete numbers in the joint.

Despite the observed effects of LXA_4 on edema and cellular infiltrate into the WT mLA joint, the chosen treatment regimen was not sufficient to hasten arthritis resolution by 35 dpi, at which point mLA was nearly resolved in both the VC- and LXA_4-treated mice. Improvements to the treatment regimen could include direct intra-articular injection of LXA_4 and repeated, frequent doses of LXA_4 until resolution. Further, as its rapid degradation causes LXA_4 to lose biological activity [99], several stable LXA_4 analogs and synthetic LXA_4 mimetics have been designed which maintain the pro-resolving actions of native LXA_4 [64, 139]. Indeed, LXA_4 mimetic AT-01-KG has been shown to ameliorate joint inflammation in mouse models of gout and adjuvant-induced arthritis [144], so using these LXA_4 analogs may yield better results in mLA than LXA_4. Lastly, as endogenous lipid mediators work in concert to resolve inflammation, a

combinatorial approach whereby LXA_4 is delivered with another SPM may further improve mLA outcomes.

While improvements could be made to the treatment regimen, our experimental administration of exogenous LXA_4 indeed demonstrated that LXA_4 could be a useful therapeutic in treating human LA. A hallmark of LA is severe swelling, but treatment with anti-inflammatory drugs during active infection would likely be detrimental to bacterial control. However, according to our findings, treatment of LA patients with LXA_4 or a stable LXA_4 analog may reduce joint edema without compromising the anti-*Borrelia* host response. This demonstrates that LXA_4, and possibly other SPM, could serve as a useful co-therapy to help reduce uncomfortable symptoms and support the formation and/or amplification of a pro-resolving program in human LA patients.

The role of mPGES-1-produced PGE_2 in mLA

In the studies described in Chapter 4, we investigated the role of PGE_2 in mLA using mPGES-$1^{-/-}$ mice. We know that COX-2 knockout results in a mLA resolution defect in C3H mice; likewise, inhibition of COX-2, even only through 14 dpi, also prevented timely arthritis resolution [71]. PGE_2 is the most highly upregulated AA-derived COX-2 product during early mLA [74] and, despite its many proinflammatory actions, has been shown to contribute to lipid mediator class switching towards lipoxin and SPM production. Indeed, PGE_2 was recently shown to drive resolution of neutrophilic inflammation by this mechanism [116].

Phagocytosis of apoptotic neutrophils has been shown to boost PGE_2 production by macrophages as a part of their post-efferocytic pro-resolving reprogramming [145]. This could explain the second peak of PGE_2 during mLA (28 dpi), as the population of apoptotic neutrophils and macrophages is highest at this timepoint and is significantly decreased by 35 dpi in WT mice [77]. These findings led us to hypothesize that while proinflammatory PGE_2 signals were dispensable for mLA development in COX-$2^{-/-}$ mice, PGE_2 activity around both its peaks is required to effectively resolve arthritis. However, our hypothesis was immediately rejected when we saw that while mPGES-$1^{-/-}$ mice indeed developed mLA as COX-$2^{-/-}$ mice do, mPGES-$1^{-/-}$ mice are still able to efficiently resolve arthritis by 35 dpi (Fig 4.2). In fact, it appears as if mPGES-$1^{-/-}$ mice may resolve mLA more efficiently than WT mice do, with significantly reduced ankle edema, arthritis severity, and neutrophil and macrophage populations by 28-35 dpi (Fig 4.2&3). These findings suggest that a prostanoid(s) aside from PGE_2 is required for inflammation resolution.

Part of the mechanism behind faster mLA resolution in mPGES-$1^{-/-}$ mice may be that they control *Bb* infection better than WT mice do (Fig 4.4). There is no difference in the kinetics or magnitude of the humoral response in mPGES-$1^{-/-}$ versus WT mice, so it may be that bacterial killing by immune cells is enhanced in mPGES-$1^{-/-}$ mice. While there is some conflicting evidence [146], PGE_2 has largely been described to inhibit the phagocytosis of bacterial and fungal pathogens by both macrophages and neutrophils [147-149]. Thus, the absence

of phagocytosis antagonism by PGE_2 may contribute to enhanced bacterial control in mPGES-$1^{-/-}$ mice. Alternatively, *Bb* may not be able to colonize mPGES-$1^{-/-}$ joints as efficiently as WT joints, but further studies are required to determine the peak of *Bb* burdens in mPGES-$1^{-/-}$ ankles during mLA.

We originally hypothesized that PGE_2 would contribute to mLA resolution by upregulating 12/15-LO transcription, thereby potentiating lipid class switching towards lipoxin and SPM production. However, as mPGES-$1^{-/-}$ mice fully resolved mLA, we hypothesized that other factors were sufficient to induce 12/15-LO and facilitate resolution. As in WT mice, *Bb*-infected mPGES-$1^{-/-}$ mice significantly upregulated *Alox15* transcript at 28 dpi (Fig 4.5A). Further, mPGES-$1^{-/-}$ BMDM were capable of producing LXA_4 in response to *Bb* stimulus (Fig 4.5B), both confirming that 12/15-LO induction and LXA_4 production still occur in the absence of PGE_2, necessitating identification of the factors that do contribute to 12/15-LO induction. This does not mean that PGE_2 cannot help facilitate SPM production in mLA, but there is not yet evidence supporting this hypothesis. The experiment that the Fig 4.5B data comes from also had groups looking at the production of LXA_4 when 40nmol PGE_2 was added to the culture. While there was a slight increase in groups which had received PGE_2 compared to their controls, the addition of PGE_2 did not significantly boost LXA_4 production by mPGES-$1^{-/-}$ or WT BMDM +/- *Bb* (MOI 10; data not shown). Therefore, we have yet to determine whether endogenous PGE_2 affects mLA resolution or if PGE_2 alters the can facilitate lipid class switching in the context of *Bb* infection.

We must also consider that PGE_2 deficiency may result in an inflammatory response quite different to that found during mLA in WT mice. As with manipulation of any enzymatic system, disruption of intricate feedback loops and alterations in substrate availability may have off-target effects. If the PGE_2 precursor PGH_2 is produced to the same level in mPGES-$1^{-/-}$ as in WT mice, then there is likely more bioavailable PGH_2 in mPGES-$1^{-/-}$ mice which could be shunted towards the production of other prostanoids [51]. In this case, we may hypothesize that because infection and arthritis are cleared faster, the lack of PGE_2 synthesis allows more substrate to be shunted towards increased production of PGD_2 and/or 15d-PGJ_2, considered the more anti-inflammatory prostanoids [150-152]. Among other mechanisms, both PGD_2 signaling through the ubiquitous D prostanoid receptor DP1 and 15d-PGJ_2 activation of peroxisome proliferator-activated receptor γ (PPARγ) dampen inflammation by antagonizing NF-κB-mediated inflammatory cytokine and chemokine production by macrophages [150, 153]. PGD_2 is also capable of inducing 12/15-LO transcription in a similar manner to PGE_2 [49], so it may support lipoxin and SPM production. Both PGD_2 and 15d-PGJ_2 are upregulated during mLA in WT mice, with their highest concentrations during early mLA (3-14 dpi) [135]. Indeed, this finding may fit with our previous report that inhibition of COX-2 up to 14 dpi prevented arthritis resolution. Thus, if we presume they are being made to similar or higher levels in mPGES-$1^{-/-}$ mice as in WT mice, their anti-inflammatory actions may potentiate improved arthritis resolution in the absence of PGE_2. Indeed, some studies have suggested that the PGE_2:PGD_2 ratio may be a

relevant factor mediating inflammation, with higher PGE_2 associated with inflammatory conditions [151, 154]. If this were the case in our model, then a predomination of PGD_2 over PGE_2 in mPGES-$1^{-/-}$ mice may shift the balance towards amelioration of inflammation.

Ultimately, it is possible that PGE_2 deficiency could so alter the inflammatory milieu that any attempt to delineate the mechanisms of mLA inflammation in mPGES-$1^{-/-}$ mice may have no correlate to WT mice. Characterization of bioactive lipid production throughout mLA in mPGES-$1^{-/-}$ mice and elucidating the mechanism of enhanced *Bb* clearance in these mice may help to discern what effects in mPGES-$1^{-/-}$ mice may be directly attributable to a lack of PGE_2, if any, and may potentially identify other key prostanoids.

While PGE_2 was not required for mLA resolution in mPGES-$1^{-/-}$ mice, we still wondered what effect PGE_2 addback would have on overall arthritis outcomes. PGE_2 addback near the peak of inflammation did not significantly alter arthritis severity or immune cell populations in the joint (Fig 4.6). However, we may anecdotally observe that many of the treated mice had higher severity scores than the mPGES-$1^{-/-}$ mice in Figure 4.2, which may indicate that the injection and/or treatments may affect inflammation resolution in some mice. Future inclusion of a mPGES-$1^{-/-}$ mouse no-treatment control would address this discrepancy.

In contrast, early PGE_2 addback resulted in significantly increased arthritis severity and more neutrophils in the joint compared to VC controls (Fig 4.7). These findings may support the hypothesis that disruption of early inflammation mechanics can negatively impact inflammation resolution. This may also point back to the proposed importance of the PGE_2:PGD_2 ratio, as it is possible that an acute shift towards higher PGE_2 presence in the joint could disrupt the inflammatory balance enough to eventually lead to exacerbated arthritis severity. These experiments emphasize the importance of inflammatory context to the activity of PGE_2.

Overall, the data in this chapter demonstrates that PGE_2 is not required for mLA development or resolution, nor is it required for induction of 12/15-LO and downstream SPM production. This does not mean that PGE_2 is not involved in mediating inflammation in WT mice but may instead exemplify the elasticity of the inflammatory response, with built-in redundancies and compensatory mechanisms to best protect the host from infection and disease.

Other factors influencing inflammation resolution

Neutrophil rTEM

Clearance of inflammatory infiltrate from the site of infection is a critical part of inflammation resolution. As neutrophils are the predominant immune cell type in arthritic joints during mLA, their apoptosis and subsequent efferocytosis by macrophages boosts inflammation resolution by reprogramming those

macrophages towards a pro-resolving phenotype [62]. However, rTEM is an alternative mechanism by which neutrophils could be cleared from the site, potentially reducing the burden of apoptotic and post-apoptotic cleanup required at the site of inflammation.

Chapter 5 describes a project in which we designed and began initial characterization of a novel *in vivo* staining method that would allow us to visualize and track neutrophils which have infiltrated the knee in response to infection or trauma. Presumably, these stained neutrophils being anywhere in the body other than the knee would indicate that the neutrophil had undergone rTEM and reentered the circulation. We are confident that we can stain these cells, but we are currently limited in the conclusions we can make. Currently, we are equipped to stain the mice and then harvest organs later to see if stained neutrophils are showing up there. While this appears to confirm that rTEM is occurring, it does not allow us to determine kinetics or frequency of rTEM from the knee or identifying a particular pattern in which the cells could be trafficking throughout the body post-rTEM. Previous researchers found that rTEM neutrophils trafficked first to the lung and then to the bone marrow [84, 115], so we looked for stained cells in both these places and found them (Fig 5.5&6). However, we still cannot discern if this trafficking pattern is common to all or the majority of rTEM neutrophils or where else in the body rTEM neutrophils may go.

This project is still in its early stages, so there are plenty of directions to take this

work. There is no published research on rTEM in the context of infectious inflammation, so future work should focus on identifying what determines whether neutrophils undergo apoptosis or rTEM. We hypothesize that only neutrophils which do not encounter PAMPs would undergo rTEM. We propose that infiltrating neutrophils that encounter *Bb* PAMPs would then either phagocytose or kill *Bb* and then undergo apoptosis at the site in an attempt to retain proinflammatory components at the site of inflammation. In contrast, responding neutrophils which do not encounter PAMPs, but instead DAMPs or anti-inflammatory/pro-resolving mediators, will be able to undergo rTEM. Further, regardless of the stimulus that the neutrophil encounters, the vasculature must be potentiated for rTEM [117, 118] and there will likely be need for a chemokine gradient [84]. Roles have also been described for PGE_2 and LTB_4 in promoting rTEM [116-118], so we can utilize our knockout mice and inhibitors to test their contribution to rTEM in an infectious inflammation model, too.

Sleep

Chapter 6 details a collaborative project we undertook with Drs. Gozal and Khalyfa in the University of Missouri School of Medicine. Their area of expertise is sleep, so we teamed up to determine the effects of experimental sleep fragmentation on mLA development and resolution in mice. Neither schema of SF during arthritis development exacerbated arthritis or affected resolution (Fig 6.1&2). However, SF starting around the peak of inflammation and continuing through the typical resolution phase prevented efficient mLA resolution in WT

mice (Fig 6.3). This was at least partly due to defective bacterial clearance from the joint (Fig 6.3F). There was no difference between the amount of *Bb*-specific IgM and IgG in SF mice compared to controls at 49 dpi, so defective phagocytosis or killing of the pathogen by innate immune cells may be responsible for elevated *Bb* burdens in the joint. Analysis of inflammatory cytokines and receptor transcript in the joints of non-resolving mice identified several genes that were significantly altered by 49 dpi following SF (Table 6.1). It is not possible to discern from these experiments whether transcription of these genes was altered by SF or by the elevated *Bb* burden, or both. Several of the differentially regulated genes could be related to development and maintenance of adaptive immune cells at the site, so it may be worthwhile to investigate the effects of SF on T and B cell populations and biology in the joint.

Conclusion

The work contained in this dissertation substantially contributes to our understanding of inflammation resolution in a murine model of Lyme arthritis. We demonstrate that 12/15-LO is required for efficient arthritis resolution in mLA, as 12/15-LO$^{-/-}$ mice have exacerbated ankle swelling and arthritis severity, as well as persistent immune infiltrate. We confirm that this non-resolution is not due to elevated *Bb* burdens in the joint, but *in vitro* findings indicate that defective efferocytosis of apoptotic 12/15-LO$^{-/-}$ neutrophils may be partially responsible for late neutrophil population persistence. We also show that exogenous LXA_4 significantly reduces ankle edema and remodels joint infiltrate populations

towards a pro-resolving phenotype. PGE_2 has previously been presumed to be a key component of the development and resolution of mLA, but we demonstrated that PGE_2 was dispensable for the inflammatory response during mLA, as mPGES-$1^{-/-}$ mice both develop and efficiently resolve mLA. In fact, mPGES-$1^{-/-}$ mice appeared to resolve mLA more efficiently than WT mice, with significantly lower arthritis severity, joint immune cell populations, and *Bb* burdens in the joint by 35 dpi. PGE_2 addback to mPGES-$1^{-/-}$ mice during early arthritis development led to exacerbated arthritis and higher neutrophil populations in the joint by 35 dpi, demonstrating the importance of early inflammatory processes on resolution outcomes. We also designed and tested an *in vivo* staining method by which we can track cells that have visited a specific tissue. We successfully utilized this method to demonstrate that some neutrophils responding to inflammatory stimuli in the knee joint undergo reverse transendothelial migration and reenter the vasculature, showing up in the lung before trafficking back to the bone marrow to presumably undergo apoptosis. We also showed that experimental sleep fragmentation for one month after the peak of inflammation (21-49 dpi) resulted in a resolution defect in WT mice which could be partially due to elevated *Bb* burdens persisting in the joint. Future studies will investigate the utility of other SPM to improve mLA outcomes. In addition, we should determine the bioactive lipid composition of the arthritic joint in mPGES-$1^{-/-}$ mice throughout mLA in order to understand how they appear to resolve more arthritis more efficiently than WT mice. We should also investigate why there appears to be enhanced *Bb* control in mPGES-$1^{-/-}$ joints. Future rTEM studies should first focus on more fully

characterizing neutrophil response kinetics and trafficking following needle injury in the knee, then investigate the roles of bioactive lipid mediators in facilitating rTEM.

REFERENCES

1. Kugeler KJ, Schwartz AM, Delorey MJ, Mead PS, and Hinckley AF. 2021. Estimating the frequency of Lyme Disease diagnoses, United States, 2010-2018. *Emerg Infect Dis*. 27(2): p. 616-619.
2. Burgdorfer W, Barbour AG, Hayes SF, Benach JL, Grunwaldt E, and Davis JP. 1982. Lyme Disease- A tick-borne spirochetosis? *Science*. 216: p. 1317-1319.
3. Ostfeld RS and Brunner JL. 2015. Climate change and *Ixodes* tick-borne diseases of humans. *Philos Trans R Soc Lond B Biol Sci*. 370(1665).
4. Stanek G and Strle F. 2018. Lyme borreliosis-from tick bite to diagnosis and treatment. *FEMS Microbiol Rev*. 42(3): p. 233-258.
5. Steere AC, Malawista SE, Snydman DR, Shope RE, Andiman WA, Ross MR, and Steele FM. 1977. Lyme arthritis: an epidemic of oligoarticular arthritis in children and adults in three Connecticut communities. *Arthrits Rheum*. 20(1): p. 7-17.
6. Steere AC, Grodzicki RL, Kornblatt AN, Craft JE, Barbour AG, Burgdorfer W, . . . Malawista SE. 1983. The spirochetal etiology of Lyme disease. *N Engl J Med*. 308(13): p. 733-740.
7. Hyde FW and Johnson RC. 1984. Genetic relationship of Lyme disease spirochetes to *Borrelia*, *Treponema*, and *Leptospira* spp. *J Clin Microbiol*. 20(2): p. 151-154.

8. Kurtenbach K, Hanincova K, Tsao JI, Margos G, Fish D, and Ogden NH. 2006. Fundamental processes in the evolutionary ecology of Lyme borreliosis. *Nat Rev Microbiol*. 4(9): p. 660-669.

9. Strle F and Stanek G. 2009. Clinical manifestations and diagnosis of Lyme borreliosis. *Curr Prob Dermatol*. 37: p. 51-110.

10. Rudenko N, Golovchenko M, Grubhoffer L, and Oliver JH, Jr. 2011. Updates on *Borrelia burgdorferi sensu lato* complex with respect to public health. *Ticks Tick Borne Dis*. 2(3): p. 123-128.

11. Mulay VB, Caimano MJ, Iyer R, Dunham-Ems S, Liveris D, Petzke MM, . . . Radolf JD. 2009. *Borrelia burgdorferi* bba74 is expressed exclusively during tick feeding and is regulated by both arthropod- and mammalian host-specific signals. *J Bacteriol*. 191(8): p. 2783-2794.

12. Schwan TG and Piesman J. 2000. Temporal changes in outer surface proteins A and C of the Lyme Disease-associated spirochete, *Borrelia burgdorferi*, during the chain of infection in ticks and mice. *J Clin Microbiol*. 38(1): p. 382-388.

13. Piesman J, Mather TN, Sinsky RJ, and Spielman A. 1987. Duration of tick attachment and *Borrelia burgdorferi* transmission. *J Clin Microbiol*. 25(3): p. 557-558.

14. Pal U, Li X, Wang T, Montgomery RR, Ramamoorthi N, Desilva AM, . . . Fikrig E. 2004. TROSPA, an *Ixodes scapularis* receptor for *Borrelia burgdorferi*. *Cell*. 119(4): p. 457-468.

15. Liang FT, Jacobs MB, Bowers LC, and Philipp MT. 2002. An immune evasion mechanism for spirochetal persistence in Lyme borreliosis. *J Exp Med*. 195(4): p. 415-422.

16. Fraser CM, Casjens S, Huang WM, Sutton GG, Clayton R, Lathigra R, . . . Venter JC. 1997. Genomic sequence of a Lyme disease spirochaete, *Borrelia burgdorferi*. *Nature*. 390: p. 580-586.

17. Zhang JR, Harham JM, Barbour AG, and Norris SJ. 1997. Antigenic variation in Lyme disease borreliae by promiscuous recombination of VMP-like sequence cassettes. *Cell*. 89(2): p. 275-285.

18. Hellwage J, Meri T, Heikkila T, Alitalo A, Panelius J, Lahdenne P, . . . Meri S. 2001. The complement regulator factor H binds to the surface protein OspE of *Borrelia burgdorferi*. *J Biol Chem*. 276(11): p. 8427-8435.

19. Rosa P. 2005. Lyme disease agent borrows a practical coat. *Nat Med*. 11(8): p. 831-832.

20. Shih C-M, Pollack RJ, Telford SR, and Spielman A. 1992. Delayed dissemination of Lyme disease spirochetes from the site of deposition in the skin of mice. *J Infect Dis*. 166(4): p. 827-831.

21. Kalish RA, Kaplan RF, Taylor E, Jones-Woodward L, Workman K, and Steere AC. 2001. Evaluation of study patients with Lyme disease, 10-20 year follow-up. *J Infect Dis*. 183(3): p. 453-460.

22. Stanek G, Wormser GP, Gray J, and Strle F. 2012. Lyme borreliosis. *Lancet*. 379(9814): p. 461-473.

23. Smith RP, Schoen RT, Rahn DW, Sikand VK, Nowakowski J, Parenti DL, . . . Steere AC. 2002. Clinical characteristics and treatment outcome of early Lyme disease in patients with microbiologically confirmed erythema migrans. *Ann Intern Med*. 136(6): p. 421-428.

24. Lochhead RB, Strle K, Arvikar SL, Weis JJ, and Steere AC. 2021. Lyme arthritis: linking infection, inflammation and autoimmunity. *Nat Rev Rheumatol*. 17(8): p. 449-461.

25. Steere AC. 2001. Lyme disease. *N Engl J Med*. 345(2): p. 115-125.

26. Wooten RM, Ma Y, Yoder RA, Brown JP, Weis JH, Zachary JF, . . . Weis JJ. 2002. Toll-like receptor 2 is required for innate, but not acquired, host defense to *Borrelia burgdorferi*. *J Immunol*. 168(1): p. 348-355.

27. Marre ML, Petnicki-Ocwieja T, DeFrancesco AS, Darcy CT, and Hu LT. 2010. Human integrin $\alpha_3\beta_1$ regulates TLR2 recognition of lipopeptides from endosomal compartments. *PLoS One*. 5(9): p. e12871.

28. Menten-Dedoyart C, Faccinetto C, Golovchenko M, Dupiereux I, Van Lerberghe PB, Dubois S, . . . Couvreur B. 2012. Neutrophil extracellular traps entrap and kill *Borrelia burgdorferi sensu stricto* spirochetes and are not affected by *Ixodes ricinus* tick saliva. *J Immunol*. 189(11): p. 5393-5401.

29. Sulka KB, Strle K, Crowley JT, Lochhead RB, Anthony R, and Steere AC. 2018. Correlation of Lyme disease-associated IgG4 autoantibodies with synovial pathology in antibiotic-refractory Lyme arthritis. *Arthritis Rheumatol*. 70(11): p. 1835-1846.

30. Barthold SW and Bockenstedt LK. 1993. Passive immunizing activity of sera from mice infected with *Borrelia burgdorferi*. *Infect Immun*. 61(11): p. 4696-4702.

31. Barthold SW, de Souza MS, Janotka JL, Smith AL, and Persing DH. 1993. Chronic Lyme borreliosis in the laboratory mouse. *Am J Pathol*. 143(3): p. 959-971.

32. Bolz DD, Sundsbak RS, Ma Y, Akira S, Kirschning CJ, Zachary JF, . . . Weis JJ. 2004. MyD88 plays a unique role in host defense but not arthritis development in Lyme disease. *J Immunol*. 173(3): p. 2003-2010.

33. Schaible UE, Gay S, Museteanu C, Kramer MD, Zimmer G, Eichmann K, . . . Simon MM. 1990. Lyme borreliosis in the severe combined immunodeficiency (*scid*) mouse manifests predominantly in the joints, heart, and liver. *Am J Pathol*. 137(4): p. 811-820.

34. Barthold SW, deSouza M, and Feng S. 1996. Serum-mediated resolution of Lyme arthritis in mice. *Lab Invest*. 74(1): p. 57-67.

35. Wang X, Ma Y, Weis JH, Zachary JF, Kirschning CJ, and Weis JJ. 2005. Relative contributions of innate and acquired host responses to bacterial control and arthritis development in Lyme disease. *Infect Immun*. 73(1): p. 657-660.

36. Steere AC, Schoen RT, and Taylor E. 1987. The clinical evolution of Lyme arthritis. *Ann Intern Med*. 107(5): p. 725-731.

37. Puius YA and Kalish RA. 2008. Lyme arthritis: pathogenesis, clinical presentation, and management. *Infect Dis Clin North Am*. 22(2): p. 289-300, vi-vii.

38. Steere AC and Glickstein L. 2004. Elucidation of Lyme arthritis. *Nat Rev Immunol*. 4(2): p. 143-152.

39. Arvikar SL and Steere AC. 2015. Diagnosis and treatment of Lyme arthritis. *Infect Dis Clin North Am*. 29(2): p. 269-280.

40. Lawson JP and Steere AC. 1985. Lyme arthritis: radiologic findings. *Radiology*. 154(1): p. 37-43.

41. Jutras BL, Lochhead RB, Kloos ZA, Biboy J, Strle K, Booth CJ, . . . Jacobs-Wagner C. 2019. *Borrelia burgdorferi* peptidoglycan is a persistent antigen in patients with Lyme arthritis. *Proc Natl Acad Sci U S A*. 116(27): p. 13498-13507.

42. Herrero-Cervera A, Soehnlein O, and Kenne E. 2022. Neutrophils in chronic inflammatory diseases. *Cell Mol Immunol*. 19(2): p. 177-191.

43. Furman D, Campisi J, Verdin E, Carrera-Bastos P, Targ S, Franceschi C, . . . Slavich GM. 2019. Chronic inflammation in the etiology of disease across the life span. *Nat Med*. 25(12): p. 1822-1832.

44. Nathan C. 2006. Neutrophils and immunity: challenges and opportunities. *Nat Rev Immunol*. 6(3): p. 173-182.

45. Serhan CN, Chiang N, and Van Dyke TE. 2008. Resolving inflammation: dual anti-inflammatory and pro-resolution lipid mediators. *Nat Rev Immunol*. 8(5): p. 349-361.

46. Serhan CN and Savill J. 2005. Resolution of inflammation: the beginning programs the end. *Nat Immunol*. 6(12): p. 1191-1197.

47. Khanapure SP, Garvey DS, Janero DR, and Letts LG. 2007. Eicosanoids in inflammation: Biosynthesis, pharmacology, and therapeutic frontiers. *Curr Top Med Chem*. 7(3): p. 311-340.

48. Serhan CN. 2014. Pro-resolving lipid mediators are leads for resolution physiology. *Nature*. 510(7503): p. 92-101.

49. Levy BD, Clish CB, Schmidt B, Gronert K, and Serhan CN. 2001. Lipid mediator class switching during acute inflammation: signals in resolution. *Nat Immunol*. 2(7): p. 612-619.

50. Nakanishi M and Rosenberg DW. 2013. Multifaceted roles of PGE_2 in inflammation and cancer. *Semin Immunopathol*. 35(2): p. 123-137.

51. Smith WL, Urade Y, and Jakobsson PJ. 2011. Enzymes of the cyclooxygenase pathways of prostanoid biosynthesis. *Chem Rev*. 111(10): p. 5821-5865.

52. Bystrom J, Evans I, Newson J, Stables M, Toor I, van Rooijen N, . . . Gilroy DW. 2008. Resolution-phase macrophages possess a unique inflammatory phenotype that is controlled by cAMP. *Blood*. 112(10): p. 4117-4127.

53. Takayama K, Garcia-Cardena G, Sukhova GK, Comander J, Gimbrone MA, Jr., and Libby P. 2002. Prostaglandin E2 suppresses chemokine production in human macrophages through the EP4 receptor. *J Biol Chem*. 277(46): p. 44147-44154.

54. Poligone B and Baldwin AS. 2001. Positive and negative regulation of NF-kappaB by COX-2: roles of different prostaglandins. *J Biol Chem*. 276(42): p. 38658-38664.

55. Gomez PF, Pillinger MH, Attur M, Marjanovic N, Dave M, Park J, . . . Abramson SB. 2005. Resolution of inflammation: prostaglandin E_2 dissociates nuclear trafficking of individual NF-kappaB subunits (p65, p50) in stimulated rheumatoid synovial fibroblasts. *J Immunol*. 175(10): p. 6924-6930.

56. Afonso PV, Janka-Junttila M, Lee YJ, McCann CP, Oliver CM, Aamer KA, . . . Parent CA. 2012. LTB4 is a signal-relay molecule during neutrophil chemotaxis. *Dev Cell*. 22(5): p. 1079-1091.

57. Serhan CN, Hamberg M, and Samuelsson B. 1984. Lipoxins: Novel series of biologically active compounds formed from arachidonic acid in human leukocytes. *Proc Natl Acad Sci U S A*. 81(17): p. 5335-5339.

58. Lee TH, Horton CE, Kyan-Aung U, Haskard D, Crea AEG, and Spur BW. 1989. Lipoxin A_4 and lipoxin B_4 inhibit chemotactic responses of human neutrophils stimulated by leukotriene B_4 and *N*-formyl-L-methionyl-L-leucyl-L-phenylalanine. *Clin Sci*. 77: p. 195-203.

59. Godson C, Mitchell S, Harvey K, Petasis NA, Hogg N, and Brady HR. 2000. Cutting edge: lipoxins rapidly stimulate nonphlogistic phagocytosis of apoptotic neutrophils by monocyte-derived macrophages. *J Immunol*. 164(4): p. 1663-1667.

60. Mitchell S, Thomas G, Harvey K, Cottell D, Reville K, Berlasconi G, . . . Godson C. 2002. Lipoxins, aspirin-triggered epi-lipoxins, lipoxin stable analogues, and the resolution of inflammation: stimulation of macrophage phagocytosis of apoptotic neutrophils *in vivo*. *J Am Soc Nephrol*. 13(10): p. 2497-2507.

61. Dalli J and Serhan CN. 2012. Specific lipid mediator signatures of human phagocytes: microparticles stimulate macrophage efferocytosis and pro-resolving mediators. *Blood*. 120(15): p. e60-72.

62. Kourtzelis I, Hajishengallis G, and Chavakis T. 2020. Phagocytosis of apoptotic cells in resolution of inflammation. *Front Immunol*. 11: p. 553.

63. Dyall SC, Balas L, Bazan NG, Brenna JT, Chiang N, da Costa Souza F, . . . Taha AY. 2022. Polyunsaturated fatty acids and fatty acid-derived lipid mediators: Recent advances in the understanding of their biosynthesis, structures, and functions. *Prog Lipid Res*. 86: p. 101165.

64. Jaen RI, Sanchez-Garcia S, Fernandez-Velasco M, Bosca L, and Prieto P. 2021. Resolution-based therapies: The potential of lipoxins to treat human diseases. *Front Immunol*. 12: p. 658840.

65. Serhan CN and Levy BD. 2018. Resolvins in inflammation: emergence of the pro-resolving superfamily of mediators. *J Clin Invest*. 128(7): p. 2657-2669.

66. Barthold SW, Beck DS, Hansen GM, Terwilliger GA, and Moody KD. 1990. Lyme borreliosis in selected strains and ages of laboratory mice. *J Inf Dis*. 162(1): p. 133-138.

67. Wooten RM and Weis JJ. 2001. Host-pathogen interactions promoting inflammatory Lyme arthritis: use of mouse models for dissection of disease processes. *Curr Opin Microbiol*. 4: p. 274-279.

68. Brown CR and Reiner SL. 1999. Genetic control of experimental Lyme arthritis in the absence of specific immunity. *Infect Immun*. 67(4): p. 1967-1973.

69. Fikrig E, Barthold SW, Chen M, Chang CH, and Flavell RA. 1997. Protective antibodies develop, and murine Lyme arthritis regresses, in the absence of MHC class II and CD4+ T cells. *J Immunol*. 159(11): p. 5682-5686.

70. Barthold SW, Sidman CL, and Smith AL. 1992. Lyme borreliosis in genetically resistant and susceptible mice with severe combined immunodeficiency. *Am J Trop Med Hyg*. 47(5): p. 605-613.

71. Blaho VA, Mitchell WJ, and Brown CR. 2008. Arthritis develops but fails to resolve during inhibition of cyclooxygenase 2 in a murine model of Lyme disease. *Arthritis Rheum*. 58(5): p. 1485-1495.

72. Blaho VA, Zhang Y, Hughes-Hanks JM, and Brown CR. 2011. 5-Lipoxygenase-deficient mice infected with *Borrelia burgdorferi* develop persistent arthritis. *J Immunol*. 186(5): p. 3076-3084.

73. Hilliard KA, Blaho VA, Jackson CD, and Brown CR. 2020. Leukotriene B4 receptor BLT1 signaling is critical for neutrophil apoptosis and resolution of experimental Lyme arthritis. *The FASEB Journal*. 34: p. 2840-2852.

74. Blaho VA, Buczynski MW, Brown CR, and Dennis EA. 2009. Lipidomic analysis of dynamic eicosanoid responses during the induction and resolution of Lyme arthritis. *J Biol Chem*. 284(32): p. 21599-21612.

75. Barthold SW, Moody KD, Terwilliger GA, Duray PH, Jacoby RO, and Steere AC. 1988. Expeirmental Lyme arthritis in rats infected with *Borrelia burgdorferi*. *J Infect Dis*. 157(4): p. 842-846.

76. Pollack RJ, Telford S, and Spielman A. 1993. Standardization of medium for culturing Lyme disease spirochetes. *J Clin Microbiol*. 31(5): p. 1252-1255.

77. Hilliard KA and Brown CR. 2019. Treatment of *Borrelia burgdorferi*-infected mice with apoptotic cells attenuates Lyme arthritis via PPAR-gamma. *J Immunol*. 202(6): p. 1798-1806.

78. Brown CR, Blaho VA, and Loiacono CM. 2003. Susceptibility to experimental Lyme arthritis correlates with KC and monocyte chemoattractant protein-1 production in joints and requires neutrophil recruitment via CXCR2. *J Immunol*. 171(2): p. 893-901.

79. Ritzman AM, Hughes-Hanks JM, Blaho VA, Wax LE, Mitchell WJ, and Brown CR. 2010. The chemokine receptor CXCR2 ligand KC (CXCL1) mediates neutrophil recruitment and is critical for development of experimental Lyme arthritis and carditis. *Infect Immun*. 78(11): p. 4593-4600.

80. Lasky CE, Pratt CL, Hilliard KA, Jones JL, and Brown CR. 2016. T cells exacerbate Lyme borreliosis in TLR2-deficient mice. *Front Immunol*. 7: p. 468.

81. Lokuta MA, Nuzzi PA, and Huttenlocher A. 2007. Analysis of neutrophil polarization and chemotaxis. *Methods Mol Biol*. 412: p. 211-229.

82. Bannenberg G, Moussignac RL, Gronert K, Devchand PR, Schmidt BA, Guilford WJ, . . . Serhan CN. 2004. Lipoxins and novel 15-epi-lipoxin analogs display potent anti-inflammatory actions after oral administration. *Br J Pharmacol*. 143(1): p. 43-52.

83. Shi Y, Pan H, Zhang H-Z, Zhao X-Y, Jin J, and Wang H-Y. 2017. Lipoxin A4 mitigates experimental autoimmune myocarditis by regulating inflammatory response, NF-κB and PI3K/Akt signaling pathway in mice. *Eur Rev Med Pharmacol Sci*. 21(8): p. 11850-11859.

84. Owen-Woods C, Joulia R, Barkaway A, Rolas L, Ma B, Nottebaum AF, . . . Nourshargh S. 2020. Local microvascular leakage promotes trafficking of activated neutrophils to remote organs. *J Clin Invest*. 130(5): p. 2301-2318.

85. Puech C, Badran M, Runion AR, Barrow MB, Qiao Z, Khalyfa A, and Gozal D. 2022. Explicit memory, anxiety and depressive like behavior in mice exposed to chronic intermittent hypoxia, sleep fragmentation, or both during the daylight period. *Neurobiol Sleep Circadian Rhythms*. 13: p. 100084.

86. Zaninelli TH, Fattori V, and Verri WA, Jr. 2021. Harnessing inflammation resolution in arthritis: Current understanding of specialized pro-resolving lipid mediators' contribution to arthritis physiopathology and future perspectives. *Front Physiol*. 12: p. 729134.

87. Arnardottir HH, Dalli J, Norling LV, Colas RA, Perretti M, and Serhan CN. 2016. Resolvin D3 is dysregulated in arthritis and reduces arthritic inflammation. *J Immunol*. 197(6): p. 2362-2368.

88. Ozgul Ozdemir RB, Soysal Gunduz O, Ozdemir AT, and Akgul O. 2020. Low levels of pro-resolving lipid mediators lipoxin-A4, resolvin-D1 and resolvin-E1 in patients with rheumatoid arthritis. *Immunol Lett*. 227: p. 34-40.

89. Gheorghe KR, Korotkova M, Catrina AI, Backman L, af Klint E, Claesson HE, . . . Jakobsson PJ. 2009. Expression of 5-lipoxygenase and 15-lipoxygenase in rheumatoid arthritis synovium and effects of intraarticular glucocorticoids. *Arthritis Res Ther*. 11(3): p. R83.

90. Hashimoto A, Hayashi I, Murakami Y, Sato Y, Kitasato H, Matsushita R, . . . Endo H. 2007. Antiinflammatory mediator lipoxin A4 and its receptor in synovitis of patients with rheumatoid arthritis. *J Rheumatol*. 34(11): p. 2144-2153.

91. Kronke G, Katzenbeisser J, Uderhardt S, Zaiss MM, Scholtysek C, Schabbauer G, . . . Schett G. 2009. 12/15-lipoxygenase counteracts inflammation and tissue damage in arthritis. *J Immunol*. 183(5): p. 3383-3389.

92. Norling LV, Headland SE, Dalli J, Arnardottir HH, Haworth O, Jones HR, . . . Perretti M. 2016. Proresolving and cartilage-protective actions of resolvin D1 in inflammatory arthritis. *JCI Insight*. 1(5): p. e85922.

93. Conte FP, Menezes-de-Lima O, Jr., Verri WA, Jr., Cunha FQ, Penido C, and Henriques MG. 2010. Lipoxin A(4) attenuates zymosan-induced arthritis by modulating endothelin-1 and its effects. *Br J Pharmacol*. 161(4): p. 911-924.

94. Barthold SW, Feng S, Bockenstedt LK, Fikrig E, and Feen K. 1997. Protective and arthritis-resolving activity in sera of mice infected with *Borrelia burgdorferi*. *Clin Infect Dis*. 25: p. S9-17.

95. Chan MM and Moore AR. 2010. Resolution of inflammation in murine autoimmune arthritis is disrupted by cyclooxygenase-2 inhibition and restored by prostaglandin E2-mediated lipoxin A4 production. *J Immunol*. 184(11): p. 6418-6426.

96. Hong S, Gronert K, Devchand PR, Moussignac RL, and Serhan CN. 2003. Novel docosatrienes and 17S-resolvins generated from docosahexaenoic acid in murine brain, human blood, and glial cells. Autacoids in anti-inflammation. *J Biol Chem*. 278(17): p. 14677-14687.

97. Silva MT, do Vale A, and dos Santos NM. 2008. Secondary necrosis in multicellular animals: an outcome of apoptosis with pathogenic implications. *Apoptosis*. 13(4): p. 463-482.

98. Buckley CD, Gilroy DW, and Serhan CN. 2014. Proresolving lipid mediators and mechanisms in the resolution of acute inflammation. *Immunity*. 40(3): p. 315-327.

99. Serhan CN, Fiore S, Brezinski DA, and Lynch S. 1993. Lipoxin A4 metabolism by differentiated HL-60 cells and human monocytes: Conversion to novel 15-oxo and dihydro products. *Biochemistry*. 32(25): p. 6313-6319.

100. Fiore S, Maddox JF, Perez HD, and Serhan CN. 1994. Identification of a human cDNA encoding a functional high affinity lipoxin A_4 receptor. *J Exp Med*. 180(1): p. 253-260.

101. Boff D, Oliveira VLS, Queiroz Junior CM, Galvao I, Batista NV, Gouwy M, . . . Amaral FA. 2020. Lipoxin A4 impairs effective bacterial control and potentiates joint inflammation and damage caused by *Staphylococcus aureus* infection. *FASEB J*. 34(9): p. 11498-11510.

102. Maddox JF and Serhan CN. 1996. Lipoxin A4 and B4 are potent stimuli for human monocyte migration and adhesion: Selective inactivation by dehydrogenation and reduction. *J Exp Med*. 183(1): p. 137-146.

103. Butenko S, Satyanarayanan SK, Assi S, Schif-Zuck S, Sher N, and Ariel A. 2020. Transcriptomic analysis of monocyte-derived non-phagocytic macrophages favors a role in limiting tissue repair and fibrosis. *Front Immunol*. 11: p. 405.

104. Ricciotti E and FitzGerald GA. 2011. Prostaglandins and inflammation. *Arterioscler Thromb Vasc Biol*. 31(5): p. 986-1000.

105. Fujino H, Salvi S, and Regan JW. 2005. Differential regulation of phosphorylation of the cAMP response element-binding protein after activation of EP2 and EP4 prostanoid receptors by prostaglandin E2. *Mol Pharmacol*. 68(1): p. 251-259.

106. Tavares LP, Negreiros-Lima GL, Lima KM, PMR ES, Pinho V, Teixeira MM, and Sousa LP. 2020. Blame the signaling: Role of cAMP for the resolution of inflammation. *Pharmacol Res*. 159: p. 105030.

107. Bombardieri S, Cattani P, Ciabattoni G, Di Munno O, Pasero G, Patrono C, . . . F. P. 1981. The synovial prostaglandin system in chronic inflammatory arthritis: Differential effects of steroidal and nonsteroidal anti-inflammatory drugs. *Br J Pharmacol*. 73: p. 893-901.

108. Park JY, Pillinger MH, and Abramson SB. 2006. Prostaglandin E2 synthesis and secretion: the role of PGE2 synthases. *Clin Immunol*. 119(3): p. 229-240.

109. Kamei D, Yamakawa K, Takegoshi Y, Mikami-Nakanishi M, Nakatani Y, Oh-Ishi S, . . . Kudo I. 2004. Reduced pain hypersensitivity and inflammation in mice lacking microsomal prostaglandin E synthase-1. *J Biol Chem*. 279(32): p. 33684-33695.

110. Trebino CE, Stock JL, Gibbons CP, Naiman BM, Wachtmann TS, Umland JP, . . . Audoly LP. 2003. Impaired inflammatory and pain responses in mice lacking an inducible prostaglandin E synthase. *PNAS*. 100(15): p. 9044-9049.

111. Feigen LP. 1981. Actions of prostaglandins in peripheral vascular beds. *Fed Proc*. 40(7): p. 1987-1990.

112. Kabashima K, Nagamachi M, Honda T, Nishigori C, Miyachi Y, Tokura Y, and Narumiya S. 2007. Prostaglandin E2 is required for ultraviolet B-induced skin inflammation via EP2 and EP4 receptors. *Lab Invest*. 87(1): p. 49-55.

113. Morimoto K, Shirata N, Taketomi Y, Tsuchiya S, Segi-Nishida E, Inazumi T, . . . Sugimoto Y. 2014. Prostaglandin E2-EP3 signaling induces inflammatory swelling by mast cell activation. *J Immunol*. 192(3): p. 1130-1137.

114. Woitzik P and Linder S. 2021. Molecular mechanisms of *Borrelia burgdorferi* phagocytosis and intracellular processing by human macrophages. *Biology (Basel)*. 10: p. 567.

115. Wang J, Hossain M, Thanabalasuriar A, Gunzer M, Meininger C, and Kubes P. 2017. Visualizing the function and fate of neutrophils in sterile injury and repair. *Science*. 358: p. 111-116.

116. Loynes CA, Lee JA, Robertson AL, Steel MJG, Ellett F, Feng Y, . . . Renshaw SA. 2018. PGE_2 production at sites of tissue injury promotes an anti-inflammatory neutrophil phenotype and determines the outcome of inflammation resolution *in vivo*. *Sci Adv*. 4(9): p. eaar8320.

117. Colom B, Bodkin JV, Beyrau M, Woodfin A, Ody C, Rourke C, . . . Nourshargh S. 2015. Leukotriene B4-neutrophil elastase axis drives

neutrophil reverse transendothelial cell migration *in vivo*. *Immunity*. 42(6): p. 1075-1086.

118. Woodfin A, Voisin MB, Beyrau M, Colom B, Caille D, Diapouli FM, . . . Nourshargh S. 2011. The junctional adhesion molecule JAM-C regulates polarized transendothelial migration of neutrophils *in vivo*. *Nat Immunol*. 12(8): p. 761-769.

119. Glatman Zaretsky A, Engiles JB, and Hunter CA. 2014. Infection-induced changes in hematopoiesis. *J Immunol*. 192(1): p. 27-33.

120. Besedovsky L, Lange T, and Haack M. 2019. The sleep-immune crosstalk in health and disease. *Physiol Rev*. 99: p. 1325-1380.

121. Mullington JM, Simpson NS, Meier-Ewert HK, and Haack M. 2010. Sleep loss and inflammation. *Best Pract Res Clin Endocrinol Metab*. 24(5): p. 775-784.

122. Imeri L and Opp MR. 2009. How (and why) the immune system makes us sleep. *Nat Rev Neurosci*. 10(3): p. 199-210.

123. Irwin MR and Opp MR. 2017. Sleep health: Reciprocal regulation of sleep and innate immunity. *Neuropsychopharmacol*. 42: p. 129-155.

124. Rebman AW, Bechtold KT, Yang T, Mihm EA, Soloski MJ, Novak CB, and Aucott JN. 2017. The clinical, symptom, and quality-of-life characterization of a well-defined group of patients with posttreatment Lyme disease syndrome. *Front Med (Lausanne)*. 4: p. 224.

125. Turk SP, Lumbard K, Liepshutz K, Williams C, Hu L, Dardick K, . . . Marques A. 2019. Post-treatment Lyme disease symptoms score: Developing a new tool for research. *PLoS One*. 14(11): p. e0225012.

126. Zubcevik N, Mao C, Wang QM, Bose EL, Octavien RN, Crandell D, and Wood LJ. 2020. Symptom clusters and functional impairment in individuals treated for Lyme borreliosis. *Front Med (Lausanne)*. 7: p. 464.

127. Weinstein ER, Rebman AW, Aucott JN, Johnson-Greene D, and Bechtold KT. 2018. Sleep quality in well-defined Lyme disease: a clinical cohort study in Maryland. *Sleep*. 41(5): p. 1-8.

128. Greenberg HE, Ney G, Scharf SM, Ravdin L, and Hilton E. 1995. Sleep quality in Lyme Disease. *Sleep*. 18(10): p. 912-916.

129. Trammell RA, Verhulst S, and Toth LA. 2014. Effects of sleep fragmentation on sleep and markers of inflammation in mice. *Comp Med*. 64(1): p. 13-24.

130. McAlpine CS, Kiss MG, Zuraikat FM, Cheek D, Schiroli G, Amatullah H, . . . Swirski FK. 2022. Sleep exerts lasting effects on hematopoietic stem cell function and diversity. *J Exp Med*. 219(11): p. e20220081.

131. Spiegel K, Sheridan JF, and Van Cauter E. 2002. Effect of sleep deprivation on response to immunization. *JAMA*. 288: p. 1471-1472.

132. Brown R, Pang G, Husband AJ, and King MG. 1989. Suppression of immunity to influenza virus infection in the respiratory tract following sleep disturbance. *Reg Immunol*. 2: p. 321-325.

133. Petzke MM, Brooks A, Krupna MA, Mordue D, and Schwartz I. 2009. Recognition of *Borrelia burgdorferi*, the Lyme disease spirochete, by TLR7 and TLR9 induces a type I IFN response by human immune cells. *J Immunol*. 183(8): p. 5279-5292.

134. Defosse DL and Johnson RC. 1992. *In vitro* and *in vivo* induction of tumor necrosis factor alpha by *Borrelia burgdorferi*. *Infect Immun*. 60(3): p. 1109-1113.

135. Blaho VA, Buczynski MW, Dennis EA, and Brown CR. 2009. Cyclooxygenase-1 orchestrates germinal center formation and antibody class-switch via regulation of IL-17. *J Immunol*. 183(9): p. 5644-5653.

136. Singh NK and Rao GN. 2019. Emerging role of 12/15-Lipoxygenase (ALOX15) in human pathologies. *Prog Lipid Res*. 73: p. 28-45.

137. Poon IK, Hulett MD, and Parish CR. 2010. Molecular mechanisms of late apoptotic/necrotic cell clearance. *Cell Death Differ*. 17(3): p. 381-397.

138. Qu Q, Xuan W, and Fan GH. 2015. Roles of resolvins in the resolution of acute inflammation. *Cell Biol Int*. 39(1): p. 3-22.

139. Serhan CN, Maddox JF, Petasis NA, Akritopoulou-Zanze I, Papayianni A, Brady HR, . . . Madara JL. 1995. Design of lipoxin A_4 stable analogs that block transmigration and adhesion of human neutrophils. *Biochemistry*. 34(44): p. 14609-14615.

140. Bandeira-Melo C, Serra MF, Diaz BL, Cordeiro RS, Silva PM, Lenzi HL, . . . Martins MA. 2000. Cyclooxygenase-2-derived prostaglandin E2 and lipoxin A4 accelerate resolution of allergic edema in Angiostrongylus

costaricensis-infected rats: relationship with concurrent eosinophilia. *J Immunol*. 164(2): p. 1029-1036.

141. Menezes-de-Lima O, Jr., Kassuya CA, Nascimento AF, Henriques M, and Calixto JB. 2006. Lipoxin A4 inhibits acute edema in mice: implications for the anti-edematogenic mechanism induced by aspirin. *Prostaglandins Other Lipid Mediat*. 80: p. 123-135.

142. Yuan J, Lin F, Chen L, Chen W, Pan X, Bai Y, . . . Lu H. 2022. Lipoxin A4 regulates M1/M2 macrophage polarization via FPR2-IRF pathway. *Inflammopharmacology*. 30(2): p. 487-498.

143. Walker J, Dichter E, Lacorte G, Kerner D, Spur B, Rodriguez A, and Yin K. 2011. Lipoxin A4 increases survival by decreasing systemic inflammation and bacterial load in sepsis. *Shock*. 36(4): p. 410-416.

144. Galvao I, Melo EM, de Oliveira VLS, Vago JP, Queiroz-Junior C, de Gaetano M, . . . Teixeira MM. 2021. Therapeutic potential of the FPR2/ALX agonist AT-01-KG in the resolution of articular inflammation. *Pharmacol Res*. 165: p. 105445.

145. Fadok VA, Bratton DL, Konowai A, Freed PW, Westcott JY, and Henson PM. 1998. Macrophages that have ingested apoptotic cells *in vitro* inhibit proinflammatory cytokine production theough the autocrine/paracrine mechanisms involving TGF-beta, PGE2, and PAF. *J Clin Invest*. 101(4): p. 890-898.

146. Aronoff DM, Canetti C, and Peters-Golden M. 2004. Prostaglandin E2 inhibits alveolar macrophage phagocytosis through an E-prostanoid 2

receptor-mediated increase in intracellular cyclic AMP. *J Immunol*. 173(1): p. 559-565.

147. Agard M, Asakrah S, and Morici LA. 2013. PGE(2) suppression of innate immunity during mucosal bacterial infection. *Front Cell Infect Microbiol*. 3: p. 45.

148. Serezani CH, Kane S, Medeiros AI, Cornett AM, Kim SH, Marques MM, . . . Peters-Golden M. 2012. PTEN directly activates the actin depolymerization factor cofilin-1 during PGE2-mediated inhibition of phagocytosis of fungi. *Sci Signal*. 5(210): p. ra12.

149. Wang Z, Wei X, Ji C, Yu W, Song C, and Wang C. 2022. PGE2 inhibits neutrophil phagocytosis through the EP2R-cAMP-PTEN pathway. *Immun Inflamm Dis*. 10(7): p. e662.

150. Herlong JL and Scott TR. 2006. Positioning prostanoids of the D and J series in the immunopathogenic scheme. *Immunol Lett*. 102(2): p. 121-31.

151. Joo M. 2010. Role of alveolar macrophages in productions of prostaglandin D_2 and E_2 in the inflamed lung. *J Life Sci*. 20(6): p. 845-852.

152. Surh YJ, Na HK, Park JM, Lee HN, Kim W, Yoon IS, and Kim DD. 2011. 15-Deoxy-delta$^{12\text{-}14}$ prostaglandin J_2, an electrophilic lipid mediator of anti-inflammatory and pro-resolving signaling. *Biochem Pharmacol*. 82(10): p. 1335-1351.

153. Appel S, Mirakaj V, Bringmann A, Weck MM, Grunebach F, and Brossart P. 2005. PPAR-gamma agonists inhibit toll-like receptor-mediated

activation of dendritic cells via the MAP kinase and NF-kappaB pathways. *Blood*. 106(12): p. 3888-3894.

154. Shim J, Park C, Lee HS, Park MS, Lim HT, Chauhan S, . . . Lee HK. 2012. Change in prostaglandin expression levels and synthesizing activities in dry eye disease. *Ophthalmology*. 119(11): p. 2211-2219.

APPENDIX I

SUPPLEMENTARY FIGURES

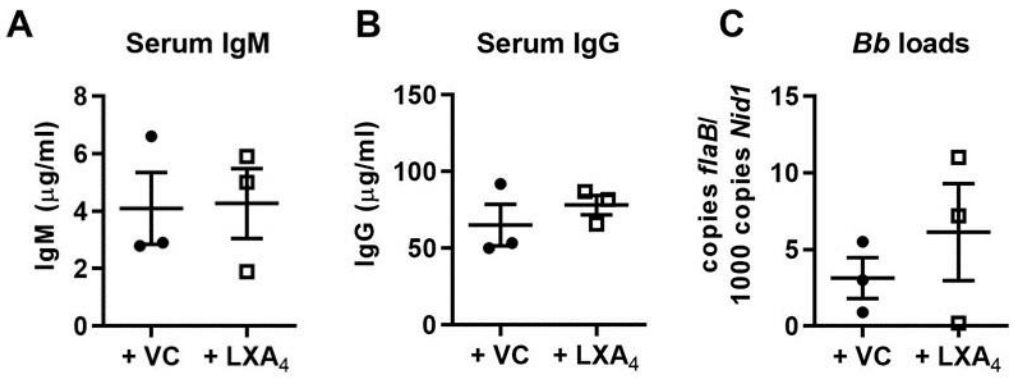

Figure 3.S1. Exogenous LXA_4 treatment does not interfere with the host anti-*Borrelia* response.

C3H WT mice were infected with *Bb* and treated with either vehicle control (VC; closed circles) or LXA_4 (open squares) i.p. on D18,19, and 20. Serum was collected and *Bb*-specific IgM (A) and IgG (B) was quantified. (C) *Bb* burdens were measured from VC or LXA_4-treated ankles on D35 by qPCR. n=3/group. Data is representative of two independent experiments.

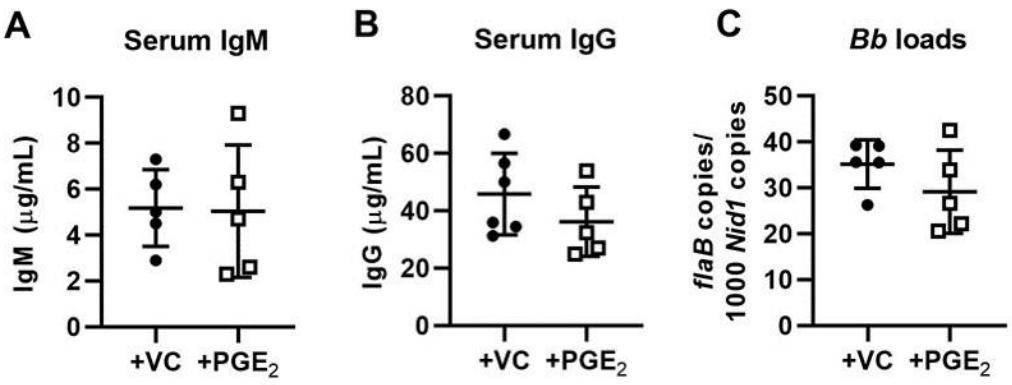

Figure 4.S1. Late PGE_2 addback to mPGES-$1^{-/-}$ mice does not affect the anti-*Bb* response.

mPGES-$1^{-/-}$ C3H mice infected with *Bb* and treated i.p. with 100μl of either VC (10% EtOH in PBS) or 100μg PGE_2 on D18,19,20, and sacrificed on D35. Blood was collected and *Bb*-specific IgM (A) and IgG (B) levels were determined by ELISA. n=5/group. (C) *Bb* burdens in ankles at D35 by qPCR. n=5/group. Data is representative of two independent experiments.

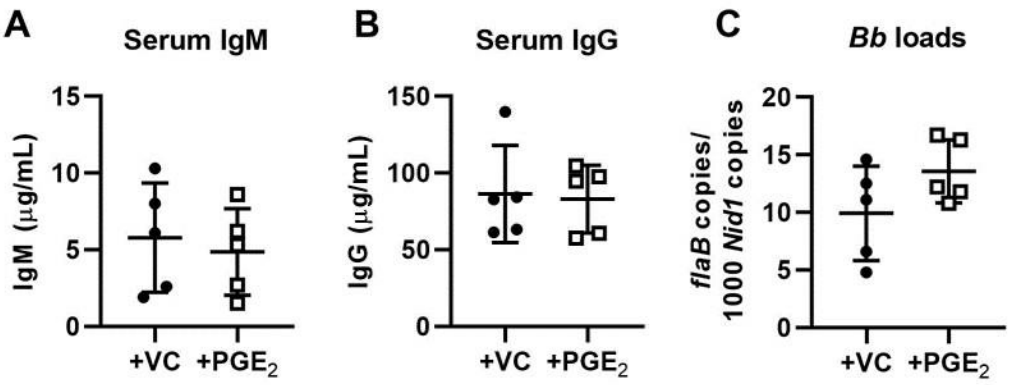

Figure 4.S2. Early PGE_2 addback to mPGES-$1^{-/-}$ mice does not affect the anti-*Bb* response.

mPGES-$1^{-/-}$ C3H mice infected with *Bb* and treated i.p. with 100μl of either VC (10% EtOH in PBS) or 100μg PGE_2 on D7,8,9, and sacrificed on D35. Blood was collected and *Bb*-specific IgM (A) and IgG (B) levels were determined by ELISA. n=5/group. (C) *Bb* burdens in ankles at D35 by qPCR. n=5/group. Data is representative of two independent experiments.

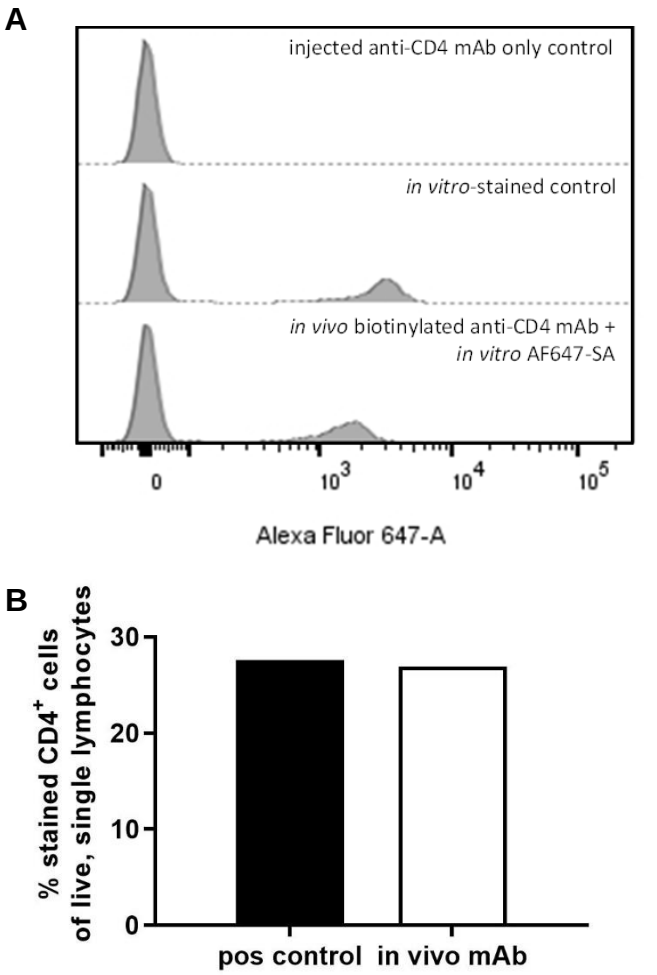

Figure 5.S1. *In vivo* biotinylated anti-CD4 mAb coverage efficiency.

Uninfected mice were injected with biotinylated αCD4 mAb (2μg in 100μl sterile PBS) i.v. alone or with AF647-SA (0.1μg in 10μl sterile PBS) in the left knee synovium. Blood was collected at 2 hps, RBCs were lysed, and white blood cells were stained for flow cytometry. Doublets and debris were excluded. (A) AF647 expression from top to bottom of cells from mice which received only the biotinylated αCD4 mAb (negative control), cells which were stained with biotin mAb + AF647-SA *in vitro* (positive control), and cells from biotinylated αCD4-injected mice with AF647-SA added *in vitro.* The proportion of blood lymphocytes expressing AF647 in the positive control sample (as in A) or the experimental sample (*in vivo* biotinylated mAb + *in vitro* AF647-SA). Lymphocyte gating by SSC v FSC plot. n=1 mouse for all groups.

APPENDIX II

PCR ARRAY RESULTS

	AVG ΔC_t (Ct(GOI) - Ave Ct (HKG))		$2^{-\Delta C_t}$		Fold Change
Symbol	**Test Group**	**Control Group**	**Test Group**	**Control Group**	**Test Group /Control Group**
Aimp1	5.61	5.86	2.0E-02	1.7E-02	1.19
Bmp2	7.67	8.50	4.9E-03	2.8E-03	1.79
Ccl1	10.60	10.73	6.5E-04	5.9E-04	1.10
Ccl11	5.22	4.89	2.7E-02	3.4E-02	0.80
Ccl12	9.40	9.55	1.5E-03	1.3E-03	1.11
Ccl17	8.88	9.50	2.1E-03	1.4E-03	1.54
Ccl19	10.34	9.16	7.7E-04	1.7E-03	**0.44**
Ccl2	8.02	8.79	3.9E-03	2.3E-03	1.71
Ccl20	9.89	9.59	1.1E-03	1.3E-03	0.81
Ccl22	11.70	10.61	3.0E-04	6.4E-04	**0.47**
Ccl24	9.39	9.88	1.5E-03	1.1E-03	1.40
Ccl3	8.99	9.61	2.0E-03	1.3E-03	1.54
Ccl4	10.16	10.63	8.8E-04	6.3E-04	1.39
Ccl5	9.43	9.15	1.4E-03	1.8E-03	0.82
Ccl6	7.00	6.40	7.8E-03	1.2E-02	0.66
Ccl7	8.72	8.66	2.4E-03	2.5E-03	0.95
Ccl8	7.60	8.85	5.2E-03	2.2E-03	**2.39**
Ccl9	10.73	9.58	5.9E-04	1.3E-03	**0.45**
Ccr1	7.52	8.84	5.5E-03	2.2E-03	**2.50**
Ccr10	10.67	10.35	6.1E-04	7.7E-04	0.80
Ccr2	7.20	7.55	6.8E-03	5.3E-03	1.28
Ccr3	7.58	8.00	5.2E-03	3.9E-03	1.34
Ccr4	10.91	9.55	5.2E-04	1.3E-03	**0.39**
Ccr5	7.20	7.97	6.8E-03	4.0E-03	1.70
Ccr6	9.99	9.47	9.9E-04	1.4E-03	0.70
Ccr8	13.77	10.73	7.1E-05	5.9E-04	**0.12**
Cd40lg	11.95	10.87	2.5E-04	5.4E-04	**0.47**
Csf1	7.56	7.72	5.3E-03	4.7E-03	1.12
Csf2	11.37	11.07	3.8E-04	4.7E-04	0.81
Csf3	11.55	9.83	3.3E-04	1.1E-03	**0.30**
Cx3cl1	10.48	10.29	7.0E-04	8.0E-04	0.88
Cxcl1	11.38	11.04	3.8E-04	4.8E-04	0.79
Cxcl10	7.21	7.95	6.8E-03	4.0E-03	1.67
Cxcl11	10.05	9.52	9.5E-04	1.4E-03	0.69

Cxcl12	2.55	2.51	1.7E-01	1.8E-01	0.97
Cxcl13	3.61	5.23	8.2E-02	2.7E-02	**3.07**
Cxcl15	10.39	9.26	7.5E-04	1.6E-03	**0.46**
Cxcl5	11.42	10.47	3.7E-04	7.0E-04	0.52
Cxcl9	10.46	9.60	7.1E-04	1.3E-03	0.55
Cxcr2	8.26	9.15	3.3E-03	1.8E-03	1.86
Cxcr3	10.00	10.58	9.8E-04	6.5E-04	1.50
Cxcr5	9.14	11.84	1.8E-03	2.7E-04	**6.50**
Fasl	11.70	9.49	3.0E-04	1.4E-03	**0.22**
Ifng	13.53	9.71	8.4E-05	1.2E-03	**0.07**
Il10ra	7.75	7.89	4.7E-03	4.2E-03	1.10
Il10rb	5.23	5.35	2.7E-02	2.5E-02	1.08
Il11	10.62	10.13	6.3E-04	8.9E-04	0.71
Il13	10.71	9.81	6.0E-04	1.1E-03	0.53
Il15	8.64	9.00	2.5E-03	2.0E-03	1.28
Il16	9.26	10.03	1.6E-03	9.6E-04	1.71
Il17a	10.57	11.47	6.6E-04	3.5E-04	1.86
Il17b	12.09	12.16	2.3E-04	2.2E-04	1.05
Il17f	11.00	10.74	4.9E-04	5.9E-04	0.83
Il1a	10.99	9.54	4.9E-04	1.3E-03	**0.37**
Il1b	7.42	7.75	5.8E-03	4.6E-03	1.26
Il1r1	7.77	7.66	4.6E-03	5.0E-03	0.92
Il1rn	6.97	7.99	8.0E-03	3.9E-03	**2.02**
Il21	12.14	10.46	2.2E-04	7.1E-04	**0.31**
Il27	10.34	9.55	7.7E-04	1.3E-03	0.58
Il2rb	13.77	11.10	7.1E-05	4.6E-04	**0.16**
Il2rg	6.45	7.09	1.1E-02	7.3E-03	1.55
Il3	11.63	11.97	3.2E-04	2.5E-04	1.27
Il33	7.26	7.63	6.5E-03	5.0E-03	1.29
Il4	10.73	9.57	5.9E-04	1.3E-03	**0.45**
Il5	10.54	10.83	6.7E-04	5.5E-04	1.23
Il5ra	11.18	10.57	4.3E-04	6.6E-04	0.66
Il6ra	7.32	7.87	6.3E-03	4.3E-03	1.47
Il6st	4.08	4.05	5.9E-02	6.0E-02	0.98
Il7	11.62	9.26	3.2E-04	1.6E-03	**0.19**
Lta	12.60	10.89	1.6E-04	5.3E-04	**0.30**
Ltb	8.47	8.72	2.8E-03	2.4E-03	1.19
Mif	4.62	4.91	4.1E-02	3.3E-02	1.22
Nampt	5.35	5.45	2.4E-02	2.3E-02	1.07
Osm	10.38	8.95	7.5E-04	2.0E-03	**0.37**
Pf4	6.40	7.03	1.2E-02	7.7E-03	1.54

Spp1	4.74	5.25	3.7E-02	2.6E-02	1.42
Tnf	8.00	9.50	3.9E-03	1.4E-03	**2.83**
Tnfrsf11b	7.31	8.33	6.3E-03	3.1E-03	**2.04**
Tnfsf10	7.55	7.43	5.4E-03	5.8E-03	0.92
Tnfsf11	9.61	9.60	1.3E-03	1.3E-03	0.99
Tnfsf13	8.92	9.61	2.1E-03	1.3E-03	1.61
Tnfsf13b	8.01	8.49	3.9E-03	2.8E-03	1.39
Tnfsf4	13.38	11.14	9.4E-05	4.4E-04	**0.21**
Vegfa	4.46	4.21	4.5E-02	5.4E-02	0.84
Actb	0.39	0.97	7.6E-01	5.1E-01	1.50
B2m	-1.39	-1.14	2.6E+00	2.2E+00	1.19
Gapdh	0.00	0.00	1.0E+00	1.0E+00	1.00
Gusb	7.41	7.42	5.9E-03	5.8E-03	1.01
Hsp90ab1	2.59	2.60	1.7E-01	1.6E-01	1.01

VITA

Christa D. Jackson (CJ) was born to Steven and Karla Jackson on August 22, 1996, in Greeley, Colorado. CJ is the oldest of four, with sisters Abby and Bethany and brother Jared. The Jacksons moved from the United States to Maputo, Mozambique in 2005. CJ attended secondary school at Rift Valley Academy in Kijabe, Kenya, graduating in July 2014. Subsequently, they earned a Bachelor of Science in Biology at John Brown University in Siloam Springs, Arkansas, graduating *summa cum laude* with honors in May 2018. CJ was accepted into the Molecular Pathogenesis and Therapeutics graduate program at the University of Missouri-Columbia in 2018, where they trained under the supervision and mentorship of Charles R. Brown, Ph.D., in the Department of Veterinary Pathobiology. CJ successfully defended their dissertation in March 2023 and received their Ph.D. in Microbiology in May 2023.